ENGINEERING
LIBRARY

JUL 1 1948

NUCLEONICS

AN INTERNATIONAL JOURNAL
FOR TECHNIQUES AND APPLICATIONS OF NUCLEAR SCIENCE

June, 1948

FUNDAMENTALS OF ISOTOPE SEPARATION

THEORY AND OPERATION OF GEIGER-MÜLLER COUNTERS—I

RADIOAUTOGRAPHY IN BIOLOGICAL RESEARCH

CHEMICAL EFFECTS OF NUCLEAR TRANSFORMATIONS

NUCLEAR PHYSICS OF THE DEUTERON
AND OTHER TWO-PARTICLE PHENOMENA—I

BETA-RAY MEASUREMENTS AND UNITS

MANHATTAN DISTRICT DOCUMENTS

Index to NUCLEONICS, Volumes 1 and 2

A McGraw-Hill Publication

SHERRON

HIGH GRADE ELECTRONICS EXPERIENCE FOR HIGH ENERGY PHYSICS

Work involving the controls for accelerators and electronic instruments for nuclear research is in the field of Sherron's activities. We can develop and manufacture equipment for the following purposes:

1. CONTROL
2. MEASUREMENT
3. POWER SOURCES

Seasoned physicists and electronic engineers are available for consultation in any auxiliary capacity—prototype through completed instrument . . . Inquiries are invited.

SHERRON CAN SERVE IN THE DESIGN, DEVELOPMENT AND MANUFACTURE OF:

- Counters, computers, servomechanisms
- Amplifiers, oscillators
- Power supplies, power regulators
- Process control, generator control
- Parameter measurement, control, production
- Temperature, flow, radiation
- Controls and accessories for synchrotrons
- Betatron, Cyclotron

SHERRON ELECTRONICS CO.

Division of Sherron Metallic Corporation

1201 FLUSHING AVENUE • BROOKLYN 6, N.Y.

NUCLEONICS VOL. 2, NO. 6, JUNE, 1948

An International Journal for Techniques and Applications of Nuclear Science

EDITORIAL BOARD

L. B. Borst
John R. Dunning
H. H. Goldsmith
Clark Goodman
F. C. Henriques, Jr.
W. F. Libby
L. D. Marinelli
I. Perlman
Edith H. Quimby
Winfield W. Salisbury
T. I. Taylor

With the cooperation of . . .

ITALY — E. AMALDI
GREAT BRITAIN — J. D. COCKCROFT
FRANCE — F. JOLIOT-CURIE
SWITZERLAND — P. SCHERRER
THE NETHERLANDS — C. J. BAKKER
DENMARK and SWEDEN — GEORGE HEVESY
GERMANY — HANS KOPFERMAN

CONTENTS

Fundamentals of Isotope Separation 3
KARL COHEN

Theory and Operation of Geiger-Müller Counters—I 10
SANBORN C. BROWN

Manhattan District Declassified Documents 22

Radioautography in Biological Research 30
AUBREY GORBMAN

Chemical Effects of Nuclear Transformations 44
R. R. EDWARDS and T. H. DAVIES

Nuclear Physics of the Deuteron and Other Two-particle Phenomena—I 57
M. E. ROSE

Beta-ray Measurements and Units 67
M. BLAU and J. E. SMITH

INDEX to Volume 1 93

Volume 2 97

EDITORIAL 2
NUCLEONIC EVENTS 75
PRODUCTS AND MATERIALS 80
ABSTRACTS 84

Walter M. DeCew ..... Technical Editor
Jerome D. Luntz ..... Assistant Editor
Ethel Pelzer ..... Assistant Editor
Robert Colborn ..... Washington Editor
Gladys Montgomery . Washington Editor
Keith Henney ..... Consulting Editor
E. J. Tangerman ..... General Manager

NUCLEONICS (with which is consolidated "Atomic Power" and "Atomic Engineering") June, 1948, Vol. 2, No. 6 Publication Office: 212 East York St., York, Pa. Editorial and Circulation Offices: 330 W. 42nd St., New York 18, N. Y. Published monthly by McGraw-Hill Publishing Company, Inc. Entered as second class matter December 17, 1947, in the Post Office at York, Pa., under the act of March 3, 1879. Copyright 1948 by McGraw-Hill Publishing Company, Inc. All rights reserved. James H. McGraw, Jr., President; J. A. Gerardi, Secretary; Curtis W. McGraw, Treasurer. Price per copy $2.00. Allow at least ten days for change of address. All communications about subscriptions should be addressed to J. E. Blackburn, Jr., Director of Circulation, 330 W. 42nd St., New York 18, N. Y. Subscription rates: United States and U. S. Possessions $15.00 a year. Canada and Latin America $20.00 a year. All other countries $25.00 a year. Return postage guaranteed. Member A.B.C.

Nuclear Engineering

ENGINEERING, by definition, is applied physics and chemistry. Nuclear engineering, concerned with the design, construction, and operation of nuclear fission reactors, might therefore presently be defined as applied fission physics and chemistry.

As a result of investigations during the last ten years, the physics and chemistry of the fission of heavy atomic nuclei are now empirically understood, and it is now possible for competent engineers to engage in the design and construction of nuclear reactors on the basis of this knowledge.

Actually, only a small fraction of the vast fund of knowledge so far achieved in nuclear physics is necessary for the theoretical and experimental foundations of nuclear chain-reacting systems. The majority of the scientists who first discovered and applied the principles and results of this chapter in nuclear physics have now advanced to the much more fundamental and challenging investigation of nuclear forces, and are seeking their explanation from information provided by high-energy accelerators, cosmic rays, meson theory, quantum electrodynamics, and other tools for the deeper study of the interaction of elementary particles.

On the other hand, very serious technical problems remain in the field of breeding and power reactors, which will require for their solution the highest type of competence in applied fission physics and chemistry. They involve, for example, the application of pile theory to the design of chain-reacting units meeting various optimum conditions, the application of nuclear chemistry to the separation and recycling of fission products, the development of materials having appropriate nuclear properties in addition to the necessary physical, chemical, and thermal properties, and the control of radioactivity hazards.

Experience on the United States Atomic Energy Commission projects has shown that capable chemical, electrical, electronic, and mechanical engineers can acquire the small amount of nuclear physics necessary for this competence in reactor design, in a relatively short time. This follows the classic pattern of all technical advances, in which it is the scientists' function to break the path with fundamental discoveries and it is the engineers' function to build upon them as the scientists pass on to new frontiers.

Although the coordinated effort of physicists, chemists, and engineers will continue to be necessary during the next several years, the central problems facing the further development of reactors for breeding and power purposes have clearly entered the engineering stage. Fortunately, the United States, with sixty percent of the world's engineers, is singularly well situated to put forth the engineering effort for their early and fruitful solution.

The efficient use of available technical manpower will now require consideration of the special conditions conducive to the greatest creative initiative in engineers. Nobody can doubt that given the same sympathetic understanding of their requirements, American engineers and industry will cooperate as enthusiastically on present fission reactor problems as the scientists have on those of the past.

—*W. M. D.*

FUNDAMENTALS OF ISOTOPE SEPARATION*

A major contributor to the design of the Oak Ridge uranium plants illustrates and discusses how a single theory of cascades provides absolute standards for raising the separative efficiency of all presently known methods of isotope separation

By KARL COHEN

The H. K. Ferguson Company, New York, New York

IN RECENT YEARS, isotope separation has changed from a laboratory curiosity to a major chemical industry. Under the pressure of the uranium problem, a great deal of thought has been expended on separation processes and much progress has been made — material progress, as well as progress in insight. The selection of topics for this article was made from the extensive report *Theory of Isotope Separation, Revised*, declassified July 14, 1947 (MDDC 1138) which contains detailed acknowledgments to the many contributors to this theory.†

The things we want to know when we decide to do an experiment with a new isotope are: First, how big a separation job is it, second, what is the best separation method to use, and then, what is the most efficient hook-up of the chosen separation apparatus?

So far we have been able to find complete and satisfying answers to these questions for binary mixtures only. But this is the most important case, and gives us considerable confidence about future generalization. Our attention, will be confined then to binary mixtures.

The problem of separating a mixture of isotopes is not fundamentally different from that of separating any other mixture. However, since the chemical and physical properties of isotopic molecules differ so little, we do not usually obtain sufficient change in isotopic abundances in a single process. Therefore we must repeat the same elementary separation process over and over again, sometimes thousands of times. This is most efficiently done in a continuous process and we arrange many separating units into a *cascade*.

The simplest possible separating element is shown in Fig. 1. A stream of material enters and is separated into two streams, one enriched in the desired isotope, and the other depleted. The electromagnetic separator, a concurrent centrifuge, and a barrier diffusion unit are of this type directly. Mathematically, they are all characterized by the relation

$$R'/R = \alpha = 1 + \epsilon, \qquad \alpha > 1 \quad (1)$$

which says that the isotopic abundance ratio of the enriched stream is increased by a constant factor over the ratio at the entrance. The factor α is large for

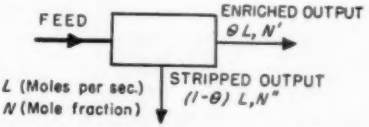

FIG. 1. A simple separating element

* Paper presented before American Chemical Society Symposium on Use of Isotopes in Biochemistry, September 18, 1947.

† A somewhat more mathematical account of the topics considered here will appear in Vol. 2 of "The Science and Engineering of Nuclear Power" (the MIT nuclear science and engineering lectures).

electromagnetic separators and very nearly 1 for the others.

The cascade (Fig. 2) may be built up out of identical small units. Each group of elements in parallel is called a *stage*. The flow in each stage is proportional to the number of elements. Or we might have different capacity elements connected in a cascade—differing in throughput but not in effective separation factor (Fig. 3). There is obviously no essential difference between these cases, and for convenience we shall consider the latter cascade.

In the cascade shown, each stage is attached directly to its nearest neighbor, the enriched stream moving forward and the depleted stream backward. Of course, more complicated cascades are permissible but analysis shows that they rarely offer any appreciable advantage over the simplest cascade.

The cascade must produce a given purity of product at a given rate from feed of a given concentration. These requirements are not sufficient to determine the cascade uniquely. Many cascades will be satisfactory. For example, we may have two different square cascades, that is, cascades with the same flow in each stage. If we

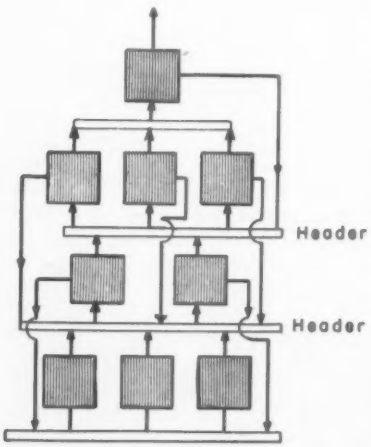

FIG. 2. A cascade of identical elements.

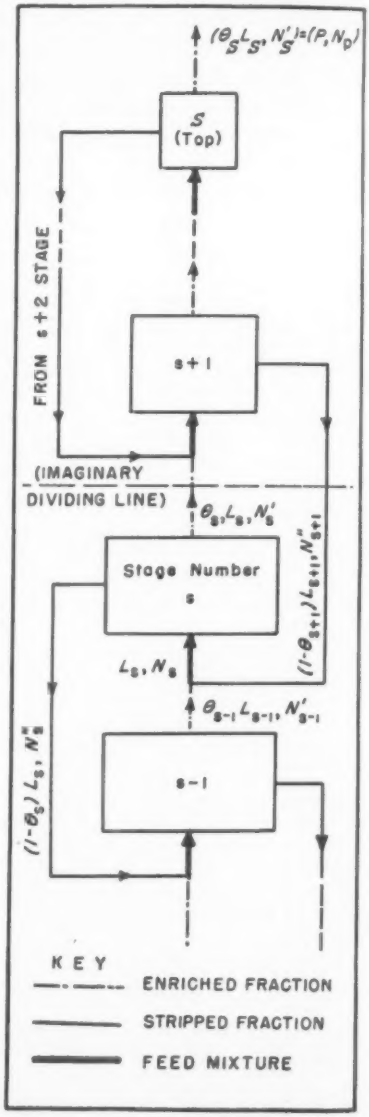

FIG. 3. A cascade of simple elements

take large flows, the cascade will be relatively short; if we take small flows, the cascade will be very long. Or we might have a triangular cascade where the flow in the top stage is $2P$, the next $3P$, and so on.

The rate of increase in concentration from stage to stage for this cascade can be readily worked out using nothing more abstruse than the conservation of matter and the fundamental relation (Eq. 1). If ϵ is small we find

$$\frac{dN}{ds} = 2\epsilon N(1-N) - \frac{2P}{L}(N_p - N) \quad (2)$$

Here N is the mole fraction of desired isotope, P the rate of production, L the throughput, and s the stage number. dN/ds has a maximum of $2\epsilon N(1-N)$, when L is infinitely large. In a square cascade, L is constant, and then all the coefficients are constant. In this case, Eq. 2 can be conveniently written in the form:

$$c_2 \frac{dN}{ds} = c_1 N(1-N) - P(N_p - N) \quad (3)$$

The constants c_2 and c_1 are deliberately meaningless, to concentrate attention on the form of the equation. Eq. 3 of course is identical with Eq. 2 if we identify

$$\begin{cases} c_1 = \epsilon L \\ c_2 = L/2 \end{cases}$$

By now you have undoubtedly recognized that this equation is the equation of a thermal diffusion column if we set

$$\begin{cases} c_1 = H \\ c_2 = K \end{cases}$$

in the usual notation. Similarly (Table 1) we can identify c_1 and c_2 for an ordinary fractionating tower, a counter-current centrifuge, and so on. In other words, a counter-current column behaves exactly like a square cascade of simple elements. We see then that a single theory of cascades is sufficient to cover all presently known methods of isotope separation.

We now consider the problem of selecting the best of all possible cascades. The total throughput in the cascade is

$$\text{Total Throughput} = \int_0^S L(s)ds = \int_{N_0}^{N_p} L(N)\frac{ds}{dN}dN \quad (4)$$

$$= \int_{N_0}^{N_p} \frac{L(N)dN}{2\epsilon N(1-N) - \frac{2P}{L}(N_p - N)}$$

TABLE 1

Separation Method	c_1	c_2
Simple element	ϵG	$G/2$
Thermal diffusion column	H	K
Chemical exchange tower	$-L(\alpha - 1)$	$+\frac{Ll}{k}$
Counter-current centrifuge	$\frac{2\pi}{RT}\frac{\Delta M\omega^2}{RT}\int_0^a r dr \int_0^r pw\, r dr$	$\frac{2\pi}{RT}Dp\frac{a^2}{2} + \frac{2\pi}{RT}\frac{1}{Dp}\int_0^a \frac{dr}{r} x\left\{\int_0^r pw\, r dr\right\}^2$

For the simple element, G is the throughput (identical with L, the throughput per stage, if there is one element per stage). For a chemical exchange tower, L and l are, respectively, the flows down and up in the tower, α is the simple process factor of the chemical exchange, and k is the mass transfer coefficient between phases. For the centrifuge, ΔM is the mass difference of two isotopes, ω is the angular velocity of centrifuge, R is the gas constant, T is the absolute temperature, a is the radius of centrifuge, p is the pressure in centrifuge, w is the velocity of axial circulation, D is the diffusion coefficient.

ds/dN is introduced from Eq. 2 where it was given as a function of L. The following notation has been used: S is the total number of stages, N_0 is the mole fraction of the feed, and N_p is the mole fraction of the product.

In this equation, for every different relation between throughput and mole fraction, we get a different total throughput. The size of each stage is proportional to its throughput; therefore, the minimum size of the whole cascade —minimum number of machines if the stages are composed of identical elements in parallel—occurs when the total throughput is a minimum. Consequently the best cascade will occur when we choose that particular function $L(N)$ which makes the total throughput a minimum. This problem in the calculus of variations has a very definite solution which is

$$L^* = \frac{2P}{\epsilon} \frac{N_p - N}{N(1 - N)} \qquad (5)$$

$$\frac{dN}{ds} = \epsilon N(1 - N)$$

$$R = \frac{N}{1 - N} = R_0 e^{\epsilon s}$$

$$S = \frac{1}{\epsilon} \log \frac{R_p}{R_0}$$

$$\int_0^S L^* ds = \frac{2P}{\epsilon^2} f(N_p, N_0)$$

$$= \frac{2P}{\epsilon^2} \left\{ (2N_p - 1) \log \frac{R_p}{R_0} + \frac{(1 - 2N_0)}{(1 - N_0)} \frac{N_p - N_0}{N_0} \right\}$$

A cascade characterized by these equations is called an ideal cascade. The first equation gives the flow as a function of mole fraction. The second shows that in an ideal cascade the enrichment per stage is exactly half the maximum. The third gives the variation of molecular abundance ratio with stage number, and combined with the first gives the flow per stage as a function of stage number. The fourth gives the total number of stages. The fifth gives the total throughput in an ideal cascade. The expression in braces defines the function f.

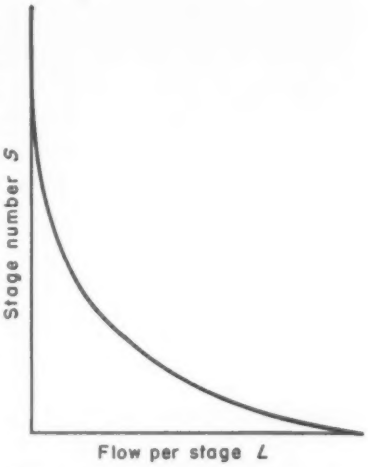

FIG. 4. Schematic ideal cascade for carbon-13 enriching section

The form of an ideal cascade according to these equations is shown in Fig. 4. Note the broad base and the very narrow and extended top. This is just the enriching section of the cascade—the engineers would call it the rectifying section. With a cascade like this, the waste is only slightly depleted in desired isotope. There would usually be, in addition, a stripping section to reduce the concentration of desired material in the waste. A cascade would then also have a roughly triangular section below the feed point (Fig. 5).

Let us put a few numbers in to get a physical feeling for these cascades. Suppose we are interested in separating C^{13} from C^{12} by some process where the effective separation factor is $\epsilon = 0.01$. We might want a plant to produce something like one mole — 13 grams — per day of C^{13} at high purity. The initial concentration of C^{13} is $N_0 = 0.011$.

For simplicity we may further suppose that our supply of raw material is so large that we are not interested in having any stripping section. The total amount of material flowing through the cascade at any one time is then given by

$$\frac{2PN_p}{\epsilon^2 N_p} f(N_p, 0.011)$$

$$= \frac{(2 \times 10^4) \times 1}{N_p} f(N_p, 0.011) \quad (6)$$

The N_p in the denominator takes account of the fact that to produce 1 mole of C^{13} at 50% concentration requires 2 moles of product. The total number of stages is

$$S = \frac{1}{0.01}\left[\log \frac{N_p}{1 - N_p} + 4.5\right] \quad (7)$$

and the flow in the base stage is

$$L_1 = \frac{2}{(0.01)N_p} \frac{N_p - 0.011}{(0.011)(0.989)} \quad (8)$$

It is interesting to examine the dependence of these expressions on N_p, the purity of the product (Fig. 6). On a log-log plot, we see that at low concentrations the total throughput increases very rapidly, but changes very little above 20%. Thus we see that as far as total amount of plant is concerned

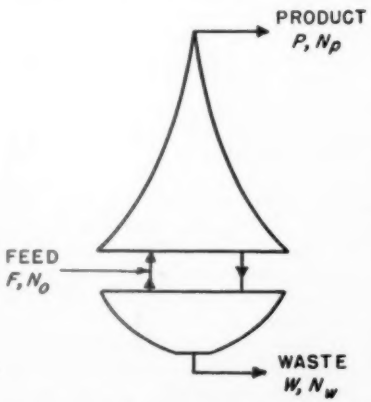

FIG. 5. Ideal cascade with rectifier and stripper for carbon-13

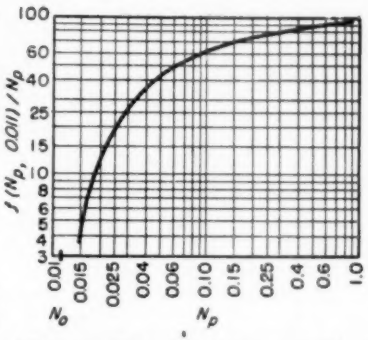

FIG. 6. Value function per mole of desired isotope versus mole fraction of product for concentration of C^{13}

it makes little difference whether we want 50% or 99% purity.

However, the number of stages increases considerably as the concentration increases. For example, for N_p = 50%, S = 450, while for N_p = 99%, S = 910. The stages which are added are, however, very small compared to the base stages: Taking N_p = 99%, stage 450, where the concentration is 50%, carries 400 moles per day while the bottom stage handles 20,000 moles per day. The upper stages correspond to the long pointed tip of the ideal cascade (refer back to Fig. 4). The total flow in the entire cascade, when producing material of 90% purity at the rate of one mole per day, is 2×10^6 moles per day.

Now let us go back and see how the cascade theory enables us to compare different separation methods. Suppose that each stage is divided into units, each of which can accommodate G moles per sec. For example, in a diffusion cascade the unit might be 1 square foot of barrier; or in a fractionating tower, take 1 square foot of tower cross section. The number of separating elements required, each of which has a throughput G, is merely the total throughput (which we already know) divided by G

TABLE 2

$$\text{Number of elements} = \frac{P f(N_p, N_0)}{\frac{1}{2} G \epsilon^2} = \frac{\text{Change in Value}}{\text{Separating Power}}$$

Type of Element	*Separating Power**
Simple element	$G\epsilon^2/2$
Electromagnetic separator	$\frac{G(\alpha - 1) \log \alpha}{\alpha + 1}$
Column or square cascade	$c_1^2/4c_8$
Thermal diffusion column	$H^2/4K$
Chemical exchange tower	$\frac{kL(\alpha - 1)^2}{4l}$

** For notation, see Table 1.*

$$\text{Number of Elements} = \frac{Pf(N_p, N_0)}{\frac{1}{2} G \epsilon^2} = \frac{\text{Change in Value}}{\text{Separating Power}} \quad (9)$$

The numerator of this expression is characteristic of the difficulty of the separation problem. It therefore depends only on the amount and mole fraction of material produced. The denominator on the other hand is characteristic only of the properties of the separating element itself—its throughput and fractionation. We call the numerator the change in value created by the cascade as a whole; we call the denominator the separating power of the element.

Table 2 gives expressions for the separating power of a few of the types of apparatus just considered. The expression for a square cascade agrees with that for a simple element for the values of c_1 and c_8 which we assigned previously. The thermal diffusion column and a chemical exchange tower are just two special cases of the square cascade. The expression for the electromagnetic separator is easily found by generalizing the theory of the simple element to the case where ϵ is not small.

An even more general method for deriving the separative power of any type of separating element is given in the M.I.T. lectures (see second footnote on page 3).

Obviously the problem of element design is to make the separative power as large as possible. Note that when the effective separation factor α is nearly 1, there is a great premium on increasing α, since the separative power varies as the square of $(\alpha - 1)$. It will be recalled that ϵ is the excess of α over 1). But for large α diminishing returns are encountered, the separative power varying only as $\log \alpha$. If increasing α is accompanied by decreasing G, as might easily be the case, there will be an optimum α, which will not necessarily be the largest physically attainable.

The theory just developed can be applied to separation problems in a more powerful way. It is clear that different apparatuses based on the same fundamental principle will have different values of the separative power. The next step is to find the largest value of the separative power in, for example, a thermal diffusion column and in a centrifuge.

If there were no circulation of gas within these instruments, an equilibrium concentration gradient would be set up. In the diffusion column, the gradient would be between the hot

and cold wall; in a centrifuge, between the axis and the periphery. When circulation is started up, this gradient is disturbed, and in seeking to return to the equilibrium state the apparatus transports material and so performs separative work. The steady-state concentration gradient of the operating instrument is therefore different from the equilibrium gradient. If the steady-state gradient is zero, no concentration difference can be established; if it equals the equilibrium gradient, no material is transported. Somewhere in between there exists an optimum. In an ideal cascade, it is recalled, the concentration gradient between stages is half the maximum possible gradient. Similarly the optimum steady-state gradient is one-half the equilibrium gradient and in the same direction.

The optimum separative power of an apparatus will thus be achieved when this condition is satisfied in every little volume element. If we integrate over the entire apparatus, we thus get a maximum attainable separative power. For a centrifuge, the result of this calculation gives

$$\frac{Dp}{RT}\left[\frac{\Delta M(\omega a)^2}{2RT}\right]^2\frac{\pi}{2}\ \text{(moles/sec-cm)} \quad (10)$$

for the maximum separative power (per unit length). For a thermal diffusion column we have

$$\frac{\pi}{2}\int_a^b \rho D\left(\frac{\alpha}{T}\frac{\partial T}{\partial r}\right)^2 r\,dr\ \text{(gm/sec-cm)} \quad (11)$$

In this expression ρ = density, D = diffusion coefficient, α = thermal diffusion constant, T = temperature, a = radius of hot wall (or wire), b = radius of cold wall. If the thermal conductivity is constant we have the maximum separative power of thermal diffusion column

$$\left(\frac{T_b - T_a}{\log b/a}\right)\frac{\pi}{2}\int_{T_a}^{T_b}\rho D\frac{\alpha^2}{T^2}dT \quad (12)$$

These equations give us absolute standards by which to measure the separative efficiency of any design. It turns out that thermal diffusion columns have efficiencies around 70%. Certain designs of centrifuges published in the German literature, on which they based their pilot plants for the separation of the uranium isotopes, have theoretical efficiencies ranging from 70% down to as low as 40%. In another application, co-current apparatus can be shown to be less efficient than countercurrent and in practical cases is at a disadvantage of 20% or more.

By approaching the optimum efficiency problem in a different way from the one just outlined, we can do more than just set up a standard of efficiency. We can find out what flow conditions within an apparatus will actually produce theoretical efficiency. Naturally this is of great importance in apparatus design. Details of this method are given in the report "Theory of Isotope Separation" (*loc. cit.*).

Theory and Operation of Geiger-Müller Counters—I

THE DISCHARGE MECHANISMS

An understanding of the characteristics of G-M counters is essential for their proper use. In this first of three articles, the author discusses the breakdown characteristics of the discharge for simple and polyatomic gas counters, properties of gas fillings, need for and method of quenching a discharge, relationship between pulse size and plateau, the nature and effect of spurious discharges, and probable life of gas filling

By SANBORN C. BROWN

Department of Physics, Massachusetts Institute of Technology
Cambridge, Massachusetts

TO A LARGE DEGREE the successful use of a Geiger-Müller counter as an ionization detector depends on an understanding of its operational characteristics and design in the light of the discharge mechanisms and the properties of the radiation to be detected. Since the characteristics are relatively complicated and new theories and practices are constantly appearing in the literature, it is worth while from time to time to survey the field and to discuss in a single group of articles material which is now mostly in the form of research papers.

This present series does not attempt to introduce new ideas or theories, but to correlate our current picture of the discharge mechanisms, and to suggest how these ideas may be used in the design and effective use of Geiger-Müller counters when wide varieties of specifications are to be met.

Breakdown Characteristics

The usual geometrical form of a Geiger-Müller counter is that of coaxial cylinders in which the axial electrode (anode) is a fine wire and the outer electrode (cathode) has an internal diameter of a few centimeters. The electric field intensity between coaxial cylinders is given by

$$E = \frac{V}{r \ln \frac{r_c}{r_a}} \qquad (1)$$

The electric field intensity at point r is measured in volts per centimeter if V is the potential in volts between the electrodes, and r is the distance from the axis of the cylinders in centimeters. The radius of the cathode is r_c and the radius of the anode is r_a.

An electron which finds itself in this electric field is accelerated toward the anode, and, where the field is sufficiently intense, the electron will cause cumulative ionization if it collides with gas atoms or molecules as it moves toward the axial wire. The magnitude of the electron avalanche so formed can be determined from gas discharge measurements of the first Townsend coefficient. The first Townsend coefficient, η, may be defined as the ionization produced by an electron falling through a potential difference of one volt. It is customary to present this coefficient as a function of the energy gained by the

electron per mean free path, writing this in terms of E/p, the ratio of the electric field strength to the gas pressure. Such a plot for a number of gases is shown in Fig. 1 (*1*). In terms of the first Townsend coefficient, the number of electrons, n, formed in the cumulative avalanche by the single entering electron is given by:

$$n = e^{\int \eta dv} \qquad (2)$$

The integral form of the exponent is required by the nonhomogeneous electric field between the coaxial cylinder electrodes of the counter.

The Townsend criterion for breakdown of a self-maintaining discharge states that:

$$\gamma n = 1 \qquad (3)$$

γ is the number of electrons liberated in the gas, or at the cathode, per ionization in the gas, and n is the number of ion pairs formed in the initial avalanche. In the counter breakdown, the number of ion pairs formed in the initial avalanche must be sufficiently high to produce by a photoelectric effect, either in the gas or at the cathode, at least one electron to form a succeeding avalanche and so maintain the discharge. Since the photoelectric efficiency from gas to gas and from cathode to cathode is approximately the same, n is approximately the same in the usual region of counter operation. Thus, from Fig. 1, for a given value of n, and hence of η, we can see the relative threshold voltages to be expected at a given pressure for various gases. To obtain a given value of η for air, a much higher value of E/p (and hence E, since the filling pressure for counters is usually about the same) is necessary than for argon or helium. For certain mixtures of neon and argon, a very low field is sufficient to maintain a discharge, as can be seen from the high values of η for low values of E/p in Fig. 1.

The quantity γ, the number of electrons liberated in the gas or at the cathode per ionization in the gas, has been studied very little. Like n, it is a function of E/p, but γ is not nearly so steep a function as n and to a rough approximation one may consider that n controls the breakdown field. A few experimental determinations of γ have been attempted for discharges between parallel plates (*1*). The breakdown criterion between coaxial cylinders has been worked out for one case, helium, and the effect of γ was related to the spectral characteristics of the singly and doubly ionized helium (*2*). No results have yet been reported on determinations of γ for the cases of discharges in polyatomic gases.

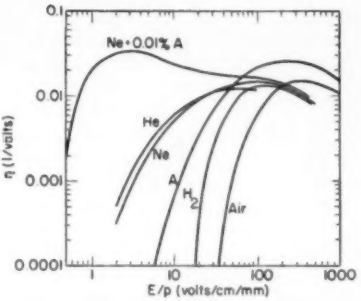

FIG. 1. The first Townsend coefficient η, the ionization per volt, is plotted as a function of the energy of the electrons per mean free path, E/p, for a few typical gases

Many detailed studies have been made of the variation of threshold voltage with pressure and the type of gas between the electrodes. One can qualitatively predict the results of these experiments from the first Townsend coefficients, shown in Fig. 1, and equation 2. Both from experiments and from consideration of Townsend coefficients, one finds that air has a high threshold voltage, argon and neon are lower, and helium the lowest of the noble gases. Recently Simpson has shown experimentally (*3*) that mixtures of neon and argon give very low voltage

counters, as would be predicted by the curves of Fig. 1. The ease with which ionization is caused in this neon-argon mixture results from the fact that not only do the electrons ionize neon directly but the metastable neon atoms ionize argon atoms for an additional source of ionization.

The conditions for breakdown control the initial avalanche. For the discharge to be of the Geiger-Müller type, it must mature from this initial avalanche to a form characteristic of the counter. This maturation of the electrical discharge depends to a large degree on the type of gas found between the electrodes. We shall discuss two different types of counters in which the general behavior is the same, but the specific details are sufficiently distinct to make it advisable to treat them separately. These two types are characterized by the filling gas and are designated as simple gas counters (H_2, A, He, air, etc.) and polyatomic gas counters (alcohol, ether, tetramethyl lead, etc., mixed with a simple gas).

Simple Gas Counters

In the simple gas counter, the discharge matures through the mechanism of a photoelectric effect. Since the electrons in the cumulative avalanche have sufficient energy to cause ionization, they also have energy enough to cause excitation of the gas atoms. During the process by which these excited atoms return to their original unexcited condition, or ground state, photons are emitted. For the energies involved in the counter mechanism, the photons lie in the ultraviolet region of the spectrum.

The photons created with the initial avalanche form photoelectrons either in the gas or at the cathode wall of the counter, and these secondary electrons cause a new succession of avalanches. By a whole series of these repetitive processes, many electrons and positive ions are produced. Since the electrons attracted toward the anode do not cause appreciable ionization until they are quite close to the anode wire, a sheath is built up in the immediate vicinity of the anode with the electrons nearest the wire surrounded by positive ions. The result of the growth of this positive ion sheath is to increase the effective radius of the anode. Referring to equation 1, we can see that if the potential across the electrodes remains constant (which will be the case since it is connected to a constant potential supply) and the effective radius of the anode increases, the field intensity at any given point decreases. The result of this is that the sheath will build up to a point where the maximum electric field will be too weak to support further ionization, and the electrical discharge between the cathode and anode will cease.

During the formation of the space-charge sheath which quenches the discharge, the motion of the positive ions can be neglected. The positive ion sheath is not really stationary, however, since it is repelled from the anode and attracted to the cathode. Consider the axial wire of the counter as one electrode of a cylindrical capacitor and the positive ion sheath as the other (*4*). The charge on this capacitor remains the same since the number of ions in the sheath remains constant. As the positive ion sheath moves outward toward the cathode, a negative voltage pulse is induced across the counter and this pulse constitutes the "count" registered by a suitable circuit connected across the electrodes.

Although the counter has successfully recorded the entrance of the ionizing radiation into its sensitive volume, the entire chain of events is not complete. The positive ion sheath moves outward and eventually hits the cathode. These positive ions have a high probability of interacting with the cathode

surface and releasing secondary electrons. A simplified picture of the mechanism involved is as follows (*5*): When a positive ion approaches a metal surface closely enough, its force field may interact with those of the electrons in the metal. The electron may be drawn out of the metal to combine with the positive ion, thus neutralizing the charge of the latter. In general, the ionization energy of the ion is much greater than the energy required (the work function of the metal) to remove an electron. Hence, by combining with the electron, the ion neutralizes its own charge to become an atom, but is left as an excited atom with its excitation energy equal to the difference between the ionization potential of the gas atom and the work function of the metal. The gas atom does not live very long as an excited atom, but radiates its excitation energy in the form of a photon. For the types of gas atoms used in the simple gas counters, the emitted photons lie in the ultraviolet region of the spectrum where they are efficient at producing photoelectrons on collision with the cathode surface. These secondary electrons can be drawn from the neighborhood of the cathode by the positive anode of the counter and will rekindle the discharge if a mechanism is not invoked to prevent their doing so.

In the simple gas counter, the usual method of preventing the rekindling of the discharge is by the action of the external circuit connected to the counter. This is called "external quenching." Unfortunately, this nomenclature is misleading since the discharge is completely over before the effect one desires to eliminate becomes important. It is not a question of quenching the discharge but of preventing the production of secondary discharges. The essential function of the quenching circuit is to prevent the total voltage across the counter from rising to threshold before all the secondary electrons produced by the positive ions at the cathode have been collected by the anode.

The entering ionizing particle causes the formation of a space-charge sheath around the anode. This sheath moves toward the cathode, causing the voltage across the counter to drop. For the counter to function properly, the voltage must drop to a value sufficiently below the threshold so that it will not recover until ionizing particles left over from the discharge are all collected. The time which elapses while the counter is thus completely insensitive is called the "dead time." The voltage recovery time depends upon the time constant of the circuit, and, since this is an exponential recovery, a relatively long time, compared to the dead time, elapses before the potential across the electrodes returns to its initial value. If an ionizing particle comes into the sensitive volume before the voltage has returned to its operating value, the counter will break down with a smaller pulse than normal. Whether or not this breakdown will be registered as a count will depend upon its size and the sensitivity of the amplifier circuit.

The recovery time of these simple gas counters depends upon the electrical characteristics of the quenching circuit. The pertinent characteristic is the constant, $\tau = RC$. The capacitance of the counter is kept small so that the pulse size will be large, but a sufficiently long time constant for the necessary quenching can be achieved by the use of large values of resistance, 10^8 to 10^9 ohms, in series with the counter and high voltage. Time constants in this simplest type of quenching circuit are long enough to interfere seriously with the usefulness of this system at even only moderately high counting rates, and various circuits have been devised to allow the external quenching to be assured without the

TABLE 1

Typical Simple Gases Used In Counters

Gas	*Formula*	*1st Excitation Potential (volts)*	*Ionization Potential (volts)*	*Electron Attachment Probability*	*Negative Ion Formed at Wall*	*Positive Ion From Which Formed*	*Negative Ion Formation Probability*	*Metastable Level (volts)*	*Emission Wave Length (A.U.)*
Argon	A	11.6	15.7	0	—	—	—	11.5	1048
Helium	He	20.5	24.5	0	—	—	—	19.7	854
Krypton	Kr	9.9	13.9	0	—	—	—	9.87	1236
Mercury	Hg	—	10.4	—	Hg^-	Hg^+	10^{-3}	5.43	1850
Neon	Ne	16.6	21.5	0	—	—	—	16.5	736
Xenon	Xe	8.3	12.1	0	—	—	—	8.27	1470
Hydrogen	H_2	11.5	15.4	0	H^-	H_2^+	10^{-5}	—	—
Atomic Hydrogen	H	10.2	13.5	0	—	—	—	None	1215
Nitrogen	N_2	6.1	15.5	0	—	—	—	6.27	—
Atomic Nitrogen	N	—	14.5	—	—	—	—	2.37	1135
Oxygen	O_2	6	12.5	10^{-4}	O^- O_2^-	O_2^+ O_2^+	10^{-4} 10^{-5}	5, 3, and 9	—
Atomic Oxygen	O	—	13.6	10^{-3}	—	—	—	2, 4, and 9	1302
Carbon Dioxide	CO_2	—	14.4	0	O_2^- CO_2^-	CO_2^+ CO_2^+	10^{-4} 10^{-4}	5.6	—

use of long time constants. These circuits will be discussed in a later section.

Polyatomic Gas Counters

In the polyatomic gas counters, the polyatomic gas is, in general, only 10 to 20% of the total gas content, the remainder being a simple gas added to achieve the desired characteristics. The production of the initial avalanche by the entering ionizing radiation appears to be the same in any type of Geiger-Müller counter. During the formation of the initial avalanche, the simple gas component of the filling mixture acts as it does when uncontaminated with polyatomic molecules. In the case of the polyatomic component of the gas, it is probable that the inelastic collisions which occur between the electrons of the forming avalanche and the polyatomic molecules result not in ionization but in increasing the rotational and vibrational energy of the molecules. This effect tends to decrease the total photoemission of the avalanche.

In the polyatomic gas counters, the maturation of the total discharge from the initial avalanche has a characteristic quite different from that of the simple gas counters. In the latter case, since the ion sheath is built up by secondary photoelectrons from the gas and cathode, it grows almost simultaneously throughout the counter. In the polyatomic gas case, the complex molecules in general prevent photons, which might be produced in the vehicular gas, from reaching the cathode. In Table 1, the wavelength of the principle emission lines of typical vehicular gases is given. In Table 2, the wavelengths of the

TABLE 2

Typical Polyatomic Gases Used In Counters

Gas	*Formula*	*Ionization Potential (volts)*	*Electron Attachment Probability*	*Negative Ion Formed in Gas*	*Energy to Form Negative Ion (volts)*	*Absorption Wave Lengths (A.U.)*	*Type of Spectra*
Bromine	Br_2	12.8	10^{-3}	Br^-		1500	Continuous
Chlorine	Cl_2	13.2	10^{-3}	Cl^-		1500	Continuous
Carbon Monoxide	CO	14.1		O^-	20.9		
Nitric Oxide	NO	9.5	5×10^{-5}	O^-	7.0		
Carbon Dioxide	CO_2	14.4	0			1360 – 600	Bands
Carbon Disulfide	CS_2	10.4				3800–1200	Bands
Hydrogen Sulfide	H_2S	10.4	0	HS^-	3.7	1600–1190	Bands
	HS		10^{-6}				
Nitrogen Dioxide	NO_2	11.0				5700–2200	Bands
Nitrous Oxide	N_2O	12.9	0	O^-	1.7	3000–1760	Continuous
						1520–1056	Bands
						< 1000	Continuous
Sulfur Dioxide	SO_2	13.1	10^{-4}	SO^-	5.7	3800–1529	Bands
Water	H_2O	13.0	0	OH^-	5.4	1240 – 983	Bands
				O^-	7.5		
	OH	13.8	10^{-4}				
Ammonia	NH_3	10.5	0	NH_2^-	6.0	1620–1450	Bands
				NH^-	3	< 1200	Continuous
	NH^-		10^{-4}				
Acetylene	C_2H_2	11.6				2400–2090	Bands
Carbon Tetrachloride	CCl_4					4600–2300	Bands
Methane	CH_4	14.4				< 1450	Continuous
Chloroform	$CHCl_3$					< 2200	Continuous
Methyl Iodide	CH_3I	10.12				3600–2110	Continuous
						2100–1215	Diffuse
Ethyl Bromide	C_2H_5Br	10.24				2850–1900	Continuous
						< 1700	Diffuse
Ethyl Chloride	C_2H_5Cl					< 1700	Continuous
Pyridine	C_2H_5N	9.8				< 2500	Continuous
Ethyl Alcohol	C_2H_5OH	11.3				1633–1602	Bands
						1518	Diffuse
						< 700	Continuous
Acetone	CH_3COCH_3	10.1				3300–2940	Bands

absorption bands of common polyatomic gas are presented. One can see from these two tables that, for the common gas mixtures used in polyatomic gas counters, the radiation from the vehicular gas is covered by absorption bands of the polyatomic gases. This photon quenching is not perfect (*6*, *7*), but due to the relative inefficiency of the cathode as a photoelectron emitter these photoelectrons can usually be neglected.

The specific ionization of the initial avalanche becomes greater as the ava-

lanche moves into the high field region near the anode wire. The ionization processes will be much more probable in the high field region because of the greater energy of the electrons. Since the energy of the photons is readily absorbed by the polyatomic molecules, any subsequent discharge following the initial avalanche will occur in the high field region near the central electrode. As we move outward from the anode wire, the field drops off very rapidly, and hence we would expect the ionization to be localized very close to the axial electrode. On the other hand, at any given distance from the wire along the length of the counter, the field is uniform. Thus the discharge, while being limited radially by the decreasing field, spreads laterally in the high field region of the wire until it meets some discontinuity which lowers the field, such as the physical end of the electrode. When this sheath has been formed, any subsequent ionizing particle which might enter the volume between the electrodes will not cause cumulative ionization.

The ion sheath which builds up near the anode decreases the electric field. This sheath will grow to the point where the field can no longer produce further ionization and this limits the thickness of the sheath. After the sheath has reached its maximum thickness and length, the discharge in the counter is over and the counter is left in a completely insensitive state from which it must recover if it is to detect any subsequent ionizing particles.

The phenomena which follow the extinction of the discharge depend both on the ion behavior within the tube and on the external circuit to which the tube is connected. The ion sheath is formed so rapidly that it may be considered stationary in the process of formation. The positive ions are attracted toward the cathode so that although they may be considered stationary during their formation they are actually moving outwards. The outward motion of the positive ions away from the anode causes a lowering of the wire potential as discussed for the simple gas counter mechanism. The function of the external circuit is to re-apply the potential across the electrodes. Again, the rate at which the potential is reapplied depends upon the time constant of the circuit. In the case of the polyatomic gas counter circuit, the resistance may be small so that, in general, the voltage is re-applied across the electrodes before the space charge sheath has moved very far out from the anode. Though the operating voltage has been restored to the counter, however, the tube is still insensitive because the electric field intensity is greatly modified by the space charge sheath within the electrode volume and has not returned to the operating field.

After the space-charge sheath has been formed and starts to move toward the cathode, it takes the order of 10^{-5} seconds for the circuit to restore the potential to the operating voltage. At this time, since the sheath has not moved very far, the field is considerably below threshold field intensity, that is, the field which would exist between the electrodes in the absence of space charge when the counter is at its threshold voltage. It takes somewhere between five and ten times longer for the space charge to move out far enough for the field intensity of the wire to rise to the threshold field than it does for the operating voltage to be re-established across the counter by a properly designed external circuit. The elapsed time, of the order of 10^{-4} seconds, between the initial breakdown of the counter and the time for the threshold field to be re-established is called the "dead time." During this time, the counter is completely insensitive to ionizing radiation. Estab-

lishing threshold field intensity at the wire does not mean that the counter has recovered its original condition. It actually takes as long again for the counter field to change from threshold field to operating field as it does to establish threshold field from the original breakdown. During the 10^{-4} seconds between the end of the dead time and the re-establishment of the operating field, any ionizing particle entering the counter will be recorded as a pulse of smaller size than normal.

Self-quenching Mechanism

The reason that the voltage may be re-applied to the polyatomic gas counters before the space charge has been collected at the cathode lies in its so-called "self-quenching" properties.

The phenomena which occur when a polyatomic ion reaches the cathode surface are different from that discussed for the simple gas counter. As in the case of the simple gas ion, the polyatomic ion interacts with the electrons in the metal and neutralizes itself by pulling an electron from the surface. The polyatomic molecule then finds itself in an excited state. The characteristic behavior of the gas leading to "self-quenching" properties is exhibited by those polyatomic molecules in which the lifetime of the excited state for emission of a photon is much longer than the lifetime for dissociation. Thus, instead of releasing the energy by emitting an electron, the energy goes into dissociation of the molecule and kinetic energy of the dissociated fragments. The self-quenching mechanism is therefore one of preventing the emission of secondary electrons by positive ion bombardment.

In the usual polyatomic gas type of counter, the filling is a mixture of only about ten percent polyatomic gas with a vehicular gas which is usually a noble gas. An additional criterion for successful self-quenching properties of a polyatomic gas is that only polyatomic positive ions reach the cathode and no simple gas ions are left in the ion space charge sheath when the sheath reaches the outer walls. The mechanism involved is one of charge transfer. In a collision between an atom and an ion, if the ion has a higher ionization potential than the atom, the ion will ionize the atom and return itself to a neutral atom. While the positive ion sheath moves outwards from the anode to the cathode, an ion makes about 10^6 collisions. This is a sufficiently high number of collisions to make it highly probable that a charge transfer will occur if the ionization conditions are suitable. Since the ionization potentials of the polyatomic molecules are all quite low, it is not at all difficult to arrange the ionization potential of the vehicular gas to be higher than the quenching agent. Again referring to Tables 1 and 2, one can see that it is quite generally true that all gases one would want to use as vehicular gases have ionization potentials higher than the ionization potentials of the polyatomic gases.

The charge transfer mechanism is not perfect and as in the case of the simple gas counter, some secondary electrons are always produced. In the polyatomic gas counters, secondary emission by ion bombardment of the cathode is unlikely enough so that for many purposes one can consider the secondary discharges as being completely quenched. Actually somewhat more than ninety percent of the secondary electrons are prevented from being produced at clean metal surfaces when the counter is operating at its threshold potential. This percentage decreases as the voltage is increased above threshold. If the figure of less than ten percent spurious pulses is important, the cathode may be treated chemically, or may be mechanically coated with a surface which will be less efficient in

producing secondary electrons than the pure metal. Various cathode treatments have been suggested and are successful in reducing the spurious discharges from ion bombardment of the cathode to about one percent at threshold. No one has yet proposed a method for reducing this effect to zero without the use of external quenching circuits.

Pulse Size

The feature which distinguishes a Geiger-Müller counter from any other ionization detector is the fact that the size of the output pulse is not a function of the initiating particle, but only of the characteristics of the counter and associated circuits. A discussion of the profound effect which associated electronic circuits may have on the pulse size from a counter will be left to the description of these circuits in a later section.

The size of the pulse in a counter depends directly on the charge transported across the space between the electrodes and inversely on the capacitance between the electrodes. The charge is a function of the characteristics of the gas in which the ions of the sheath are formed. The capacitance is determined by the physical dimensions of the counter.

The fundamental factors which control the number of ion pairs formed in the space-charge sheath are not easily discussed theoretically. Enough empirical data has been accumulated, however, to serve as a guide in a discussion of the magnitude of the charge. One of the advantages of organic gas filling for counters lies in the fact that the useful polyatomic gases exhibit copious ion production and hence the pulses are large. As a general rule, counters filled with the noble gases support considerably less charge and hence have considerably smaller pulses than the simple molecular gases, which in turn produce smaller pulses than the polyatomic gas counters. The simple gases also show wide variation among themselves. Helium is remarkable for the smallness of its pulses. The size of the space-charge sheath in hydrogen is among the largest of the simple gases.

Plateau Characteristics

The size of the counter pulse is not of itself an important characteristic since one can, in general, make up for lack of pulse size by electronic amplification. However, inasmuch as the pulse size controls the plateau characteristics of the counter, it becomes a significant quantity.

One of the characteristics which accounts for the popularity of a Geiger-Müller counter as an ionization detector is its peculiar voltage-counting-rate behavior. In the ideal counter, a region exists just above the threshold value, over which the counting rate is independent of the applied potential. The counter is not operating correctly unless the counter potential is depressed below threshold by each pulse. In general, the pulse lowers the potential considerably below the breakdown voltage. This means that the potential across the counter can be varied considerably and the pulse will still cause the counter voltage to go below threshold. Hence, there exists a region of voltage above threshold where each single pulse will depress the potential below threshold to guarantee extinction of the discharge. As long as this can occur, the behavior of the counter should be independent of voltage.

It is clear that the size of the pulse must be one of the governing factors in the width of the voltage plateau. The larger the negative voltage pulse coming from the breakdown of the counter, the farther up in voltage the total counter potential may be raised and still maintain the necessary conditions that the electrode field drop

below the threshold value during the pulse. Counters filled with gases which produce large pulses, such as hydrogen and polyatomic vapors, exhibit wider voltage plateaus in general than gases such as helium.

We define the plateau as the region in which the counting rate for a given radiation intensity is independent of the voltage across the counter. However, this is quite a theoretical description. In practice, it is seldom, if ever, that one can achieve complete independence of voltage over any considerable range. Lack of a flat plateau can usually be associated with either discontinuities in the electric field, or with spurious discharges due either to geometrical factors or peculiarities of the gas discharge mechanisms.

Long Versus Short Counters

Other things being equal, long counters have flatter plateau characteristics than short ones. The counting volume does not extend to the physical limits of the counter electrodes. Increasing the voltage across a counter increases the sensitive volume by allowing the counter field to approach the actual limits of the cathode and anode more closely. This effect will cause more relative change in the sensitive volume of short counters than long, and hence, will militate against a flat plateau where the fringing field is appreciably compared with the total length of the counter.

Various gas discharge mechanisms can lead to spurious discharges. Because of the importance of understanding these phenomena, the subject will be discussed at some length. The longer the plateau of a particular counter, in general, the more success has been achieved in eliminating spurious discharges.

As a test for the usefulness of a counter, the length of the plateau tends to be overrated. One would like to operate a counter in a region where changes of potential would not change the sensitivity and operation of the counter during an experimental investigation. On the other hand, the development of stabilized high-voltage circuits has become good enough so that one need not rely on plateau characteristics of the Geiger-Müller counter to guarantee reproducible electrical conditions.

Spurious Discharges

Spurious pulses are defined as discharges occurring in the counter which are not directly associated with the entering radiation. Spurious discharges can take place due to local discontinuities of the electric field. However, at this point, we will discuss only those causes of spurious discharges which arise from the gas discharge mechanisms. For a spurious discharge to show up as an unwanted count, it must produce a secondary breakdown after the true pulse has been recorded as a count. Thus, in general, only those phenomena associated with the slow moving ions will be of interest here.

In Tables 1 and 2 are tabulated those properties of gases which are useful in predicting the behavior of the ions which may be formed. Not all possible gases are included in these tables, but enough variety is given to illustrate the main types of processes that may occur.

If the charge transfer mechanism does not remove all simple gas ions from the positive ion sheath in a "self-quenching" counter discharge, secondary discharges will be produced by the secondary electrons released by the simple gas ions. These electrons are released after the counting field is restored between the electrodes, and they will cause spurious counts. Since it is found experimentally that a few percent of a polyatomic gas mixed with

the vehicular gas is enough to give a maximum charge transfer effect, the usual practice of using five to ten percent quenching gas is more than sufficient.

Cause of Spurious Counts

In simple gas filled counters, a common cause of spurious counts is the secondary electron released by metastable atoms colliding with the walls. Table 1 shows that most of the simple gases used in counters can exist in metastable states. Since a metastable atom is uncharged, it will drift around in the counter, unaffected by the electric field, and may have a very long life until a collision (in general with the wall) releases the energy from the metastable state. This may give rise to a secondary electron from the wall. However, if we deal with a mixture of gases including a small amount of a gas which has an ionization potential lower than the metastable level of the vehicular gas, the collisions which occur in the gas will allow the metastables to be removed by ionizing the contaminant gas. The usual practice of filling counters on vacuum systems in which the pressure is read by mercury gauges takes care of this automatically. The mercury ionization potential is lower than the metastable states of the vehicular gases normally used, and the concentrations are sufficient to quench these metastable states. With the polyatomic gas counters, Tables 1 and 2 show that the ionization potential of the polyatomic gases are lower than the metastable states of the usual vehicular gases which have metastable levels, and hence, these polyatomic gases quench the metastables.

Gases which form negative ions by electron attachment in the gas in general show spurious discharges due to this effect. In the simple gas counter, the time constant of the quenching circuit is so arranged that the counter field has returned to its operating value as soon as possible after all electrons produced by ion bombardment at the cathode have been collected. If these electrons attach to gas atoms to form negative ions, these negative ions, because of their much greater mass, arrive at the intense field of the anode very much later than the electrons. The negative ions will in general lose their electrons in the high field region and thus cause a breakdown after the counter has recovered from its initial pulse. This would cause a spurious pulse. In the case of polyatomic gas counters, negative ions may be formed as dissociation fragments at the walls, or in the gas discharge, and these may arrive in the counting field after the field has recovered from the initial pulse. Thus, we would expect some spurious discharges from this effect in most polyatomic gas counters.

Some gases, of which carbon dioxide is a good example, show no electron attachment in the gas, but may form negative ions at the walls (*8*). The interaction between the positive ion and the cathode is similar to that discussed for the simple gases, except that the electron which is released by the excited neutral atom does not escape into the gas. It is captured by the gas atom as it is released from the metal,

TABLE 3

Electron Affinities

Argon	−1.0*
Bromine	3.54
Chlorine	3.70
Fluorine	3.94
Helium	−0.53
Hydrogen	0.76
Neon	−1.20
Nitrogen	0.04
Oxygen	3.80

* All values in electron volts. These are calculated values for the atoms. Negative values indicate unstable ions.

TABLE 4

Work Functions

Aluminum	4.56–3.57*
Bismuth	4.4–4.0
Cadmium	4.0
Carbon	4.82
Copper	4.5–4.1
Gold	4.82–4.73
Iron	4.72–4.2
Lead	4.1–3.5
Mercury	4.53
Nickel	5.01–4.12
Platinum	6.3–4.4
Silver	4.73–3.85
Tantalum	4.05–3.92
Tin	4.21–4.5
Zinc	3.68–3.32

* All values in electron volts

thus forming a negative ion. The condition for this phenomenon is that the sum of the ionization potential of the atom plus the electron affinity of the atom must be in excess of twice the work function of the cathode surface. Electron affinities of some of the common gases are shown on Table 3, and work functions of cathode surfaces are given in Table 4. From these tables one can predict when this phenomenon might be expected to occur.

Counter Tube Life

When a simple gas is used for filling a counter, there is very little to limit its life to any given period. The energy of the electrical discharge is not great enough to change the gas composition, and chemical changes of the electrodes can be largely eliminated. Changes which do occur after prolonged operation of simple gas counters can usually be attributed to one of the two following causes. If the electrode metals have not been properly outgassed, gases other than the filling gas may gradually diffuse out of the body of the electrodes and change the filling composition. If chemical changes can occur at the surface of the cathode, changes in secondary-electron emission of the surface will result in differing characteristics.

Mixtures of gases are frequently used to achieve specific characteristics. If any gas in the mixture is of a sufficiently complicated nature to decompose in the electrical discharge or if it is chemically active toward the electrodes, changes in the counter behavior will result.

For the case of counters filled with a polyatomic gas, the decomposition of these molecules is a necessary condition for the operation of the self-quenching mechanism. This does not mean that the useful life of the counter is inconveniently short, since an effort is made to choose organic molecules of such a nature that the products of the first few decompositions are themselves satisfactory quenching molecules. A point is reached eventually, however, in all counters filled with polyatomic gases when the self-quenching properties are lost. It is not uncommon to achieve between 10^9 and 10^{10} counts with a polyatomic gas filled counter before the desirable characteristics are lost.

Deterioration of Gas

The deterioration of a polyatomic gas filling appears to be not so much the result of the loss of the quenching gas as the depositing of the decomposed molecular fragments on the cathode. Merely refilling a polyatomic gas counter which has ceased to function does not in general restore its operating properties. It is usually necessary to wash the counter electrodes with an appropriate solvent to revive the surface coating of the molecular decomposition fragments before the counter can be refilled to exhibit its original characteristics. In this connection some diatomic molecules such as the halogens (*10*), which exhibit self-

quenching properties, and which do not permanently decompose, should not show this type of deterioration.

BIBLIOGRAPHY

For a very complete bibliography of Geiger-Müller counter literature, reference should be made to:

Monica Healea, Bibliography: Geiger and Proportional Counters, NUCLEONICS **1**, No. 4, 68 (1947)

1. M. J. Druyvestyn, F. M. Penning, *Revs. Mod. Phys.* **12**, 99 (1940)
2. S. C. Brown, *Phys. Rev.* **62**, 244 (1942)
3. J. A. Simpson, Jr., *Phys. Rev.* **72**, 181 (1947)
4. C. G. Montgomery, D. D. Montgomery, *Phys. Rev.* **57**, 1030 (1940)
5. N. F. Mott, H. S. W. Massey, "Theory of Atomic Collisions," (Oxford University Press, New York, N. Y., 1933)
6. W. E. Ramsey, *Jour. Franklin Inst.* **231**, 393 (1941)
7. J. D. Craggs, A. A. Jaffe, *Phys. Rev.* **72**, 784 (1947)
8. F. L. Arnot, *Proc. Roy. Soc.* **158**, 137 (1937)
9. H. S. W. Massey, "Negative Ions," (Cambridge University Press, New York, N. Y., 1938)
10. R. D. Present, *Phys. Rev.* **72**, 243 (1947); S. H. Liebson, *Phys. Rev.* **72**, 181 (1947)

MANHATTAN DISTRICT DOCUMENTS

ADDITIONAL TITLES of Manhattan District Declassified Documents recently made available to NUCLEONICS appear below and supplement the eight lists previously published therein.

Listed with the name of the paper are its author(s) and MDDC (Manhattan District Declassification Code) number.

Requests for further information concerning the documents may be directed to the Atomic Energy Commission, Technical Information Division, Oak Ridge Directed Operations, Oak Ridge, Tenn. The Technical Information Division will advise requestors where the information contained in the document has been published or otherwise made available, or will provide copies of documents for purchase if the information in them cannot be obtained otherwise.

Flow Diagrams, Pictures of the Plant and Equipment used in the Production of Fluorine, Fluoro-Lube, Hexafluoroxylene and Chlorohexafluoroxylenes. Hooker Electrochemical Company. MDDC 324

Analytical Chemistry of the Manhattan Project Vanadium, Columbium, and Tantalum. S. W. Rasmussen, C. J. Rodden. MDDC 373

Tracer Studies with Inhaled 1.0 *Year Ruthenium.* Mary Dailey, Irving Wender, Richard Abrams. MDDC 420

Some Aspects of the Biological Action of Radiation. E. S. Guzman Barron. MDDC 484

Heats of Reaction of the Oxidation-Reduction Couples: H_2O-H_2O_2, Fe^{+2}-Fe^{+3}, Ce^{+3}-Ce^{+4} and U^{+4}-UO_2^{+2}. B. J. Fontana. MDDC 542

Report on a Magnetic Drive Design for the Fercleve Corporation. General Engineering and Consulting Laboratory. MDDC 548

Continuous Purification of Water for Isotopic Analysis by Density Determination. Robert L. Burwell, Jr., W. E. Roake, Malcolm Dole. MDDC 549

Industrial Health and Medical Rehabilitation at an Atomic Energy Laboratory. J. S. Felton, M.D. MDDC 554

The Half-life of the Be^{10}. D. J. Hughes, C. M. Huddleston. MDDC 556

The Application of Certain Metallic Fluorides to the CoF_3 *Process.* W. B. Burford. MDDC 565

Production of High Boron Steel. R. M. Fowler. MDDC 567

Supplementary Table of Copper Spark Sensitivities. Mark Fred, Frank S. Tompkins. MDDC 568

Correlation of Tissue Responses Following Exposure to Penetrating Radiations. P. S. Henshaw, R. S. Snider. MDDC 569

Review of Information Bearing on the Tumor Inducing Action of Superficial Radiation. P. S. Henshaw, R. S. Snider. MDDC 570

Plant Studies (The Fixation and Absorption of Fission Products by Plants). L. Jacobson, R. Overstreet. MDDC 571

Nitrogen, (Analytical Chemistry of the Manhattan Project). K. J. Jensen, R. J. Mundy. MDDC 572

The Measurement of the Surface Tension of UF_6 *at Two Temperatures.* H. F. Priest. MDDC 573

The Preparation of Tungsten Hexafluoride. H. F. Priest, R. Colton. MDDC 574

The Production of Fluorocarbons by the Reaction of Fluorine with Silicon Carbide. H. F. Priest, A. V. Grosse. MDDC 575

A Simple Laboratory Electrolysis Cell for the Production of Fluorine. H. F. Priest. MDDC 576

Thermocouple Elements of the Concentric Type for Use in Small Wells. H. F. Priest 577

The Effects of External Irradiation with Beta Rays on the Peripheral Blood of Rabbits. J. R. Raper, K. K. Barnes. MDDC 579

Effects of Periodic Total Surface Beta Irradiation. J. R. Raper, P. S. Henshaw, R. S. Snider. MDDC 580

Analytical Chemistry of the Manhattan Project. Chap. XXI—Carbon, Hydrogen and Oxygen. C. J. Rodden. MDDC 581

Histopathological Studies on Mice Following External Beta Ray Treatment. R. S. Snider. MDDC 583

Comparative Effectiveness and Additivity of Fission Neutrons, Gamma Rays, and Beta Rays on Drosophila Eggs. G. E. Stapleton, R. E. Zirkle. MDDC 584

Analytical Chemistry of Manhattan Proj. Chapter XXXI—Iron, Cobalt, and Nickel. R. W. Bane, W. R. Grimes. MDDC 596

Qualitative Description of the Arc Plasma in a Magnetic Field. D. Bohm. MDDC 597

The Quantitative Estimation of the Activity of Beta Particle Emitters. A. Broido, J. D. Teresi, P. Tompkins. MDDC 598

Disposal of Fluorine by Caustic Scrubbing. W. B. Burford, III. MDDC 599

Biological Bases for Maximum Permissible Exposures. S. T. Cantril. MDDC 601

Industrial Medical Program—Hanford Engineer Works. S. T. Cantril. MDDC 602

Preparation of Cerium by Electrolysis of Molten Salts. E. D. Eastman, B. J. Fontana, C. D. Thurmond, W. K. Wilmarth. MDDC 603

Capture Cross Section of Pb^{208} for C Neutrons. J. S. Levinger. MDDC 604

The Rate of Sublimation of Solids. G. E. MacWood. MDDC 605

Crystal Structure of Tetragonal Bismuth Arsenate. R. C. L. Mooney. MDDC 606

Identification and Crystal Structure of Barium Hydrogen Phosphate. R. C. L. Mooney. MDDC 607

Report on Determination of Densities of Several Uranium Compounds. H. F. Priest, G. L. Priest. MDDC 609

Report on Methods of Preparation of Inorganic Fluorides. H. F. Priest. MDDC 610

The Clinical Sequence of Physiological Effects of Ionizing Radiation in Animals. C. Ladd Prosser, *et al.* MDDC 611

The Use of the Ion Exchangers for the Determination of Physical Properties of Substances, Particularly Radiotracers, in Solution I. Theoretical. J. Schubert. MDDC 612

Chemistry of the Fission Products. N. Sugarman. MDDC 614

Short-Lived Ge and As Fission Activities. E. P. Steinberg, D. W. Engelkemeir. MDDC 614-A

Absence of Long-Lived Ge in Fission. L. Winsberg. MDDC 614-B

Absence of Long-Lived As in Fission. L. Winsberg. MDDC 614-C

Fission Yield of the 2.4h Br^{83} and Absence of Long-Lived Br. S. Katcoff, B. Finkle, N. Sugarman. MDDC 614-D

Absence of Long-lived Se in Fission. L. Winsberg. MDDC 614-E

Short-lived Kr and Xe Isotopes. Introduction. R. M. Adams. MDDC 614-F

Search for Gas Ancestry of Some Fission Products. E. L. Brady, N. Sugarman. MDDC 614-G

Half-Lives of Some Short-lived Krypton and Xenon Activities. C. Dillard, R. M. Adams, H. Finston, A. Turkevich. MDDC 614-H

Determination of Gas Half-lives by the Charged Wire Technique. R. Overstreet, L. Jacobson. MDDC 614-I

Determination of Gas Half-lives by the Charged Wire Technique. II. C. Dillard, R. M. Adams, H. Finston, A. Turkevich. MDDC 614-J

Discovery of 10-y Kr^{85} in Fission. E. J. Hoagland, N. Sugarman. MDDC 614-K

Quantitative Studies of the Neutron Activation of Kr. E. J. Hoagland, N. Sugarman. MDDC 614-L

Characteristics of 2.7-h $Sr^{(92)}$. Gotte. MDDC 614-M

Fission Yield and Radiation of the 3.5-h

Note: The Atomic Energy Commission has recently announced that, beginning with document number 1780, the notation will be changed from MDDC to AECD. AECD means Atomic Energy Commission Document. Future listings of these documents in NUCLEONICS, therefore, will be made under the title of "Atomic Energy Commission Documents."

$Y^{(92)}$. E. J. Hoagland, S. Katcoff. MDDC 614-N

The Characteristics and Decay Relationships of 9.7-h Sr^{91} and 51-m Y^{91}. B. Finkle, S. Katcoff, N. Sugarman. MDDC 614-O

Fission Yield of 20-m Y. C. R. Dillard, R. M. Adams, H. Finsten, A. Turkevich. MDDC 614-P

Energies of Radiation of 17-h $Zr^{(97)}$ and 75-m $Cb^{(97)}$. S. Katcoff, B. Finkle. MDDC 614-Q

The Discovery of Long-Lived Zr and Cb in U Fission. B. L. Goldschmidt, I. Perlman. MDDC 614-R

The Characteristics of the 65-d Zr by Chemical Study. E. L. Brady, D. W. Engelkemeir, E. P. Steinberg. MDDC 614-S

The Note on the β and γ Energies of 65-d Zr and 35-d Cb by Coincidence Counting. A. C. G. Mitchell, L. J. Brown. MDDC 614-T

The β-Ray Spectrum of 65-d Zr. V. A. Nedzel. MDDC 614-U

The Characteristics of 35-d Cb by Chemical Study. D. W. Engelkemeir, E. L. Brady, E. P. Steinberg. MDDC 614-V

A Note on the Spectrum of 35-d Cb by Coincidence Counting. D. W. Engelkemeir. MDDC 614-W

The β-Ray Spectrum of 35-d Cb. V. A. Nedzel. MDDC 614-X

The Mass Assignment of the Chain 65-d Zr → 35-d Cb. L. Jacobson, R. Overstreet. MDDC 614-Y

The Existence of an 80–85-h Cb in U Fission. D. W. Engelkemeir, E. L. Brady. MDDC 614-Z

The Characteristics of the 90-h Cb^{95} by Chemical Study. MDDC 614-AA

Preliminary Spectrometer Examination of 90-h Cb. J. S. Levinger. MDDC 614-BB

Absence of Long-Lived Rh in Fission. J. A. Seiler, L. Winsberg. MDDC 614-CC

Pd-Ag Chains in Fission. J. A. Seiler. MDDC 614-DD

Absence of Long-lived Pd Isotopes in Fission. J. A. Seiler. MDDC 614-EE

Study of The 43-d Cd^{115} in Fission. R. P. Metcalf. MDDC 614-FF

The Chain 2.33-d Cd^{115}–4.5-h In^{115}. R. P. Metcalf. MDDC 614-GG

The Chain 2.83-h Cd^{117}–1.95-h In^{117}. R. P. Metcalf. MDDC 614-HH

Sn Isotopes in Fission. J. A. Seiler. MDDC 614-II

The Toxicology of U-Compounds—Progress Report on Injection and Ingestion. A. Tannenbaum, H. Silverstone. MDDC 615

Methods of Analysis of Fission Products in the Experimental Biology Section. P. C. Tompkins, A. Broido, L. Wish. MDDC 616

General Electric Company's Part in Manhattan District Electromagnetic Process. T. R. Rhea. MDDC 624

Berkeley Isotope Chart. R. Segre. MDDC 626

Absorption and Scattering of Beta Particles and Application to Determination of Disintegration Rates of Radioactive Sources. N. E. Ballou. MDDC 630

A Comparison of the Sum of the Individual Fission Product Activities with the Gross Activity of Neutron Irradiated Uranium. N. E. Ballou. MDDC 631

Radiochemistry of the La, Ce, and Pr Fission Products. N. E. Ballou, W. H. Burgus, R. R. Edwards, H. Gest, R. Hein, A. Kant, A. S. Newton. MDDC 632

Survey of Ruthenium and Rhodium Isotopes formed in the Fission Process. N. E. Ballou. MDDC 633

MDDC 634. Abstract of MDDC 840.

Experimental Investigation of Threshold Pressure for Stable Operation of Arcs. E. H. Burhop, H. S. W. Massey, G. Page. MDDC 636

Attempted Preparation of a Volatile Uranium Carbonyl. G. Callingaert, *et. al.* MDDC 637

The Preparation of Fission Radioisotopes for Radiotoxicological Studies. W. E. Cohn. MDDC 638

Boron Absorption of Resonance Activation. S. M. Dancoff. MDDC 639

Properties of Br at Tracer Concentrations. R. R. Edwards, T. H. Davies. MDDC 640

Radiochemical Beta Radiation Measurements. N. Elliott, D. W. Engelkemeir, W. Rubinson, E. Shapiro. MDDC 641

Biologic Effects of Long-continued Whole Body Irradiation with Gamma Rays on Mice, Guinea Pigs, and Rabbits. A. B. Eschenbrenner. MDDC 642

The Geochemistry of Columbium and Tantalum. J. O. Harder, M. Fleischer. MDDC 644

Geochemistry of Germanium. M. Fleischer, J. O. Harder. MDDC 645

The Geochemistry of Indium. M. Fleischer, J. O. Harder. MDDC 646

Some Studies of the Reactions of Uranium Oxides with Hydrogen, Oxygen and Water, D. M. Gilles. MDDC 647

The Metabolism of Thorium, Protoactinium and Neptunium in the Rat. H. Lans, K. G. Scott, J. Growley, J. G. Hamilton. MDDC 648

Measurement of C^{14} Activity. W. B. Leslie, C. J. Borkowski. MDDC 649

Synthesis of Organic Compounds from $C^{14}O_2$. W. B. Leslie, L. B. Spector. MDDC 650

Capture of Fast Neutrons by Pb^{208}. J. S. Levinger. MDDC 651

The n-Gamma Reaction for Fast Neutrons for Pb^{208}, Bi, and Al. J. S. Levinger. MDDC 652

Biologic Effects of Long-continued Whole Body Irradiation With Gamma Rays on Mice, Guinea Pigs and Rabbits, Part I. Egon Lorenz, Walter E. Heston. MDDC 653. *Part II.* MDDC 654. *Part III.* MDDC 655

Biologic Effects of Long-continued Whole Body Irradiation With Gamma Rays on Mice, Guinea Pigs, and Rabbits. Part VI. Conclusions and Applicability of Results to the Problems of Human Protection. E. Lorenz. MDDC 656

Thermodynamic Properties of Uranium Compounds. George E. MacWood. MDDC 657

Electrolytic Reduction of Uranl Ion. A. R. Nichols, Jr. MDDC 658

Discharge Cathodes. W. E. Parkins. MDDC 660

Techniques of External Irradiation with Beta Rays. J. R. Raper, R. E. Zirkle, K. K. Barnes. MDDC 661

Infrared Spectrum of Benzene. J. Flanagan, R. Gardner, F. McKee, R. Schlegel. MDDC 663

The Lightest Elements Formed in Fission (Zn, Ga, Ge, As), E. P. Steinberg, D. W. Engelkemeir, L. E. Glendenin, J. M. Siegel. MDDC 664

Accumulation of Uranium in the Tissues of Mice Ingesting Uranyl Nitrate. A. Tannebaum, H. Silverstone. MDDC 665

Uptake of Plutonium, Yttrium, and Strontium by the Callus of Healing Bone Fractures. L. Van Middlesworth, D. H. Copp, J. G. Hamilton. MDDC 666

Samarium and Europium Isotopes Formed in Fission. L. Winsberg. MDDC 667

The Crystal Structure of $Ba_3(PO_4)_2$ and $Sr_3(PO_4)_2$. W. H. Zachariasen. MDDC 668

Metabolism and Distribution of Inhaled Plutonium in Rats. R. Abrams, *et al.* MDDC 677

Variation in Yield Among Members of Fission Chains. R. M. Adams, *et al.* MDDC 678

The Use of the Szilard-Chalmers Reaction to Prepare Radio-isotopes in High Specific Activity. A. W. Adamson, *et al.* MDDC 679

The Chemical and Radiochemical Identification of Isotopes of Nd and Element-61 Formed in Fission. N. E. Ballou, L. E. Glendenin, J. A. Marinsky, J. Sellar, L. Einsberg. MDDC 680

Theoretical Consideration Regarding Minimum Pressure for Stable Arc Operation. D. Bohm. MDDC 681

Laboratory Techniques in High-level Radiochemistry. E. L. Brady *et al.* MDDC 682

Long-lived Zirconium and Columbium Isotopes in Fission. E. L. Brady *et al.* MDDC 683

Quarterly Report, August to October, 1946 *Biology Division.* A. M. Brues. MDDC 684

Colorimetric Measurements of Gross Fission Product Decay Energy. C. V. Cannon, R. A. Day. MDDC 685

The Requirements of an Adequate Health Service in Relation to Atomic Research and Industrial Development. S. T. Cantril, J. J. Nickson, J. E. Wirth, R. S. Stone. MDDC 686

Chemical Effects Following Nuclear Transformations. T. H. Davies. MDDC 687

Spectroscopic and Photochemical Properties of Uranium Compounds with Particular Reference to Isotopic Separation. G. H. Dieke, A. B. F. Duncan. MDDC 688

Chemical Effects Accompanying the Decay of Radioactive Selenium to Bromine. T. H. Davies, R. R. Edwards, H. Gest. MDDC 689

A Method for the Determination of Certain Metals Present in Minor Concentration in Various Substances. N. Howell Furman, C. E. Bricker. MDDC 691

The Chemical Effects of Nuclear Transformation. I. β-Decay of Lanthanum to Cerium. II. β-Decay of Selenium to Bromine. H. Gest, *et al.* MDDC 692

Quantitative Chemical Isolation of Fission Product Radioactivities. D. N. Hume. MDDC 694

Control Chart Method Applied to Errors in Radioactive Counting. W. G. Schlecht. MDDC 695

The Effects of Fast Neutrons on the Ability of Mice to take Forced Exercise. G. E. Stapleton, H. J. Curtis. MDDC 696

Failure to Affect Toxicity of Ingested Uranium Chloride by Dietary Acid (HCl) or Base ($NaHCO_3$). A. Tannenbaum, H. Silverstone. MDDC 697

Relationship of Uranium Excretion to the Total Amount of Uranium in the Mouse. A. Tannenbaum, H. Silverstone. MDDC 698

Methods for the Quantification of Radium. P. C. Tompkins, W. P. Norris, L. Wish, R. D. Finkle. MDDC 699

Radiation-induced Changes in Ultraviolet Absorption on Spectra of Urine; I. Central Effects. L. Wattenberg, S. Schwartz. MDDC 700

Radiation-induced Changes in Ultraviolet

Absorption Spectra of Urine: II. Quantitative Spectrophotometric Studies. L. Wattenberg. MDDC 701

Boundary Conditions at Interface between Medium and Vacuum; The Extrapolation Distance. A. M. Weinberg. MDDC 702

Standardization of the pD Scale. R. B. Fischer, R. A. Potter. MDDC 715

Metabolism of Plutonium. W. Langham, *et al.* MDDC 719

Assembly of Thin Wall Geiger Counter. Argonne National Laboratory. MDDC 746

Neutron Temperature Measurement in Graphite and in Uranium-Graphite Reactor. G. M. Branch. MDDC 747

Slowing Down of Neutrons. G. Breit. MDDC 748

The +5 Oxidation State of Plutonium. R. E. Connick, M. Kasha, W. H. McVey, G. E. Sheline. MDDC 749

The Transmission of Radiostrontium and Plutonium from Mother to Offspring in Laboratory Animals. M. P. Finkle. MDDC 750

Analytical Chemistry of the Manhattan Project. Chapter VII—Photometric Methods. M. Fred, C. J. Rodden. MDDC 751

Analytical Chemistry of the Manhattan Project. Chapter IX—Spectrochemical Methods. M. Fred, B. F. Scribner. MDDC 752

An Investigation of the β Ray Spectrum of 93^{239}. H. W. Fulbright. MDDC 753

Effects of Periodic Doses of Slow Neutrons on Mice. P. S. Hensaw, *et al.* MDDC 754

Analytical Chemistry of the Manhattan Project. Chapter XXIX—Zinc, Cadmium and Mercury. K. J. Jensen. MDDC 755

Drawings on an Electrolysis Assembly. Robert Loevinger. MDDC 756

Tissue Metabolism of Rats Treated with Uranyl Nitrate. J. Meyer, *et al.* MDDC 757

High-Temperature Heat Contents of Uranium, Uranium Dioxide, and Uranium Trioxide. G. E. Moore, K. K. Kelley. MDDC 758

Effects of Uranium on the Metabolism of Yeast and Bacteria. J. A. Munts, *et al.* MDDC 759

The Transport of Uranium to the Tissues. Some Properties of Uranium in Solutions and in Combinations with Proteins. J. A. Munts, E. S. G. Barron. MDDC 760

Physiological Observations on Rabbits Exposed to Single Doses of X-Rays. E. E. Painter, C. L. Prosser, M. C. Moore. MDDC 761

An Introduction to Nuclear Chemistry Lecture Series. G. T. Seaborg. MDDC 763

Photo-Neutron Produced in D_2O and Beryllium by Fission Product Gamma Rays. W. D. B. Spatz, D. J. Hughes, A. Cahn. MDDC 764

Experiments to Test the Validity of the Linear R-Dose/Mutation Frequency Reaction in Drosophila at Low Dosage. W. P. Spencer. MDDC 765

Counting Rate Meter Based on a Design by M.I.T. R. L. Sternberg. MDDC 766

Nuclear Energy for Power Production. W. F. Davidson. MDDC 767

The Equation of State of Air. K. Fuchs, R. E. Peierls. MDDC 772

The Model 200 Pulse Counter. W. A. Higinbotham, J. Gallagher, M. Sands. MDDC 773

Purification of Uranium Oxide. J. I. Hoffman. MDDC 777

Velocity Analyzer. W. C. Meecham. MDDC 781

Health-Physics, Instrumentation, and Radiation Protection. H. M. Parker. MDDC 783

Atomic Power Engineering. F. C. Von der Lage. MDDC 792

Production and Analysis of Radioactive Aerosols. E. Abrams. MDDC 795

Abstract of Material for Possible Presentation to Radiotracer Conference at the University of Chicago. MDDC 796. D. S. Anthony.

The Average Gamma Energy Emitted per Beta Particle for Several Radioactive Isotopes. E. C. Barker. MDDC 798

MDDC 799. Abstract of MDDC 839.

The Beta-Gamma Hand and Foot Counters. W. H. Bradley. MDDC 800

Test Results on Bias Setting for the Chicago Scaler Offner Models. W. Bradley, B. Epstein, E. Wakefield. MDDC 801

A Threefold Coincidence System Based Upon a 10^{-6} *Second Resolution Time.* W. H. Bradley, B. Epstein. MDDC 802

The Electronic Pressure Transmitter and Self-Balancing Relay. S. Cromer. MDDC 803

Diffraction of Neutrons by Hydrogen and Deuterium Containing Crystals. W. L. Davidson, G. A. Morton, C. G. Shull, W. O. Wollan. MDDC 804

Manufacturing Specifications for the Portable G-M Tube Survey Meter. J. Dorsey. MDDC 805

The Shielding of Nuclear Reactions. M. L. Goldberger. MDDC 806

Resonance Scattering of Neutrons by Mn^{55}. S. P. Harris, F. G. P. Seidl, A. S. Langsdorf, Jr. MDDC 807

Physical Properties of Uranyl Sulfate Solutions. L. Helmholz, G. Friedlander. MDDC 808

MDDC 809. Abstract of MDDC 849.

A Linear Amplifier for General Laboratory Use. W. H. Jordon, P. R. Bell. MDDC 810

New Developments in Instruments for Counting and Detecting Nuclear Particles. W. H. Jordon. MDDC 811

Ranges in Air of Plutonium Fission Fragments as a Function of Their Mass. S. Katcoff, J. A. Miskel. MDDC 812

The Rate of Exchange of U (IV) and U (VI). E. L. King. MDDC 813

Oxidation-Reduction Potentials of Plutonium Couples as a Function of pH. K. A. Kraus. MDDC 814

Drawings. (Circuit diagrams and panel and chassis layouts of miscellaneous electronic equipment.) Los Alamos Laboratory. MDDC 815

Spectrophotometric Determination of Submicrogram Amount of Boron. C. F. Metz. MDDC 816

Test Results on Clinton Alpha Amplifier Used with an Offner Columbia Scaler. H. E. Osdahl. MDDC 817

Polymerized Trifluorochlorethylene. Plax Corporation. MDDC 818

High Energy Photo-Disintegration of the Deuteron. M. E. Rose, G. Goertzel. MDDC 820

A Report on the Columbia Scaling Circuit. B. Schloss, S. Robinson. MDDC 821

MDDC 822. Abstract of MDDC 869.

Criticality Studies of the Enriched Uranium-Heavy Water Chain Reacting System. A. H. Snell, *et al.* MDDC 823

Response of Hematopoietic Systems to X-Rays. G. M. Suter. MDDC 824

Studies on Acquired Tolerance to Uranium. A. Tannenbaum, H. Silverstone. MDDC 825

Power Supply. E. W. Titterton. MDDC 826

Pulse Unit Model I. E. W. Titterton. MDDC 827

300 *Mc Transmitter Pulser (Mock-Up).* E. W. Titterton. MDDC 828

Video Amplifier and Scope. E. W. Titterton. MDDC 829

Emissivity and Temperature Scale for Vacuum Heated Uranium. H. B. Wahlin. MDDC 830

Manufacturing Specifications for Higinbotham Scaler. E. Wakefield. MDDC 831

A Preliminary Report on the Higinbotham Scaler. E. Wakefield, S. E. Cooper. MDDC 832

Specifications for the Types 961-*A Scaler.* E. Wakefield. MDDC 833

The Technical Associates Scaler. E. Wakefield. MDDC 834

The Chemical Consequences of Nuclear Changes in Tellurium. R. R. Williams. MDDC 835

The Average Gamma Energy Emitted per Beta Particle for Several Radioactive Isotopes. E. C. Barker. MDDC 838

Radioactive Isotope Tracer Techniques. G. E. Boyd. MDDC 840

Meteorological Equipment of the Hanford Engineer Works. P. E. Church, C. A. Gosline, Jr. MDDC 841

The Slowing Down of Neutrons by Air. D. H. Frisch. MDDC 846

Determination of Andoic Current Efficiency in the Counter Flow Electrolysis of Uranyl Chloride Solutions. W. J. Hamer. MDDC 847

Protection of Laboratory Personnel Handling Radioactive Materials. L. H. Hempelmann. MDDC 848

The Specific Activity of Radium. Truman P. Kohman, Donald P. Ames, Jacob Sedlet. MDDC 852

Dynamics of a Mass of Hot Gas Rising in Air. G. I. Taylor. MDDC 919

The Uptake by Plants of Plutonium and Some Products of Nuclear Fission Adsorbed on Soil Colloids. Louis Jacobson, Roy Overstreet. MDDC 1006

Cosmic-Ray Induced Fission. Darol K. Froman, Bruno B. Rossi, Louis Rosen. MDDC 1034

Portable Probe Types Ionization Meter, Mark II, Model 10. G. R. Carlson. MDDC 1057

Los Alamos Fast Reactor. David B. Hall, Jane Hall. MDDC 1080

Cobalt-62 Radioactivity. Thomas J. Parmley, Burton J. Moyer. MDDC 1190

The Natural Abundance of Isotopes of Stable Elements. J. R. White, A. E. Cameron. MDDC 1195

Ion Exchange as a Separation Method. III. Equilibrium Studies of the Reactions of Rare Earth Complexes with Synthetic Ion Exchange Resins. Edward R. Tompkins, Stanley W. Mayer. MDDC 1225

The Half-life of Tritium. M. Goldblatt, E. S. Robinson, R. W. Spence. MDDC 1229

Half-life of Tritium. Aaron Novick. MDDC 1236

Inelastic Scattering of Fast Neutrons. S. Bernstein, B. T. Feld, L. Szilard. MDDC 1292

Note on Zero-Zero Transitions. Marvin L. Goldberger. MDDC 1298

The Effects of Irradiation from the Atomic

Bomb on the Japanese. Joe W. Howland, Stafford L. Warren. MDDC 1301

A Method of Assay for C^{14}. C. D. Janney, B. J. Meyer. MDDC 1303

Colorimetric Determination of Uranium with 1-Ascorbic Acid. C. D. Rothenberger, E. F. Orlemann, W. R. Grimes, C. E. Larson. MDDC 1314

Methods of Driving a High Q-Cavity with Many Self-excited Oscillators. J. R. Woodyard, E. A. Marinelli, W. Toulis, W. K. H. Panofshy. MDDC 1323

Low-energy Yield of $D(D,p)H^3$ and the Angular Distribution of the Emitted Protons. E. Bretscher, A. P. French, F. G. P. Seidl. MDDC 1348

Alpha-Particle and Deuteron Tracks in Eastman NTA Photographic Plates. Robert L. Brock, Eugene Gardner. MDDC 1350

Further Evidence for a γ-p Process in Be^9. Richard L. Conklin, William E. Ogle. MDDC 1398

Some New β-Diketones Containing the Trifluoromethyl Group, Part I. Keto-Enol Relationships in β-Diketones containing the Trifluoromethyl Group, Part II. J. C. Reid, M. Calvin. MDDC 1405

Effect of X-Ray on Mortality, Weight, Length, and Counts of Erythrocytes and Hematopoietic Cells in Fingerling Chinook Salmon Oncorhynchus Tschawytscha Walbaum. Kelshaw Bonham, *et al.* MDDC 1416

Neutron Absorption in Samarium. A. J. Dempster. MDDC 1419

"Shielded Contact" Grounding Key for Electrometers. G. Failla. MDDC 1420

Medical and Biological Research Activities of the Los Alamos Laboratory. Wright Langham. MDDC 1439

Photoelectrons for Space-Charge Neutralization. S. C. Curran. MDDC 1476

Energy Distribution of Protons from a Target Bombarded by 190 Mev Deuterons. Warren W. Chupp, Eugene Gardner, T. B. Taylor. MDDC 1483

Inelastic Scattering of Fe, Pb, and Bi. L. Szilard, S. Bernstein, B. Feld, J. Ashkin. MDDC 1536

The Thermodynamic Properties and Equilibria at High Temperatures of Uranium, Halides, Oxides, Nitrides, and Carbides. L. Brewer, L. Bromley, P. Gilles, N. Lofgren. MDDC 1543

Inelastic Scattering of Neutrons. K. L. Greisen. MDDC 1545

X-Ray Structural Studies of the Tetrachlorides of Uranium and Thorium. Rose C. L. Mooney. MDDC 1559

Electromagnetic Deflector for the Beam of the 184-inch Cyclotron. W. M. Powell, I. R. Henrich, Q. A. Kerns, D. C. Sewell, R. L. Thornton. MDDC 1560

Some Procedures for the Preparation of Highly Purified Adenosine Triphophate. Aser Rothstein. MDDC 1561

The Mechanism of Action of Uranium on Carbohydrate Metabolism of Yeast. Aser Rothestein. MDDC 1562

The Determination of Small Amounts of Nitrate in U_3O_8 and other Uranium Oxides. E. Staple, E. Marshall, W. Simon. MDDC 1564

The Determination of the Composition of Fluorine-Nitrogen Mixtures by the Thermal Conductivity Method and the Construction of a Field Apparatus for Such Analyses. E. Staple, E. R. Grilly. MDDC 1565

Short-lived Halogen Fission Products. Nathan Sugarman. MDDC 1566

A New Radioactive Series—The Protactinium Series. Martin H. Studier, Earl K. Hyde. MDDC 1567

Effect of Energy on the Mass-Yield of Thorium. A. Turkevich. MDDC 1568

A New Colormetric Method for Determining Traces of Beryllium. A. L. Underwood. MDDC 1569

Relation of Adrenal Cortical Hormone to Lymphoid Tissue and Lymphocytes. W. N. Valentine, C. G. Craddock, Jr., J. S. Lawrence. MDDC 1570

Relative Effectiveness of Different Intensities of Gamma Radiation in Retarding Mitosis in the Grasshopper Neuroblast. J. Carlson, M. Snyder, A. Hollaender. MDDC 1576

Proton Angular Distribution for 90-Mev Neutron-Proton Scattering. James Hadley, Cecil E. Leigh, Herbert F. York. MDDC 1580

Disintegration of Be^8. Arthur Hemmendinger. MDDC 1582

Uranium Hydride. Part I—Preparation, Composition, and Physical Properties. F. H. Spedding, *et al.* MDDC 1585

Excretion of Radium From the Mouse. J. Weikel, E. Lorenz. MDDC 1587

The Intermediate Uranium Fluoride Compounds (α-UF_5, U_2F_9, and U_4F_{17}). P. Agron, A. Grenall, R. Kunin, S. Weller. MDDC 1588

Programs in Toxicity and Metabolism of Commonly Used Isotopes. A. M. Brues. MDDC 1601

Electric Time-Switch for Closing Circuits at Accurately Regular Intervals. J. A. Crawford, A. H. Jaffey. MDDC 1602

The Preparation of Thin U_3O_8 Films. M. Kahn. MDDC 1605

Metabolism of Phosphorus in Paramecium Aurelia. E. L. Powers, Jr. MDDC 1606

An Investigation of the Delayed Neutron Decay Curves Resulting from Uranium and Plutonium Fission. C. Redman, D. Saxon. MDDC 1607

The Structure of the Carbides, Nitrides and Oxides of Uranium. R. Rundle, N. Baenziger, A. Wilson, R. McDonald. MDDC 1608

The Transuranium Elements. G. T. Seaborg, E. Segre. MDDC 1609

The Bromine Displacement Method for the Determination of Fluorine in Gas Mixtures. E. Staple, J. G. Schaffner, E. Wiggin. MDDC 1610

Firing Unit for X-Ray Generator (Circuit Drawings). E. W. Titterton. MDDC 1611

A General Basis for the Resonance Formula. E. P. Wigner, L. Eisenbud. MDDC 1612

Negative 4 KV and Positive 6 KV High Voltage Power Supply. W. A. Hane. MDDC 1613

Radiation Meter Model "B." R. Watts. MDDC 1614

Technique for Irradiating Microorganisms with Artificially Radioactive Materials. Part II—External Radiation Sources. E. Anderson, G. Stapleton, A. Newton. MDDC 1615

A Modified Method for the Determination of Chromium in Uranium or Its Compounds. C. E. Bricker, N. H. Furman. MDDC 1616

The Solubility of Sodium Uranyl Carbonate in Water and in Solutions of Various Salts. W. E. Bunce, N. H. Furman. MDDC 1617

The Determination of Water in Uranyl Nitrate and in Ethereal Solutions of Uranyl Nitrate. J. A. DiPace, N. H. Furman. MDDC 1618

The Use of Cupferron in Inorganic Analysis with Special Reference to the Determination of Uranium. I.—Introduction. The Properties of Various Cupferrates. N. H. Furman, W. B. Mason. MDDC 1619

The Use of Cupferron in Inorganic Analysis with Special Reference to the Determination of Uranium. II.—The Factors that Control the Extraction of Various Elements from Aqueous Solution by Cupferron Plus an Organic Solvent. N. H. Furman, W. B. Mason. MDDC 1620

The Use of Cupferron in Inorganic Analysis with Special Reference to the Determination of Uranium. III.—The Isolation of Uranium as the Quadrivalent Cupferrate. N. H. Furman. W. B. Mason, J. S. Pekola. MDDC 1621

The Interference of Nickel in the Reduction of Uranium Solutions in the Jones Reductor. N. H. Furman, J. B. Heberling. MDDC 1622

Uranyl Cupferrates. The Extraction of Traces of Uranium Cupferrate by Ether from Concentrated Uranyl Solutions. The Preparation of $UO_2(O(NO)NC_6H_5)_2NH_4O(NO)NC_6H_5$. N. H. Furman, D. R. Norton. MDDC 1623

A Critical Study of the Turneric Procedure for the Determination of Small Quantities of Boron. R. J. Mundy, N. H. Furman. MDDC 1624

Electronic Classifying, Cataloging, and Counting Devices. J. H. Parsons. MDDC 1625

Thermal Neutron Absorption Cross Sections of Separated Isotopes. H. S. Pomerance, J. I. Hoover. MDDC 1626

Considerations on the Existence of Element-61 in Nature. N. E. Ballou. MDDC 1627

Heat Transfer in Film Boiling from Horizontal Tube. L. Bromley. MDDC 1628

Mixed Oxide-Sulfides of Cerium and Thorium. E. D. Eastman, *et al.* MDDC 1629

Determination of the Melting Points of Plutonium Chloride and Plutonium Bromide. T. O. Jones. MDDC 1630

Note on the Preparation of Plutonium (III) Oxalate. R. L. Patton. MDDC 1631

Mission Yields in Uranium 233. E. P. Steinberg, J. A. Seiler, A. Goldstein, A. Dudley. MDDC 1632

Technique for Observing Nuclear Disintegrations and Scattering in Small Gas Volumes. R. F. Taschek. MDDC 1663

Variable Energy Neutrons from Accelerated Particles. A. O. Hanson, R. F. Taschek. MDDC 1634

Chemistry of Element-93. VI. First Preparation and Solubilities of Some Neptunium Compounds in Aqueous Solutions. T. J. LaChappelle, L. B. Magnusson, J. C. Hindman. MDDC 1635

The Acute Toxicity of Some Zirconium and Thorium Salts in Rats. L. T. McClinton, J. Shubert. MDDC 1636

The Preparation of Perfluorocarbons. L. Spiegler. MDDC 1637

Unsteady-State Separation Performance of Cascades. A. M. Squires, *et al.* MDDC 1638

Construction of a Hand-Contamination Counter and Radiation Monitor. R. J. Watts. MDDC 1639

Preparation of Plutonium Nitride. B. M. Abraham, N. R. Davidson. MDDC 1640

An Ion "Velocitron." A. E. Cameron, D. F. Eggers, Jr. MDDC 1641

Electromagnetic Separation of Bromine and Chlorine Isotopes. L. G. Chelius, C. P. Keim. MDDC 1642

The Origin, Detection, Identification, and Removal of Radioactive Contaminants in Tracers. W. E. Cohn. MDDC 1643

Exchange of Uranium between UF_4 *and* UF_6. A. V. Grosse. MDDC 1644

Radioautography in Biological Research

This survey of the biological fields in which radioautography has proved useful illustrates the extensive range of applications the technique has for precise determination of the spatial distribution of radioactivity in both plant and animal tissues

By AUBREY GORBMAN

Department of Zoölogy, Barnard College
Columbia University, New York

RADIOAUTOGRAPHY is a system for detecting and recording radiant energy within tissues or other materials through its effect upon photographic plates. It is, therefore, the instrument of choice in determining the precise topographic or spatial distribution of radioactive substances.

In a sense, radioautography may be considered the morphologic aspect of radioisotope study, just as Geiger or electroscopic measurements might, analogously, be considered physiological or functional. Since the radioautograph provides the means for correlating anatomical structure with functional properties, it is a tool that is finding application especially in the hands of biologists. Although exploitation of this new technique has hardly begun, it is now obvious that radioautography can be of greatest value in studying many difficult biological problems.

This review has been designed to provide a survey of the biological fields in which radioautography has proved useful. It is hoped that such a presentation may indicate the areas of research in biology in which the graphic studies of radioisotopes may be employed most rewardingly.

One of the most attractive features of the radioautographic techniques, in the eyes of many biologists, is their simplicity. The preparation of a radioautograph requires no equipment which is not usually found in a biological laboratory other than the radioactive material itself. The technical and procedural data of radioautography were reviewed in this journal by Titus C. Evans (*13*) and will not be dealt with in this survey.

Limits of Usefulness

Their nonquantitative or semiquantitative character frequently has been mentioned as a disadvantage of the radioautographic techniques. It should be pointed out, however, that, within the dimensions in which the radiographic method is most useful, the instruments of more exact measurement, the Geiger counter and electroscope, offer no solution. For example, radioactive phosphorus is selectively accumulated by certain randomly occurring lymphoid structures in the wall of the intestine. Geiger counts of whole intestinal segments, since they are made from masses of tissue containing a greatly predominating proportion of structures not participating in the function in question, offer a poor measure of radiophosphorus concentration in each punctate area of accumulation. By microdensitometric measurements of radioautographs, Axelrod and Hamilton (*2*) recently have provided a method of quantitation

which should prove of great value in this respect.

The radiographic and counting methods have at times been compared, with varying conclusions, as to their relative sensitivities. Since the areas of greatest usefulness of the methods do not very often overlap, this comparison probably is not of great moment. Hamilton has estimated that a total density of 2,000,000 to 10,000,000 disintegrations per square centimeter are required for sufficient blackening of a photographic emulsion to yield a satisfactory radioautograph. From a practical standpoint, then, the counting methods are clearly the more sensitive. On the other hand, by extending exposure of the film over a period of nine to ten months, enough radiation has been accumulated to produce a satisfactory radioautograph under conditions in which Geiger counting might have given equivocal results (*7*).

A very pertinent feature in considering the limits of usefulness of radioautography is its ultimate resolving power, or ability to discriminate between adjacent sources of radiation. Certainly some of the most valuable contributions of the radioautographic technique may be expected eventually in studies of microdistribution of chemicals within the cell. With the best application of beta and gamma-ray-emitting isotopes in the autographic technique, however, different workers report limits of resolution of twenty to forty micra. This places the present usefulness of the technique within the histological, and outside of the cytological, range. Individual alpha particles, in traversing a photographic emulsion, create a definite straight line. This line can be traced backward to the exact point of emission, providing the ultimate in resolving power in a radioautograph. Several investigators have reported such use of alpha emission from histological sections, and one from micro-organisms (*8*, *11*, *14*), but none have as yet reported observations of intracellular localization, though such observations would seem to be feasible. Unfortunately, none of the alpha-particle emitters are elements ordinarily encountered in living systems. Isotopes of some of the physiologically important elements such as carbon-14, phosphorus-32, sulfur-35, chlorine-36, and calcium-45 are pure beta-particle emitters, having no gamma radiation. It is hoped that by forming radioautographs of such beta emission in a strong magnetic field the direction of the charged beta particles can be influenced sufficiently to afford considerable improvement in resolution (*38*).

Botanical Applications

Botanists were among the first to adopt the radioautographic technique when cyclotron-produced radioisotopes became available. Arnon, Stout, and Sipos (*1*) studied the distribution of radiophosphorus, P^{32}, given as phosphate in a nutrient solution fed through the roots of tomato plants. They were able to lend support to the view that phosphate moves upward with the transpiration stream, and that the initial regions of accumulation of phosphate were the regions of greatest transpiration. Radioautographs of tomato fruits in various stages of maturity showed a marked difference in phosphate localization between green and ripe fruit. Green tomatoes exhibited an avidity for phosphate, and an intense localization in the pulp and especially the seeds. In ripe tomatoes very small amounts of P^{32} appeared, and were restricted to the pulp. The investigators interpreted this as meaning that mineral metabolism in the seed is halted at some point in the development of the fruit. The seed of ripe fruit had already embarked upon a resting state in their experiment, at

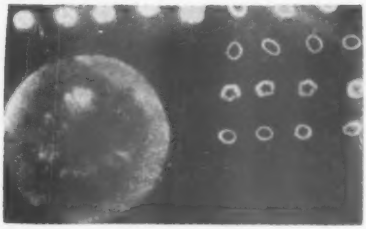

FIG. 1. Radioautograph of a section of squash fruit and of sections of petiole and stem from a squash plant given radiophosphate. Concentrations are visible on the surface and in seeds of the fruit and in phloem and interfascicular cambium of the stem. Colwell (8)

least insofar as phosphorus metabolism was concerned.

Colwell (7) followed the rate and routes of distribution of P^{32} applied to the leaves of squash plants as an aqueous solution of Na_2HPO_4. He found that the normal channel of distribution of phosphate from the leaf to the plant was through the tubules in the phloem (Fig. 1). Autographs of cross sections of the stem showed this. Treating the leaf petiole with boiling water appeared to plug the phloem tubes by coagulation. Under this circumstance radioactive material applied to the leaf did not reach the stem but was restricted to spreading instead through all parts of the treated leaf (Fig. 2). By altering the conditions under which the radiophosphate was administered (dehydrating the plant as a whole, increasing the area of application), Colwell could induce flow of the mineral through the xylem tubes of scalded petioles. This was demonstrated in radioautographs.

Colwell observed other peculiarities of distribution of radiophosphate in the squash plant. In the fruit P^{32} concentrated in the seeds and on the surface. In autographs of seeds the embryo was quite distinct as a region of P^{32} accumulation. Another zone of accumulation was the interfascicular cambium in the stem. Colwell considers that P^{32} accumulation in the embryo and cambium is evidence of the higher rate of mineral metabolism there.

Harrison, Thomas, and Hill (27) have made a radioautographic study of the distribution of radioactive sulfur in wheat kernels after giving the isotope to growing plants as gaseous SO_2 or as sulfate through the roots. Kernels were examined when they first formed, two to five weeks after treatment. S^{35} was in much greater concentration in the kernels than elsewhere in the plant. Within kernels, the heaviest localization was in the embryo, the aleurone layer, and the cells just beneath it. A smaller amount of S^{35} appeared in the inner part of the endosperm, but the pericarp was almost free of it. This distribution coincided with the known distribution of protein in the kernel, and other evidence indicated that the S^{35} was most likely present in combination with protein in the seed.

Isotope Studies in Invertebrates

It seems remarkable that only a few studies have appeared in the literature dealing with isotope distribution in an invertebrate. Such investigations would seem to offer great promise in metabolic studies, and in identification of the character of organs whose function is unknown or subject to controversial interpretation.

The distribution of P^{32}-labeled phosphate has been followed in four insects (wax moth, mealworm, cockroach, and firebrat) by Lindsay and Craig (34). The insects were fed the radiophosphate and sectioned by the freezing method (sections subject only to aqueous extraction) or the paraffin method (subject to aqueous, alcoholic and fat solvent extraction). Autographs prepared from the two kinds of sections yielded essentially similar results, indicating that very little P^{32} was in phospholipid

combination; most of that detectable was in phosphoprotein combination, even in the fat bodies. In all four insect species the epithelium of the midintestine was an active site of P^{32} accumulation, suggesting to Lindsay and Craig that it might be a region of phosphorylation, possibly for the mobilization of fat. Newly formed tissues like the wing bud, the gonad, and the gonoducts also stored much P^{32} as phosphoprotein. This suggested a comparison with neoplastic tissues which behave in a similar fashion.

The deposition of I^{131} in larval and adult Drosophila fed with radio-iodide has been demonstrated autographically (*45*). By far the greatest accumulation in this insect was in the chitinous exoskeleton. Solubility behavior appeared to indicate that the radio-iodine was coupled with a scleroprotein, and was not incorporated in the carbohydrate of the chitin itself.

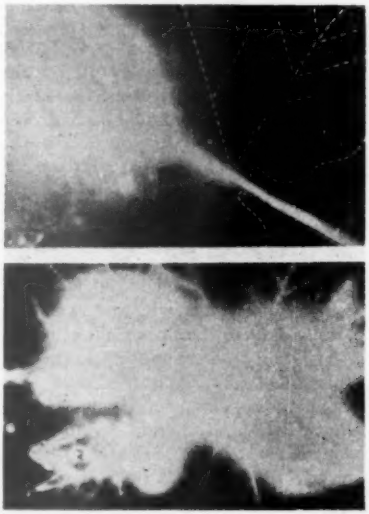

FIG. 2. Radioautographs of leaves upon the surface of which radiophosphate solution was placed. In normal leaf in upper figure, collection of absorbed phosphate and flow into petiole is evident. Petiole tubules of lower leaf were plugged by heat, causing phosphate to spread throughout leaf. Colwell (*8*)

Radioautographic Studies of Thyroid

The early availability of radioactive I^{131} of high specific activity from deuteron bombardment of tellurium has made possible a considerable volume of research in thyroid problems. The thyroid in vertebrates is essentially unique in its ability to accumulate very high concentrations of iodine, converting it into the globulin-coupled hormone thyroxine.

Comparative anatomy and physiology of the thyroid. In invertebrates there is no organ morphologically comparable to the vertebrate thyroid gland. However, in the protochordates, which are the invertebrates most closely allied to the vertebrates, the endostyle, a ciliated groove in the ventral pharynx, has long been considered homologous to the thyroid. Gorbman (*17*) found no evidence of radioiodide accumulation in radioautographs of the endostyle of three protochordate species, *Amphioxus*, *Styela montereyensis*, and *Perophora annectens*. In *Perophora*, however, a species which has finger-like stolons anchoring it to its rock substratum, a tissue within the stolon, the stolonic septum was found to store I^{131}. This tissue is an embryologic derivative of the endostyle, and so is probably more acceptable as a homologue of the thyroid than the endostyle itself.

Embryology of the thyroid. Autographic studies have been made of three species, the lamprey, frog, and rat, to determine at what stage of embryonic development their thyroids first have the ability to store, in protein-bound form, I^{131} which is given as iodide. In the fresh-water lamprey *Entosphenus lamottenii*, which spends five years as a larva. I^{131} accumulation is demonstrable during the first year of life (*19*). At this time iodine metabolism appears

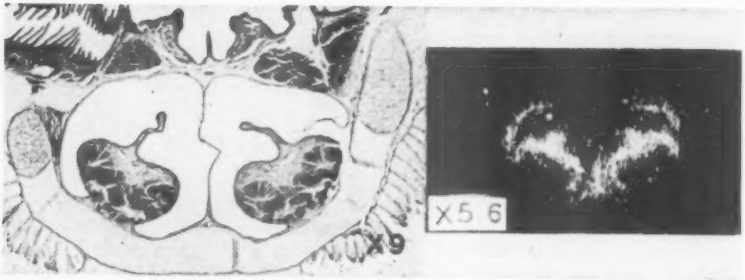

FIG. 3. Photomicrograph of endostyle of lamprey larva which had been placed in radioactive iodide-containing water for 24 hours. Right figure is a radioautograph prepared from this section (note difference in magnification). The accumulation of iodide is restricted to a single layer of epithelial cells in the endostyle. Gorbman and Creaser (*19*)

limited in radioautographs to the single layer of cells lining a pouch, known as the endostyle, which is derived from the ventral pharynx (Fig. 3). Iodine metabolism here can be said to occur in the morphologic precursor, or anlage, of the thyroid, even before it has undergone its definitive differentiation into follicles.

Similar tests made in the frog embryo (*20*) showed that in this form, too, thyroid function begins early in development, in the tailbud stage, when follicle formation was just beginning in the thyroid rudiment (Fig. 4). In the fetal rat this test was made by injection of radioactive iodide into the mother (*21*). Autography of fetal thyroids showed that iodine accumulation was delayed until the eighteenth day of gestation (Fig. 5). This was correlated with the first formation of glandular follicles. Since the total length of pregnancy in the rat is 21 days, this means that thyroid function does not begin until 90% of gestation is completed. It would be interesting to learn what factors initiate such early thyroidal function in the free-living larvae of the lamprey and frog or delay it so long in uterine embryos of the rat.

Radioautographic work has shed some light on another problem of thyroidal embryology. The thyroid of virtually all vertebrates studied has been found to form by the fusion of both median and lateral pharyngeal rudiments. It has been maintained by some embryologists, though not without controvery, that lateral rudiments degenerate without contributing appreciably to the adult gland.

Recently it was reported (*18*) that in a mouse a duct was found leading from the lateral pharynx into one lobe of the thyroid. Within the thyroid, tissue derived from this duct was seen to assume the form of typical thyroidal follicles. Radioautographs showed that follicles most directly continuous with the lateral pharyngeal duct did not store iodine, while those which were further removed from the duct showed transitionally an increased ability to perform this function (Fig. 6). These data would seem to lend support to the view that the lateral thyroid rudiments do contribute to the definitive thyroid gland. Further, they indicate the possibility that the thyroid gland may not be physiologically equivalent in all its parts.

Studies of adult mammalian thyroids. In considerations of the hormonal synthesis and storage in the thyroid gland it has always been a

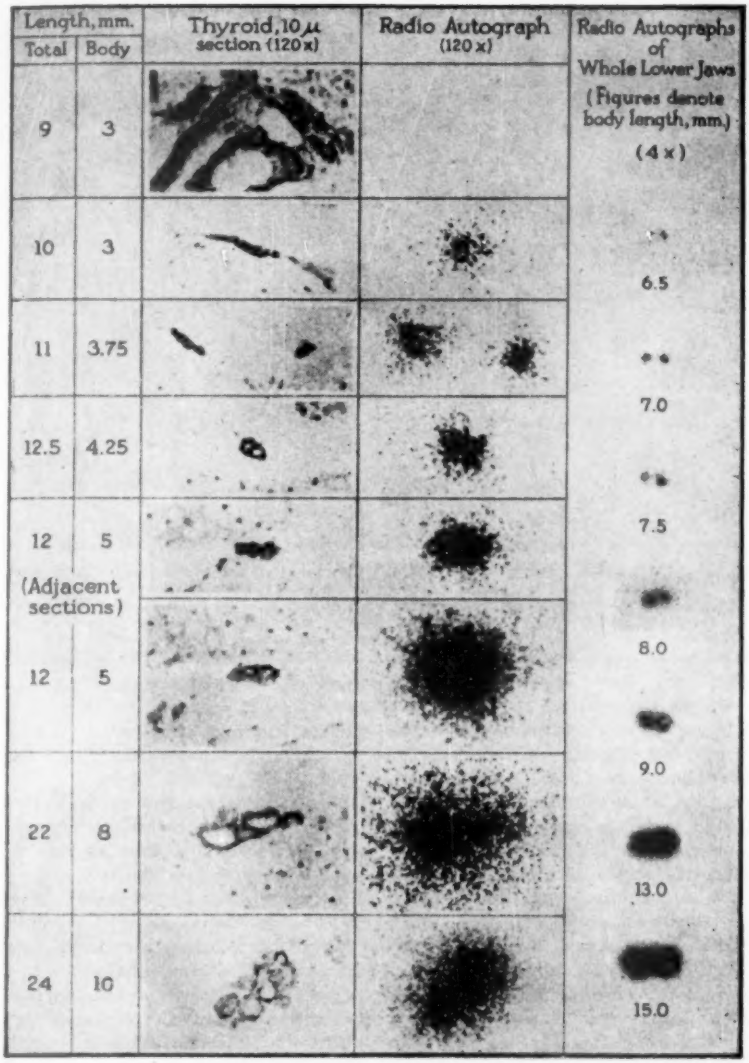

FIG. 4. Radioautographs of thyroids of frog larvae of different ages, and photomicrographs of the sections from which these autographs were prepared. In the last column are autographs of the whole lower jaws of tadpoles of different age. The growth in size and iodine accumulativeness of the two thyroid lobes is evident. Gorbman and Evans (*20*)

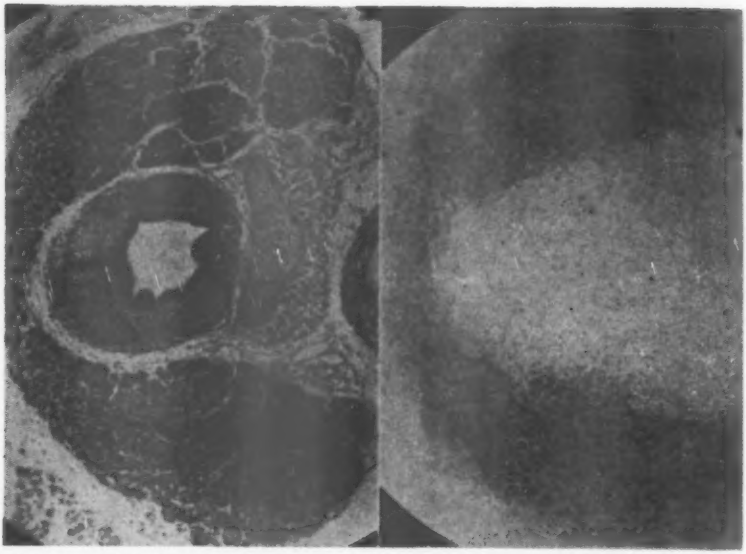

FIG. 5. Photomicrograph of the thyroid (large half-moon shaped mass of tissue) and its radioautograph from 19-day rat fetus whose mother was injected with radio-iodide. This autograph is relatively feeble compared to that of a 20-day fetus and therefore represents the beginning of iodine-storage ability in the fetal thyroid. Gorbman and Evans (*21*)

difficult matter to determine the site of these activities. Leblond (*22*) was able to show in radioautographs that soon after administration radio-iodide is diffusely distributed in the gland. Shortly, organically bound I^{131} can be found in the cells, and finally, in the storage phase, it is located in the colloid. Storage within the colloid also has been shown in radioautographs of developing thyroids of frogs (*16*). Leblond has shown, further, (*22*, *31*) that when areas of iodine accumulation are correlated with the staining reactions in the colloid of trichrome stained glands, the first loci of accumulation are in follicles with basophilic colloid. He, therefore, considers basophilic colloid as that containing recently formed hormone, while acidophilic colloid is regarded as "older."

Interesting application has been made of radioautography as a means of checking the completeness of surgical thyroidectomy in experimental animals (*41*, *42*). If tracer doses of I^{131} are given such animals shortly before autopsy, films exposed to the tissues of the cervical region reveal the presence and location of bits of thyroid tissue which escaped surgery, or which are of an accessory and anomalously placed nature.

A number of autographic studies have been made of normal, hypoplastic, and hyperplastic thyroids of man and experimental animals (*10*, *25*, *26*, *31*, *33*) confirming the quantitative data which have been found in connection with iodine accumulation under these varying conditions.

Neoplastic thyroid tissue. A great deal of interest has devolved on whether or not thyroid carcinoma has the ability

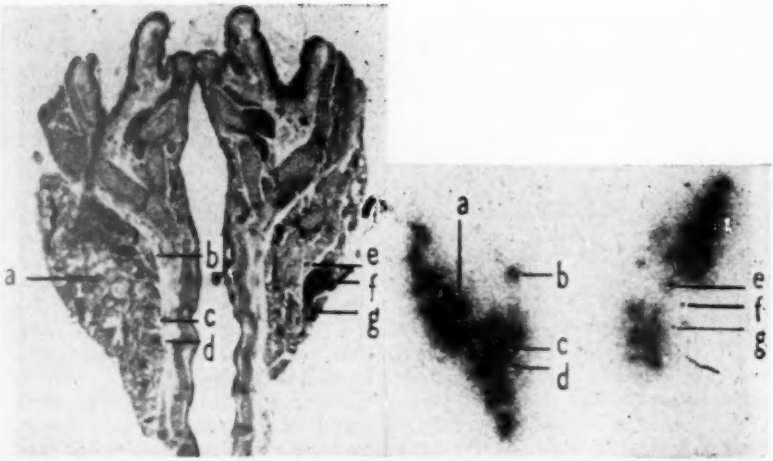

FIG. 6. Frontal section of the thyroid and trachea of an adult female mouse, and its radioautograph. Point-by-point comparison may be made by reference to the letters a, b, c, d, e, f, and g in both photographs. A large area of thyroid between a and b is connected to an anomalous lateral pharyngeal duct and stores no iodine. The areas of f and g are parathyroid and thymus, respectively. Gorbman (*18*)

of normal thyroid to store iodine. If it has, then it would seem that therapy through auto-irradiation by localized high doses of I^{131} would be possible. The earlier autographic data of Hamilton, Soley, and Eichorn (*25*) seemed to deny this possibility. In two patients with thyroidal adenocarcinoma, they found a lack of iodine in the carcinomatous tissue when tracer doses of I^{131} were actively localized in adjacent normal thyroid tissue. More recently, however, others (*37*) have found autographically that some thyroidal carcinomas do retain administered I^{131} and that at least temporary remission may be obtained with large doses of the isotope. Frantz *et al.* (*16*) have used films wrapped around the leg of such a patient to locate a femoral metastasis.

Embryology of the Chick

A very interesting application of radioautography has been made recently by Smith and Gray (*43*) in a study of the distribution of copper in chick embryos. They injected Cu^{64} ion into the egg white and later removed the incubated chick embryos. Radioautographs were made of the whole mounts. Regional localizations of copper were found in all ages studied (19 to 84 hours' incubation). Earliest localization was in the primitive streak. A succession of localizations occurred in an anterior-posterial gradient. This was especially marked in the early central nervous system in which the most anterior brain structures autographed very strongly. As they became organized and underwent early growth, Cu^{64} accumulated in the eye, auditory and olfactory placodes, limb and tail buds, allantois, pharyngeal pouches, and somites. The authors point to the parallel distribution in the embryo of oxygen uptake and cytochrome oxidase concentration, shown by previous authors. They suggest that copper may play an important part in those metabolic activities of the embryo which accompany or accomplish differentiation.

It would seem that the radioautographs of Smith and Gray point to the possibility of a new experimental tool for the embryologist. Localized accumulation of isotopes could provide the means for selective radiant destruction of certain embryonic structures without the use of microsurgery. This would be decidedly advantageous in experimenting with embryos like those of the chick or mammal which are relatively difficult to approach.

Normal and Neoplastic Lymphoid Tissue

It has been, of course, a primary task in cancer research to discover chemical substances which accumulate selectively in cancerous tissue to permit radioisotope irradiation therapy, if possible. As long as investigations are limited to the use of simple inorganic compounds of the radioactive elements, it does not seem very likely that this objective will be achieved. It is to be hoped that when specific organic compounds of these isotopes become more generally available further progress can be made.

The use of radioactive iodides in treatment of thyroidal carcinoma has been described. The only other possibility which has appeared in the literature is implied in the high concentration of radioactive polonium (*28, 29*) and phosphorus (*30, 36*) in lymphoid tissue which has been shown by both the counting and radioautographic techniques. Lacassagne clearly demonstrated the localization of polonium in lymphoid and haematopoietic tissues as early as 1924, and was the first to make radioautographs from histological sections. He observed that the polonium accumulated as well in placental chorionic tissue, in interstitial cells of the testis, in atretic follicles of the ovary, and in the zona reticularis of the adrenal cortex. The use of polonium has not yet been attempted for treatment of tumors of lymphoid tissue though it was obviously suggested in Lacassagne's work. Beneficial effects have been claimed in treatment of lymphatic and myelogenous leukemia, polycythemia vera, and lymphosarcoma with radiophosphate (*36*).

Autography of Bone and Teeth

Discussion of radioisotope work with bony tissues should be divided into those studies involving elements ordinarily encountered there (P, C, Ca, and the chemically similar Sr), and those considered strange to bone (Pb, Ra, I, Th, Pu, etc.).

Pecher has made a series of autographic observations (*40*) on the localization of strontium in skeletal tissues. In the long bones, the first and strongest deposition of strontium occurred in the regions of new-bone formation in the epiphyseal disc and accumulation occurred in the metaphysis as well. Pecher and others (*40, 44*) have found that strontium localizes in osteogenic sarcoma. Calcium behaves in the same manner as strontium in bone (*40*), but use of Ca^{45} in radioautographic work in the past has been attended by such disadvantages as low available specific activity and low beta-radiation energy.

Phosphorus, though a normal constituent of skeletal tissue, localizes in numerous other foci in the body, as has been brought out in earlier parts of this survey. A number of workers (*12, 30, 32, 40*) have supplied radioautographs showing accumulation of radiophosphate in bone, zones of calcifying cartilage, and in teeth (both dentine and enamel).

The accumulation of radio-carbon (C^{14}), given as carbonate, has been pictured recently in autographs by Bloom, Curtis, and McClean (*6*). In contrast with the tendency of P^{32} and Sr^{8} to appear in areas of newly forming bone, C^{14} accumulated in regions of pre-

existing bone. The danger should be obvious to workers who deal with this isotope (half-life more than 5,000 years) from the fact that measurements for as long as four months after the original deposition in bone showed no appreciable decrease in radioactivity.

Deposition of radiophosphate in teeth, as in bone, is greatest in areas of new deposition of enamel or dentine (*22*, *32*). Bartelstone *et al.* (*3*) made an interesting application of radioautography in the study of I^{131} distribution in adult teeth. They injected radioiodide into cats and rats and exposed to film prepared sections of the animals' teeth. The autographs showed a rather uniform iodine distribution in dentine, and enamel, and slightly more in the cementum. This was taken by the authors as evidence of a dynamic fluid equilibrium between the calcified structures and the blood.

Metabolism and Osteal Localization of Heavy Metals and Fission Products

Finkel (*15*) has described some interesting experiments on the effects on offspring of injection of plutonium and of Sr^{89} into pregnant mice. The young were born with higher equivalent amounts of Pu and Sr per body weight than the mothers retained. Severest effects on the young were seen after radiostrontium salt injections. In these animals, as was shown in radioautographs, Sr^{89} accumulated in bone with resulting retardation of growth, skeletal malformations, and anemia. In such mice living more than 200 days, osteogenic sarcoma was found, apparently induced by the radiation localized in the bones. If treated mothers suckled normal young of untreated mothers, Finkel found that they received Pu and Sr^{89} through the milk.

Accumulation of radiolead (radium D or thorium B) has been shown in radioautographs to occur in bone, liver, kidney cortex, spleen, and mucosa of the alimentary tract. Adipose tissue, skin, brain, and muscle were essentially free of lead, as were the submucosa and muscularis of the digestive organs (*4*). Behrens and Baumann (*4*, *5*) made an extensive study of the circumstances under which lead deposition occurs in the bones of rats and mice. They found that the principal concentrations of radiolead were in the regions of new epiphyseal and periosteal bone formation. They found, further, that lead accumulated in any other area where calcification was in progress either normally, or experimentally induced. For example, accompanying atypical calcification in the stomach, kidney, lung, or heart, consequent to massive treatment with calcium salts or irradiated ergosterol, depositions of lead could be radioautographed in these organs (Fig. 7, *8*).

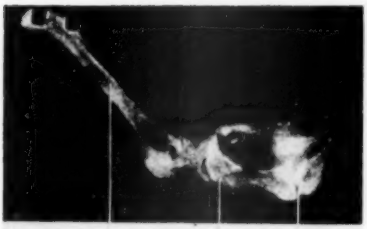

FIG. 7. Radioautograph of the leg bones of a rat given radiolead after fracture of the tibia. Radiolead is most energetically deposited in the healing callus at the point where calcification is most active. Behrens and Baumann (*5*)

In a more extensive study, Lisco, Finkel, and Brues (*35*) have noted the appearance of osteogenic sarcomas in rabbits, rats, and mice following administration by injection or feeding of radioactive strontium, yttrium, cerium, or plutonium. Localization in the skeleton was demonstrated autographically. Sarcomas appearing after plutonium treatments were predominantly

FIG. 8. Radioautograph of the heart of a rat given radiolead after a massive dose of vitamin D. Areas where calcium is being deposited in the large vessels, and apparently in coronary vessels, are sites of radiolead deposition. Behrens and Baumann (*5*)

in the vertebral column. Tumors induced by Sr, Y, and Ce were found principally in the long bones. No reason for this difference was apparent. Carcinoma of the colon was found after Y^{91} feeding, seemingly because of the lack of intestinal absorption of this substance which resulted in extended epithelial irradiation.

Hamilton (*24*) recently reported the results of experiments with a large number of radioactive fission products and heavy metals whose distribution and metabolism in the organism was followed by autographic and by counting technique. The elements studied were strontium (Sr^{89}, Sr^{90}), yttrium (Y^{91}), columbium (Cb^{95}), zirconium (Zr^{95}), ruthenium (Ru^{103}, Ru^{106}), tellurium (Te^{127}, Te^{129}), iodine (I^{131}), xenon (Xe^{133}), cesium (Cs^{135}), barium (Ba^{140}), lanthanum (La^{140}), cerium (Ce^{141}, Ce^{144}), praseodymium (Pr^{142}), element 61 (61^{147}), protoactinium (Pa^{231}), thorium (Th^{234}), neptunium (Np^{239}), plutonium (Pu^{239}), americium (Am^{241}), curium (Cm^{242}).

The elements were given parenterally, orally, or in some cases by inhalation in an aerosol. Only Sr, Ba, Te, I, and Cs were found absorbable from the gut. Xe was easily absorbable through the lungs, and eliminated by the same route. It was necessary to give the remaining elements parenterally. Iodine, as was to be expected, accumulated in the thyroid. Te was rapidly lost from the body after a transitory accumulation in blood and kidney. Cs also was rapidly lost after an initial slight concentration in muscle tissue. Except for ruthenium, which was quickly excreted, all other elements studied, including Ba and Sr (Fig. 9), had a high degree of skeletal localization and retention.

In the case of La, Ce, Pr, 61, Am, and Cm there was a brief concentration in the liver which soon decreased, apparently by way of excretion through bile. Once localized within the bones, the slowest rates of elimination were found for Sr, Y, Zr, Ba, La, Ce, Pr, Pu. Radioautographs showed details of histological localization differed for Sr on the one hand and Y, Zr, Ce, Th, Pu, and Am on the other hand. Some months after administration, strontium was found generally distributed throughout the mineral structure of bones.

Plutonium, and the elements behaving like it, were found associated with

FIG. 9. Section of bone from radiostrontium injected rat, and its radioautograph Sr is apparently distributed throughout the mineral part of the bone. Hamilton (*24*)

FIG. 10. Section of bone from plutonium-injected rat, and its radioautograph. Pattern of plutonium distribution is essentially that of periosteum and endosteum. Hamilton (*24*)

the periosteum, endosteum, and trabecular bone. Hamilton was able to correlate this distribution in autographs with the presence of osteoid matrix material (Fig. 10). Essentially the same type of autograph was obtained after a year as shortly after injection, indicating that the presence of Pu in osteoid matrix was not, as in the case of lead (*4*), associated with new calcium deposition. It is pointed out (*9, 24*) that the osteoid accumulation of such alpha-particle-emitting isotopes, of long half-life, presents a dangerous situation, since it exposes the bone marrow to prolonged irradiation of a very destructive type. Furthermore, plutonium inhaled as an aerosol was found to remain in the pulmonary alveoli, in a significant concentration, for more than eight months.

These findings are of undoubted value. It would be of greatest interest to learn more of the metabolism of these substances since the behavior of most of them is unknown in living systems. Some of them are new even to the periodic table, having only recently emerged from laboratories of atomic nuclear study.

Distribution of War Gases in the Skin

Axelrod and Hamilton (*2*) have been able to observe radiographically the integumentary penetrativeness of mustard gas labeled with S^{35} and lewisite labeled with As^{74}. These studies were made on the skin of man and pigs, and on the cornea of rabbits. Mustard gas in radioautographs was seen to penetrate the epidermis rapidly, reaching the dermis soon after administration. Within the dermis, it accumulated in hair follicles, sebaceous glands, and walls of blood vessels. Lewisite, on the other hand, was fixed principally in hair follicles and epidermis and blood vessels in the dermis. The authors consider the deep penetration of labeled mustard gas as explanatory of the deep burns it produces, and the selective effect of both poisons on deep blood vessels as responsible for the disturbances in circulation characteristic in affected areas.

Summary

The radioautographic technique has proved of greatest usefulness in the precise identification of areas of distribution or localization of radioactive isotopes within the organism. It has been applied profitably in a diverse series of fields of study in biology and medicine.

In botany the vascular routes of movement of phosphorus have been studied, and localization in cambium, seeds, and other foci has been demonstrated. The distribution in the seed of radiosulfur given to the plant as a whole also has been shown in radioautographs.

The early availability of radio-iodine has made possible numerous studies of the thyroid. Radioautographs have been used to identify iodine metabolizing tissues in lower chordates which have no thyroid, to indicate when the thyroid of embryos begins to function, and to show that ultimobranchial-derived follicles in the adult thyroid do not metabolize iodine. Autographs have furnished visual evidence that colloid is the site of hormonal storage, and that basophilic colloid is of recent formation. Further, autography has provided a practical means for locating scraps of thyroid remaining after incomplete thyroidectomy, and for locating metastatic growths of thyroidal carcinoma. The ability or inability of thyroidal cancers to engage in iodine metabolism has been shown in this way.

The localization of radiophosphorus and polonium in lymphoid tissue has been recorded in radioautographs. Neoplastic lymphoid tissues also have been shown to be foci for phosphorus deposition.

Bone has proved to be the place of selective localization of a large number of radioisotopes. This is of especial interest in understanding the health hazard inherent in these isotopes, and the pattern of toxicity to be expected from them. Ca, Sr, P, and C are readily deposited in the mineral structure of bone, and the details of their behavior in relation to the epiphyseal, periosteal, and endosteal zones of ossification have been visualized in autographs.

Accumulation of Sr in osteogenic sarcoma has suggested therapeutic usefulness. On the other hand, Sr and several other osteotropic radioactive elements have themselves proved to be carcinogenic, inducing the appearance of osteogenic sarcoma in experimental animals.

Numerous heavy metals and radioactive fission products have been autographed in bone. The conditions under which radiolead accumulates there have been especially well studied in this way. Autographs of plutonium and several similar elements in bone proved that their concentrations occurred in the mineral-poor osteoid regions rather than the mineral part of bone, as is the case for Ca, Sr, P, and C.

The details of integumentary and corneal penetration have been autographed for mustard gas and lewisite labeled with radioactive S and As.

BIBLIOGRAPHY

1. D. I. Arnon, D. R. Stout, F. Sipos. Radioactive phosphorus as an indicator of phosphorus absorption of tomato fruits at various stages of development, *Am. J. Botany* **27**, 791 (1940)
2. D. J. Axelrod, J. G. Hamilton. Radioautographic studies of the distribution of lewisite and mustard gas in skin and eye tissues, *Am. J. Path.* **23**, 389 (1947)
3. H. J. Bartelstone, D. Mandel, E. Oshry, S. M. Seidlin. The use of radioactive iodine as a tracer in the study of the physiology of teeth, *Science* **106**, 132 (1947)
4. B. Behrens, A. Baumann. Zur Pharmakologie des Bleis. IX. Weitere Untersuchungen über die Verteilung des Bleis mit Hilfe der Methode der Autohistradiographie, *Z. ges. exptl. Med.* **92**, 241 (1933)
5. B. Behrens, A. Baumann. Zur Pharmakologie des Bleis. X. Die Beziehung der Bleiablagerung zum Calciumstoffwechsel, *Z. ges. expt. Med.* **92**, 251 (1933)
6. W. Bloom, H. J. Curtis, F. C. McClean. The deposition of C^{14} in bone, *Science* **105**, 45 (1947)

7. G. A. Boyd. The physical principles and techniques of autoradiographs, *J. Biol. Phot. Assoc.* **16,** 65 (1947)
8. R. N. Colwell. The use of radioactive phosphorus in translocation studies, *Am. J. Botany* **29,** 798 (1942)
9. D. H. Copp, D. A. Axelrod, J. G. Hamilton. The deposition of radioactive metals in bone as a potential health hazard, *Am. J. Roentgenol.* **58,** 10 (1947)
10. A. Couceiro, L. G. Veira, J. De Moraes. Acao da tiouracila sobre a fixacao de iodo pela tiroide. *Rev. brasil. biol.* **4,** 173 (1944)
11. P. Demers, V. Fredette. New autoradiographic method, *Bull. Am. Phys. Soc.* **22,** (No. 3), 20 (abst.) (1947)
12. M. J. Dois, B. C. P. Jansen, G. J. Sizoo, G. J. Van der Maas. Distribution of phosphorus in the leg bones of the chicken, *Nature* **142,** 953 (1938)
13. T. C. Evans. Selection of Radioautographic Technique for Problems in Biology, NUCLEONICS **2,** No. 3, 53 (1948)
14. K. M. Endicott, H. Yagoda. Microscopic historadiographic technique for locating and quantitating radioactive elements in tissues, *Proc. Soc. Exptl. Biol. Med.* **64,** 170 (1947)
15. M. P. Finkel. The transmission of radiostrontium and plutonium from mother to offspring in laboratory animals, *Physiol. Zoöl. 20,* 405 (1947)
16. V. K. Frantz, R. P. Ball, A. S. Keston, W. W. Palmer. Thyroid carcinoma with metastases: studied with radioactive iodine, *Ann. Surg.* **119,** 668 (1944)
17. A. Gorbman. Identity of an iodine storing tissue in an ascidian, *Science* **94,** 192 (1941)
18. A. Gorbman. Functional and morphological properties in the thyroid gland, ultimobranchial body, and persisting ductus pharyngobranchials IV of an adult mouse, *Anat. Record* **98,** 93 (1946)
19. A. Gorbman, C. W. Creaser. Storage of radioactive iodine in the endostyle of larval lampreys and the problem of homology of the thyrcid, *J. Exptl. Zoöl.* **89,** 391 (1942)
20. A. Gorbman, H. M. Evans. Correlation of histological differentiation with beginning of function of the thyroid gland of the frog, *Proc. Soc. Exptl. Biol. Med.* **47,** 103 (1941)
21. A. Gorbman, H. M. Evans. Beginning of function in the thyroid of the fetal rat, *Endocrinology* **32,** 113 (1943)
22. J. Gross, C. P. Leblond. Histological localization of radioactive elements, *McGill Med. J.* **15,** 1 (1946)
23. J. G. Hamilton. The use of radioactive tracers in biology and medicine, *Radiology* **39,** 541 (1942)
24. J. G. Hamilton. The metabolism of the fission products and the heaviest metals, *Radiology* **49,** 325 (1947)
25. J. G. Hamilton, M. H. Soley, K. B. Eichorn. Deposition of radioactive iodine in human thyroid tissue. *Univ. Calif.* (*Berkeley*) *Publs. Pharmacol.* **1,** 339 (1940)
26. J. G. Hamilton, M. H. Soley, W. A. Reilley, K. B. Eichorn. Radioactive iodine studies in childhood hypothyroidism, *Am. J. Diseases Children* **66,** 495 (1943)
27. B. F. Harrison, M. D. Thomas, G. R. Hill. Radioautographs of the distribution of sulphur in wheat, *Plant Physiol.* **19,** 245 (1944)
28. A. Laccassagne, J. Lattes. Methode autohistoradiographique pour la detection, dans les organes, du polonium injecte, *Compt. rend.* **178,** 488 (1924)
29. A. Laccassagne, J. Lattes, J. Lavedan. Etude experimentale des effets biologiques du polonium introduit dans l'organisme, *J. Radiol. Electrol.*, **9,** 1 (1925)
30. J. H. Lawrence. The new nuclear physics and medicine, Caldwell Lecture, 1941, *Am. J. Roentgenol.* **48,** 283 (1942)
31. C. P. Leblond. Behavior of radioiodine in resting and stimulated thyroids, *Anat. Record* **88,** 285 (1944)
32. C. P. Leblond, L. F. Belanger. Detection of radioactive phosphorus by the autographic method in the newborn mouse, *Anat. Record* **94,** 542 (1946)
33. C. P. Leblond, M. B. Fertman, I. D. Puppel, G. M. Curtis. Radioiodine autography in studies of human goitrous thyroid gland, *Arch. Path.* **41,** 510 (1946)
34. E. Lindsay, R. Craig. The distribution of radiophosphorus in wax moth, mealworm, cockroach, and firebrat, *Ann. Entomol. Soc. Am.* **35,** 50 (1942)
35. H. Lisco, M. P. Finkel, A. M. Brues. Carcinogenic properties of radioactive fission products and of plutonium, *Radiology* **49,** 361 (1947)
36. B. V. A. Low-Beer, J. H. Lawrence, R. S. Stone. The therapeutic use of artificially produced radioactive substances, *Radiology* **39,** 573 (1942)
37. L. D. Marinelli, F. W. Foote, R. F. Hill A. F. Hocker. Retention of radioactive iodine in thyroid carcinomas, *Am. J. Roentgenol.* **58,** 17 (1947)
38. L. Morton, P. Abelson. Tracer micrography, *Phys. Rev.* **72,** 161 (abst.) (1947)
39. C. Pecher. Biological investigations with radioactive calcium and strontium: Preliminary report on the use of radioactive strontium in treatment of metastic bone cancer, *Univ. Calif.* (*Berkeley*) *Publs. Pharmacol.* **2,** 117 (1942)
40. C. Pecher. Biological investigations with radioactive calcium and strontium, *Proc. Soc. Exptl. Biol. Med.* **46,** 86 (1942)
41. W. O. Reinhardt. Method for determining completeness of thyroidectomy using radioactive iodine, *Proc. Soc. Exptl. Biol. Med.* **50,** 81 (1942)
42. R. O. Scow, M. E. Simpson. Thyroidectomy in the newborn rat, *Anat. Record* **91,** 209 (1945)
43. E. Smith, P. Gray. The distribution of copper in the early chick embryo, *Anat. Record* **99** (suppl.), 52 (abst.) (1947)
44. A. Treadwell, B. V. A. Low-Beer, H. L. Friedell, J. H. Lawrence. Metabolic studies on neoplasm of bone with the aid of radioactive strontium, *Am. J. Med. Sci.* **204,** 521 (1942)
45. B. M. Wheeler. The iodine metabolism of Drosophila gibberosa studied by means of radioiodine I^{131}, *Proc. Nat. Acad. Sci.* **33,** 298 (1947)

Chemical Effects of Nuclear Transformations*

The extensive chemical changes induced by nuclear processes are described, with a review of the contribution which their study has made to the understanding of nuclear and molecular phenomena. The new field of "hot atom chemistry" is defined and logically developed from basic considerations

By R. R. EDWARDS and T. H. DAVIES

Department of Chemistry and Laboratory for Nuclear Science and Engineering Massachusetts Institute of Technology Cambridge, Massachusetts

Institute for Nuclear Studies University of Chicago Chicago, Illinois

SINCE THE DISCOVERY of artificial radioactivity and its rapid development into an important and complex field in its own right, chemistry has grown steadily in importance as an ally of nuclear physics. Illustrative of this is the expanding range of applications of radioactive tracers to the study of *chemical* phenomena. Of equal interest, however, is the use of chemistry in the study of *nuclear* phenomena; for example, the products of nuclear reactions can be readily isolated and identified by means of analytical chemistry.

This application was demonstrated dramatically in the case of fission of uranium. In 1938, four years after fission was first observed, Hahn and Strassmann (*1*) recognized the true nature of the process when they identified barium and lanthanum among the reaction products. Later a large fraction of the spectrum of fission products of U^{235} was determined by chemical means (*2*).

The study of the chemical changes resulting from nuclear transformations is further evidence of the alliance of chemistry with nuclear physics. Although little attention has been given this subject, it is of scientific interest from several points of view. The energy release in nuclear processes provides recoiling atoms with energies as high as 95 Mev. The behavior of such species is of interest to the chemist since the energy required for ionization, for destruction of molecular species, and for the formation of new compounds is obviously available in many cases. The occurrence and origin of such phenomena will be illustrated in the material which follows.

Chemical study of newly formed energetic atoms may yield information about the nuclear processes themselves, since the energy, degree of ionization, and, consequently, the chemical state of the recoiling atom are functions of the nature of the nuclear process. Applications of this sort have already appeared in the literature and will be reviewed below.

Thus, the so-called "chemistry of hot atoms" may be defined as the subject which considers primarily the behavior of atoms energized by virtue of recoil momentum, or by virtue of electronic excitation, arising from transitions in the nucleus of the same atom. The subject may well be taken as part of, or closely associated with, the general field of radiation chemistry.

* Work supported in part by the Office of Naval Research.

TABLE 1

Nuclear Transformations

Classification	*Process*	*General Equation*	*Example*
Particle emission	α-decay	${}_ZA^M \rightarrow {}_{(Z-2)}B^{(M-4)} + {}_2He^4$	${}_{92}U^{238} \rightarrow {}_{90}Th^{23} + {}_2He^4$
	β-decay	${}_ZA^M \rightarrow {}_{(Z+1)}B^M + \beta^-$	${}_{35}Br^{83} \rightarrow {}_{36}Kr^{83} + \beta^-$
Photon emission	Isomeric Transition	${}_ZA^{M*} \rightarrow {}_ZA^M + \gamma$	${}_{35}Br^{80*} \rightarrow {}_{35}Br^{80} + \gamma$ (or e^-)
Neutron absorption —Photon emission	n,γ	${}_ZA^M + {}_0n^1 \rightarrow {}_ZA^{M+1} + \gamma$	${}_{35}Br^{81} + {}_0n^1 \rightarrow {}_{35}Br^{82} + \gamma$
Neutron absorption —Proton emission	n,p	${}_ZA^M + {}_0n^1 \rightarrow {}_{(Z-1)}B^M + {}_1H^1$	${}_{52}Te^{128} + {}_0n^1 \rightarrow {}_{51}Sb^{128} + {}_1H^1$
Nuclear Fission	nf		${}_{92}U^{235} \rightarrow {}_{36}Kr^{91} + {}_{56}Ba^{143} + 2{}_0n^1$

ENERGY PARTITION

The energy relationships between the particles or radiations and the emitting nuclei can be grouped in a few categories: (*a*) particle emission, (*b*) photon emission, (*c*) particle absorption, and (*d*) nuclear fission. Combinations of the above reactions are, of course, quite common, and sometimes require special treatment in energy calculations.

Some nuclear reactions illustrating these phenomena and their combinations are listed, with examples, in Table 1. The nature of the various processes will be discussed in more detail after the general equations for energy partition have been developed.

Particle Emission

The kinetic energies of heavy particles seldom require relativistic treatment. In β emission, however, the relativity correction is usually necessary. Since this nuclear process is especially prominent, we shall derive relativistically the equation relating energy of the emitted particle with that of the recoil atom.

For any particle the kinetic energy is given by

$$E = (m - m_0)c^2 \qquad (1)$$

and the momentum by

$$p = mv \qquad (2)$$

where m_0 is the rest mass of the particle, c is the velocity of light, and m is the relativistic mass

$$m = \frac{m_0}{\sqrt{1 - (v^2/c^2)}} \qquad (3)$$

The energy and momentum of the recoil atom may be expressed nonrelativistically since the velocity of the latter is small compared with the velocity of light. Thus, for the recoil nucleus

$$E_R = MV^2/2, \quad p_R = MV \qquad (4)$$

If momentum is conserved,

$$MV = mv = \frac{m_0 v}{\sqrt{1 - (v^2/c^2)}} \qquad (5)$$

Squaring and multiplying by $[(c^2/v^2) - 1]$ gives

$$\frac{M^2V^2c^2}{v^2} - M^2V^2 = m_0^2c^2 \qquad (6)$$

From equations 5 and 6

$$M^2V^2 = (m^2 - m_0^2)c^2 \qquad (7)$$

or

$$\frac{M^2V^2}{m + m_0} = (m - m_0)c^2 = E \quad (8)$$

From equations 8 and 4,

$$E_R = \frac{m + m_0}{2M} E \quad (9)$$

Equation 9 is the general expression for the recoil energy of a nucleus following particle emission. For non-relativistic particles, equation 9 reduces to

$$E_R = (m_0/M)E \quad (10)$$

Particle Absorption (Capture)

When a stationary nucleus captures an energetic particle, the equation of momentum conservation (equation 5) must apply as in the case of particle emission. In this case, the mass M is that of the compound nucleus, m is the relativistic mass of the incident particle, E is the kinetic energy of the particle, and E_R that of the compound nucleus. By means of an identical derivation, equation 9 is seen to apply to the capture process as well as to that of emission. The non-relativistic simplification (equation 10) will usually suffice unless the (heavy) bombarding particle is of extremely high energy, such as that obtained with the linear accelerators or frequency-modulated cyclotrons. A 100-Mev proton, for example, moves with about one-third the velocity of light, so that the relativistic mass is only about eight percent above the rest mass. The interaction of relativistic electrons with nuclei is not of sufficient importance to require special treatment here.

Photon Emission

A photon of energy $E = h\nu$ carries a momentum equal to $h\nu/c$, or E/c. In photon emission, the momentum of the recoil nucleus must equal that of the photon

$$MV = E/c \quad (11)$$

The kinetic energy of the recoil nucleus $E_R = \frac{1}{2}MV^2$; thus

$$E_R = \frac{(MV)^2}{2M} = \frac{E^2}{2Mc^2} \quad (12)$$

The recoil energy can be obtained in units of ergs, electron volts, or Mev by substituting the values of E^2 and Mc^2 (energy equivalent) in the corresponding units. The mass M, in this case, is the mass of the atom in grams rather than its mass number. Solving the equation, and expressing Mc^2 in Mev, we see that

$$E_R = \frac{536 \times 10^{-6} E^2}{M} \quad (13)$$

where M is the mass of the recoiling atom in atomic mass units and both energies are in Mev.

Nuclear Fission

The energetics of fission can be treated as a special case of particle emission in which the two resulting fragments are of comparable mass and energy. Let E_t represent the total kinetic energy of the fission fragments, and let M_1, M_2, V_1, and V_2 be the masses and velocities of the fragments. Then, from conservation of momentum*

$$M_1V_1 = M_2V_2 \quad (14)$$

Conservation of energy requires that

$$\frac{M_1V_1^2}{2} + \frac{M_2V_2^2}{2} = E_t \quad (15)$$

From equations 14 and 15

$$\frac{(M_1V_1)^2}{2M_1} + \frac{(M_1V_1)^2}{2M_2} = E_t$$

Solving for $(M_1V_1)^2/2M_1 = E_1$:

$$E_1 = \frac{M_2}{M_1 + M_2} E_t \quad (16)$$

The lighter of the two fission fragments, then, will have greater energy, and consequently greater velocity, than the heavy product. The value of E_t may be estimated by calculating the electrostatic potential energy $(Z_1Z_2e^2/r)$ of the two product nuclei in contact

* The small contribution to the momenta by the excess neutrons released in fission is neglected here.

at the instant of fission; r may be obtained approximately from the equation

$$r = 1.5 \times 10^{-13}(M_1^{1/3} + M_2^{1/3}), \quad (17)$$

and the ratio of the charge values (Z_1/Z_2) may be considered approximately equal to that of the mass values (M_1/M_2).

Use of these equations to find the reaction energy for the case of symmetrical fission, *i.e.*, when $Z_1 = Z_2 = 46$, and $M_1 = M_2 \approx 118$, yields 208 Mev in approximate agreement with experiment. Extrapolation of Jentschke's data (*25*) to the case of symmetrical fission gives 175 Mev as the most probable total kinetic energy of the fission products.

NATURE OF CHEMICAL EFFECTS

Experimental study of the chemical effects accompanying nuclear processes has been meager. Nevertheless, theory and results can be compared in selected cases.

Radioactive Decay Processes

β Particle Emission. In equation 9 it is shown that a β particle of energy E_β imparts to the decaying nucleus a recoil energy $E_R = [(m + m_0)/2M]E_\beta$. The relativistic mass m of the β particle relative to its rest mass can be calculated from equation 1, and is

$$\frac{m}{m_0} = \frac{E_\beta + m_0c^2}{m_0c^2} \quad (18)$$

Substituting the energy values in Mev,

$$\frac{m}{m_0} = \frac{E_\beta + 0.51}{0.51} \quad (19)$$

For convenience in calculating recoil energies, some typical values of this ratio are given in Table 2. From equations 9 and 19, the specific equation applicable to β emission can be obtained. Thus, since $m = (m_0E_\beta + 0.51\ m_0)/0.51$,

$$E_R = \frac{m_0(E_\beta + 1.02)}{0.51}\left(\frac{E_\beta}{2M}\right) \quad (20)$$

Introducing the rest mass of the electron and simplifying

TABLE 2

Relativistic Mass of β Particles

E_β(Mev)	m/m_0
0.01	1.02
0.10	1.10
0.50	1.98
1.0	2.96
2.0	4.92
3.0	6.88
5.0	10.8
12.0	24.5

$$E_R = 536 \times 10^{-6}E_\beta\left(\frac{E_\beta + 1.02}{M}\right) \quad (21)$$

where all energies are in Mev, and M is the mass of the recoil nucleus in amu.

Figure 1 shows the magnitude of the recoil energies as a function of β energy to be a few ev for the characteristic β emitter. The most energetic β emitters known are B^{12} and Li^8, which emit particles with the maximum energy at 12 Mev. The recoil energy in these cases is quite high (particularly so because the nuclei are of low mass) and

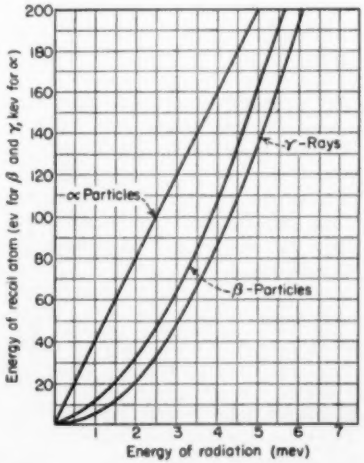

FIG. 1. Recoil energy versus energy of radiation for $M = 100$

approaches 7 kev per nucleus for the boron.

However, the energies of β particles emitted by a given nuclide vary from zero to a definite maximum. The residual energy when $E < E_{max}$ is assigned to the neutrino. An approximate equation for a β spectrum (allowed transition), is, by the Fermi theory,

$$N_E = AE^{1/2}(1 + 2E)(1 + E)^{1/2} (E_{max} - E)^2 dE \quad (22)$$

where N_E is the probability that a β particle will have energy between E and $E + dE$, and A is a constant.

The difference between the maximum energy and the actual energy of the β particle is carried by the neutrino, which has a rest mass less than $1/50$ that of the β particle (*34*), and may indeed have zero rest mass. The recoil spectrum therefore is more complicated to calculate than that for single, monoenergetic particle emission. Unfortunately very little information is available concerning angular correlation, if any, of neutrino and β particle. Jacobsen (*3*), in retarding potential experiments with Kr^{85}, found that recoil energies were frequently greater than accounted for by the β particle alone, thus indicating a high probability for emission in the same direction. Hamilton (*4*) has calculated from theoretical considerations that emission in the same direction should be preferred, and has shown that it is quantitatively dependent on the choice of interaction terms employed in the calculations, and upon the order of forbiddenness of the β transition.

Other recent experimental work, however, suggests that there is no highly preferred angular correlation. Christy *et al.* (*5*), in cloud chamber studies of β-radioactive Li^8 (whose Be^8 daughter undergoes spontaneous disintegration into two alpha particles), observed that the momenta of recoils due to the β decay were too great to be accounted for by the β particle alone, and were best described by equations assuming no preferred angle between β and neutrino. Sherwin (*6*) reports that momentum is not conserved between β and recoil atom in P^{32}, and his results (time of flight measurements) indicate that the probability for emission of β and neutrino in the same hemisphere is low. The energy spectrum of the recoil atoms could not, however, be simply expressed. Above 25 ev the spectrum was given by a $(1 - b \cos \theta)$ expression, but more recoils were observed below 25 ev than predicted. Although this phenomenon could not be satisfactorily explained, it might have been due in part to a "work function" for removal of the recoils from the surface on which they are formed, and perhaps also to scattering of recoils by the surface.

The recoil spectra for the three cases discussed should differ markedly. Unidirectional emission leads to total recoil momenta equal to the sum of those of β and ν; emission in opposite direction, the difference; and isotropic emission, the vectorial sum, as treated by Libby (*7*). If the neutrino is regarded as a quantum, its momentum can be expressed as E_ν/c, while that of a relativistic β particle (from equation 2) is

$$p_\beta = mv = \left[\frac{E_\beta + m_0c^2}{c^2}\right] v \quad (23)$$

Solving the Einstein relation (equations 1 and 3) for v, we find

$$v = \frac{c\sqrt{E_\beta^2 + 2m_0c^2E_\beta}}{E_\beta + m_0c^2} \quad (24)$$

Substitution of this value into equation 23 gives

$$p_\beta = \frac{\sqrt{E_\beta^2 + 2m_0c^2E_\beta}}{c} \quad (25)$$

for the momentum of the β particle. We may solve directly for the energy of the (non-relativistic) recoil nucleus from the relationship $E_R = p^2/2M$ where p is the resultant of the β and ν momenta in the particular case of angular correlation chosen. Thus

(*a*) For emission in the same direction ($\theta = 0$ deg):

$$E_R = \frac{(p_\beta + p_\nu)^2}{2M} = \frac{536 \times 10^{-6}}{M} \times (\sqrt{E_\beta^2 + 1.02E_\beta} + E_\nu)^2 \text{ Mev} \quad (26)$$

(*b*) For emission in opposite directions ($\theta = 180$ deg):

$$E_R = \frac{(p_\beta - p_\nu)^2}{2M} = \frac{536 \times 10^{-6}}{M} \times (\sqrt{E_\beta^2 + 1.02E_\beta} - E_\nu)^2 \text{ Mev} \quad (27)$$

(*c*) For isotropic emission, as treated by Libby (7):

$$E_R = \frac{p_\beta^2 + p_\nu^2 + 2p_\beta p_\nu \cos\theta}{2M} = \frac{536 \times 10^{-6}}{M} [E_\beta^2 + 1.02E_\beta + E_\nu^2 + 2E_\nu \sqrt{E_\beta^2 + 1.02E_\beta} \cos\theta] \text{ Mev} \quad (28)$$

Figure 2 shows the general features of the spectra for these three cases; the probability $N(E)$ for a given energy partition is taken from the Fermi equation (22), and the recoil energies calculated for a β emitter whose E_{max} is 2.0 Mev. The three curves have the same probability scale (ordinate) and energy scale, and each has been normalized to unit probability.

Chemical studies might prove useful in resolving this uncertainty. From Fig. 2, the fraction of recoils having energies above any given minimum is strongly dependent on the angular correlation of β and neutrino. Consequently, the efficiency of rupture of chemical bonds in the decay process might also show such dependence. In illustration, a bond whose energy is 100 kcal/mol (4.3 ev) might be broken in every case if the angle is near 0 deg, whereas a large fraction of the molecules would remain intact if there is no preferred angle, or particularly if emission tends to occur at angles near 180 deg. Clear-cut results in such experiments should be welcome because of the difficulties in direct determinations of the angular correlation (inability to detect the neutrino, difficulty in detecting recoil nuclei).

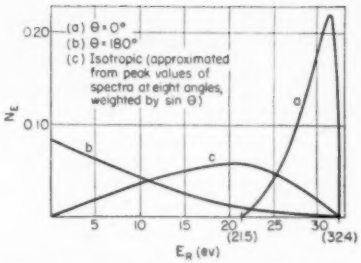

FIG. 2. Recoil spectra for various cases of $\beta - \nu$ angular correlation; $M = 100$ amu, $E_{max} = 2.0$ Mev

The fraction of the recoil energy which may be utilized in bond rupture in such processes has been considered by Suess (8). If the atom M in the molecule Mm is given a momentum p, the resultant energy, $E_M = p^2/2M$, is divided between translational energy of the total mass (E_{M+m}) and internal energy (E_i) of the molecule leading to activation or dissociation. Thus

$$E_M = E_{(M+m)} + E_i \quad (29)$$

If the molecule does not dissociate instantaneously, its kinetic energy (conservation of momentum) must be

$$E_{M+m} = \frac{p^2}{2(M+m)} \quad (30)$$

The difference between this energy and the initial energy of the individual recoil atom must go into excitation or bond strain. Thus

$$E_i = \frac{p_2}{2M} - \frac{p_2}{2(M+m)}$$

or

$$E_i = \frac{m}{M+m} E_M \quad (31)$$

The fraction of the recoil energy available for bond rupture will thus be appreciable if the radioactive atom is bonded to another atom or group of the same or greater mass, and will become small only when a heavy radioactive atom is bonded to a very light partner.

The velocity of a recoil atom after β emission is of the order of 10^5 cm per sec ($M = 100$, $E_R = 5$ ev). This is considerably less than the velocity of orbital electrons.

Under these conditions, orbital electron loss because of acceleration of the nucleus is regarded as unlikely (*32*).

If no disturbance of the orbital electrons occurs, the daughter atom will be in an oxidation state one unit more positive than its parent, since the nuclear charge is increased by one unit. This phenomenon has been observed (*9*) in the case of trivalent La^{143} (19 m half-life) decaying to Ce^{143} (33 h half-life), an experimental minimum of 60% of the Ce being found in the tetravalent state. In the decay of Se^{83} as SeO_3^- ion, only about 35% of the Br^{83} product was found as BrO_3^-, the remainder being present in more reduced forms (*9*). The origin of the reduced bromine species is unclear. If the neutrino is strongly oriented *with* the β particle the resulting recoil energy appears sufficient to disrupt the BrO_3^- ion in the majority of disintegrations. For the other postulated modes of angular correlation, outright disruption seems unlikely. However, in all cases the radioactive BrO_3^- ions which survive the recoil process will be highly excited. The decomposition to BrO^- and O_2 is exergic and may have an activation energy no greater than the excitation from recoil. Radiohypobromite ion thus produced would be counted as reduced bromine in the experiments as would part of its disproportionation products.

The assumption above that orbital electrons are not disturbed by the β process *per se* is, however, insecure. The probability of K-electron ejection subsequent to β emission, according to Feinberg (*10*), is $0.3/Z^2$. The loss of valence electrons is stated to be much more probable. In processes with increase in nuclear charge, the electronic configuration which constitutes the ground state of the atom before the transformation becomes an excited state after the event. Energy which may add up to several hundred electron volts must be dissipated; this may be accomplished through ionization. Thus, chemical effects may follow β decay even when the recoil is small and the presumptive product molecules chemically stable.

α-Particle Emission. The expression for recoil energy in α-particle emission can be simplified to the nonrelativistic form, since the relativistic mass is very nearly equal to the rest mass in all known cases of α radioactivity. Therefore, from equation 10,

$$E_R = \frac{4}{M} E_\alpha \qquad (32)$$

where E is the energy of the α particle, and M is the mass number of the recoil nucleus.

Study of the chemical state of recoil atoms from α decay has not progressed beyond examination of the charge on the particles. Ordinarily the source is a solid foil and the discordant results obtained probably reflect the interaction of the recoil atoms with the varying material of the source and the gas between source and collector (*29*). Two apparently significant determinations of the charge resulting from the nuclear process itself have been reported. McGee (*30*) deposited RaC(Bi) on a highly polished nickel plate taking great care to obtain a very thin clean layer. The RaD(Pb) recoils from the α decay of RaC'(Po), produced in turn by the β decay of RaC, were examined for charge in an ion chamber. The recoils carried an average of one positive electronic charge. The author commented that if the recoils were initially Pb^{++} ions, one charge would probably have been removed by interaction with the nickel foil. Mund, *et al.* (*31*), observed the behavior in an electric field of recoil

RaA(Po) atoms from the α decay of radon at very low pressures and concluded that the average charge carried was close to two positive electronic charges.

The results are not in accord with the rule which predicts self-ionization only if the nuclear velocity exceeds orbital velocities of the least stable electrons (*32*, *33*). The orbital velocities of the first and second valence electrons of Pb calculated from ionization potentials are approximately 1.5×10^8 and 2×10^8 cm per sec, respectively, while the velocity of the Pb atom from a 9 Mev α decay of RaC′ is only 3.9×10^7 cm per sec. The relative velocities for the case of the Po atom from radon decay are yet more disparate. However, the rule has been formulated to deal with collisions of high velocity particles with stationary atoms, whereas a nuclear process intrudes as an additional factor in the case under discussion. The ionization observed may be evidence of a perturbation resulting from the passage of an α particle through the electron shells of the radiating atom or from the abrupt decrease in nuclear charge with loss of the α particle.

γ Emission; Internal Conversion. The transition from one isomeric nuclear state to another usually involves rather small amounts of energy compared with that in β decay. The isomeric transitions which have reasonably long half-lives generally involve energies of only a fraction of a Mev. The recoil energies (Fig. 1) of the nuclei in such low energy processes may be insufficient to produce observable chemical effects.

The problem is best illustrated with an example which has been rather extensively studied. The nuclide Br^{80*} undergoes isomeric transition according to the following scheme:

4.4 h $Br^{80*} \rightarrow$ 18 m Br^{80} + 48.9 kev

The recoil energy of the 18 m Br^{80} nucleus in the emission of a 48.9 kev γ-ray is calculated from equation 13 to be 0.016 ev. This value approximates thermal energies and should not induce chemical changes. However, if the γ-ray is converted in the *L*-shell of the atom, so that an *L*-electron is emitted, the electron has an energy of 47.2 kev, giving the recoil atom an energy of 0.34 ev. This amounts to about 7.8 kcal/mole, which, although it represents an appreciable activation, is still less than the energies of most chemical bonds. Furthermore, conversion in the *K*-shell is much more probable, leading to recoils of only 5.9 kcal/mole.

Nevertheless, Segrè, Halford, and Seaborg (*36*), and, at the suggestion of these, DeVault and Libby (*14*), sought and found a peculiar reactivity for the 18 m Br isomer. The decay of 4.4 h Br^{80*} in $(CH_3)_3Br$ produced 18 m Br separable from the organic products with aqueous HBr (*36*), while that from aqueous BrO_3^- precipitated from ammoniacal solution with AgBr (*14*). Further, Willard (*15*) observed that the daughter isomer from the parent as Br_2 displaces chlorine in CCl_4, while DeVault and Libby (*16*) noted reaction with CS_2. Similar behavior is reported for other compounds of bromine under varied conditions (*8*, *13*, *16*).

Since such reactions are not characteristic of thermal bromine atoms, and since insufficient recoil energy is available to induce them, an alternative explanation was required. This was found in the Auger process of ionization associated with internal conversion. When an electron is ejected from the *K*-shell of the radiating atom, the vacancy is filled by an electron from a higher shell and a characteristic X-ray is emitted. The new vacancy is filled in a similar manner producing a second X-ray. The X-radiation in turn may be internally converted, increasing the number of unfilled orbitals. The

process ends when the vacancies have migrated to the least stable orbitals.

From theoretical calculation on the Auger effect by Wentzel (*38*) and fluorescent yields, DeVault and Libby (*16*) estimated that at least 16% of the transition in Br^{80*} caused loss of all valence electrons, over 60% caused loss of four or more, less than 10% lose only two, and less than 2% lose only one. Cooper (*17*) has calculated the average excess charge on the Br^{80} atom to be 4.7 units after the hole in the *M*-shell is filled. If the Br atom is bound in a molecule this charge will probably be distributed among the various atoms, producing electrostatic repulsions of sufficient force to rupture the bonds. For the case of two atoms 10^{-8} cm apart, each carrying a single electronic charge, the repulsive energy is $e^2/10^{-8} = 2.3 \times 10^{-11}$ ergs, equivalent to 331 kcal/mole, which is greater than the energies of chemical bonds. The highly reactive radioactive ion thus produced may subsequently add directly to neighboring molecules. Or if decomposition of the latter is induced and the radioactive atom remains in the vicinity by virtue of a solvent "cage" effect, combination with a fragment may follow.

The hypothesis that the chemical effects observed in isomeric transition stems from the ionization in internal conversion rather than from recoil was tested by Seaborg, Friedländer, and Kennedy (*18*). With the upper isomer of Zn^{69} in diethyl zinc molecules, no disruption was observed in the isomeric transition. In the case of Te^{127} and Te^{129} as diethyl tellurium, a large fraction of molecules were destroyed. The calculated recoil energy from the Zn^{69} γ-ray is 40 kcal/mole, while that of Te^{127} is 9.2, and of Te^{129} only 6.6. However, the Zn^{69} γ-ray is not converted, and no charge is produced. On the other hand, the γ-rays from the Te isomers are highly converted, ionization should follow, and the observed bond rupture finds an explanation.

As an illustration of the contributions of these studies to nuclear physics, the extent of conversion of the γ-rays of Br^{80} has been shown by chemical methods to be greater than 85% (*35*). Accurate physical measurements in the case of such soft radiations are not easily made, but the efficiency of chemical bond rupture in the isomeric transition can be determined directly.

Nuclear Bombardment

Under the classification of nuclear bombardment is included the wide range of particle bombardments and photon excitations which have now been studied. Bombardment with a given particle or with photons can lead to a variety of stabilizing reactions, depending on the nuclear charge of the target and the bombarding energy. For the present purpose, the reactions will be divided into high-energy (particle and photon) bombardments, and thermal neutron bombardments.

High-energy Bombardments. When a nucleus absorbs a highly energetic bombarding particle, it attains a kinetic energy E_R given by equation 10, and an excitation energy $E - E_R$. The compound nucleus will undergo a stabilization reaction in a period of 10^{-21} to 10^{-6} seconds (*19*): (*a*) usually by particle emission if this is energetically possible; or (*b*) by photon emission if insufficient energy is available for particle emission.

In these processes, the kinetic energy of the bombarding particle, E_1, plus the mass decrease of the reaction in energy units, Q, equals the sum of the kinetic energies of the emitted particle, E_2, and residual nucleus, E_3:

$$E_1 + Q = E_2 + E_3 \qquad (33)$$

This equation holds for any three particle process provided the bombarded nucleus is initially at rest or the kinetic energies are relative to the center of

mass. The relative magnitudes of E_2 and E_3 depend upon the masses of the product particles and the angular correlation, if any, between the bombarding and emitted particles. The energy partition for the case of no angular correlation is treated by Libby (*7*, appendix B).

If the nucleus is highly excited by the bombarding particle, the secondary process may occur within an extremely short time. If the binding energy of a neutron is exceeded, stabilization by neutron emission may occur in 10^{-21} to 10^{-18} seconds (*19*); similarly, if, in addition to the binding energy, the energy equivalent to the Coulomb barrier is supplied, a proton or alpha particle may be emitted within such short periods.

Lifetimes of the excited states will be much longer, however, when a potential barrier must be penetrated, and in general when stabilization occurs by photon emission.* Lifetimes for the latter may extend from 10^{-17} to 10^{-6} seconds (*19*) depending on the spin change and multipole order of the transition. In such cases of relatively long-lived excited states, particularly in condensed media, the compound nucleus may attain near thermal kinetic energy by collisions before undergoing the secondary stabilization process. As an example let us take a recoiling compound nucleus with a reasonable velocity, say 5×10^7 cm per sec., whose life expectancy is 10^{-13} seconds. If its path is to be collision-free until the stabilization process occurs, it must travel several hundred atomic diameters. This is extremely improbable in a liquid, impossible in a close-packed solid, and has only a 50% chance in a gas at atmospheric pressure. A few collisions will, in general, reduce the energy greatly since the collision partner will frequently have a mass near that of the compound nucleus.

For many purposes, therefore, the high energy reactions should be treated as two separate processes particularly when the bombardments are of solids or liquids. The energy equations for the two processes involved can then be written as follows:

PROCESS (*a*):

When the bombarding particle or photon reacts with the nucleus, the momentum of the resulting compound nucleus will be equal to that of the incident particle or photon, so that from equation 10, $E_R = (m/M)E$, where M is the mass of the compound nucleus and E is the incident energy.

PROCESS (*b*):

The compound nucleus will be reduced to near thermal energy by collision, so that the total energy of the secondary process will be the sum of the excitation energy $(E - E_R)$ and the mass-energy released in the overall reaction (Q). Thus, if the subscripts 1, 2, and 3 refer to incident particle, emitted particle, and residual nucleus, respectively, and M is the mass of the compound nucleus:

$$E_2 + E_3 = E_1\left(1 - \frac{m_1}{M}\right) + Q \quad (34)$$

The momenta $(mv)_2$ and $(mv)_3$ are equal, so that

$$\frac{(mv)_2^2}{2m_2} + \frac{(mv)_3^2}{2m_3} = E_1\left(1 - \frac{m_1}{M}\right) + Q \quad (35)$$

Therefore, since $m_2 + m_3 \approx M$,

$$E_3 = \frac{m_2}{M}\left[E_1\left(1 - \frac{m_1}{M}\right) + Q\right] \quad (36)$$

E_3 then is the recoil energy in the secondary process. For heavy nuclei, particularly when Q is large (positive), the equation may be expressed approximately as

$$E_3 = \frac{m_2}{M}(E_1 + Q) \quad (37)$$

* An important reaction of this type is the (d,p), in which the nucleus may attain a high translational momentum without achieving great excitation energy. In the efficient Oppenheimer-Phillips process, the nucleus actually undergoes an (n,γ) reaction with the polarized deuteron.

Equation 36 will apply to all reactions involving particle bombardment and single particle emission. For the $(d,2n)$ reaction, the angular dependence of the emitted neutrons is not known, so that no definite equation can be derived.

For such reactions as the (p,γ) involving photon emission in process (b), the radiation energy may be obtained as a good approximation from the equation neglecting the recoil energy:

$$E_2 = E_1\left(1 - \frac{m_1}{M}\right) + Q \qquad (38)$$

and the recoil energy can be obtained then from equation 13.

No chemical studies of the products of such reactions as those discussed above have as yet been reported. The energetic character of the processes indicates that extensive chemical changes should be induced.

Thermal Neutron Bombardments. The nuclear reactions produced by thermal neutrons are of two types: (a) the (n,γ) reaction which occurs with all stable nuclei, and (b) the $(n, particle)$ reactions, which occur only with nuclei of low atomic numbers, *i.e.*, where such reactions are exergic.

Among the latter are found such reactions as the three (n,p) reactions: $S^{32}(n,p)P^{32}$; $Cl^{35}(n,p)S^{35}$; $N^{14}(n,p)C^{14}$. The recoil energy is given by equation 36, with the simplification that E_1 is essentially zero. The chemical nature of S^{35} produced by neutron bombardment of KCl crystals is now under study. The indications are that it exists in the crystal as S^{VI}, or is in some reactive atomic form which is oxidized in water to $SO_4^{=}$, since the latter form is found to contain all the active S^{35} after the irradiated KCl is dissolved in water (*20*, *21*). The high-energy S^{35} recoils from neutron-bombarded CCl_4 exchange efficiently with the S atoms in CS_2, a reaction which does not occur at ordinary temperatures. A solution 10 volume per-cent CS_2 in CCl_4 was irradiated with neutrons, and about half of the active S^{35} produced was found in the CS_2 molecules (*37*).*

The (n,γ) reaction is the most extensively studied with regard to chemical consequences. Szilard and Chalmers (*22*) found in 1934 that on neutron irradiation of ethyl iodide an appreciable fraction of the radioactive iodine could be obtained as free iodine. This procedure has since proved to be a valuable source of radioactive materials of high specific activity, and has been applied to a large number of elements. The energy released in thermal neutron capture is just the binding energy of the neutron in the new nucleus, and approximates 8 Mev as an average. If this energy is released as a single quantum, a nucleus of mass 100 receives a recoil (equation 13) of 344 ev, or 7950 kcal/mole. This is much greater than the energies of chemical bonds, and should lead to rupture of the parent compound in every case. However, the energy of the nucleus is sometimes dissipated in two quanta of comparable energy. In this case, if one assumes isotropic distribution of the quanta, the recoil spectrum would extend to zero energy for the cases when the two momenta cancel, and a fraction of the parent molecules might remain intact.

In the earliest experiments where solids and liquids were bombarded, it was indeed observed that a good fraction of the radioactive atoms produced were present chemically in the original form. However, the experiments of Suess (*8*) with ethyl bromide in the gas phase showed complete separation of the radioactive Br from EtBr. This served as conclusive evidence that the bonds are broken in every instance, and required an alternative explanation for the so-called "retention" observed in

* The yield of S^{35} by the reaction $S^{34}(n,\gamma)S^{35}$ is unimportant here.

the liquid bombardments. This was found in the Franck-Rabinowitch "cage hypothesis." In liquid alkyl halides, the recoiling halogen atom may collide with atoms either much lighter than itself (C and H) or with those essentially its own weight. In the former cases, only a small fraction of the recoil energy is imparted to the struck particle, whereas in a halogen-halogen collision, much or all of the excess energy may be transferred. If such a collision occurs while the recoil atom still has enough energy to break a C-X bond, it may be immobilized in the vicinity of a reactive free radical or ion. In condensed media, the probability is high that reaction between the two will occur, and this is observed to be the case.

Dilution with a compound of light elements, as demonstrated in the case of CBr_4 and C_2H_5OH (*23*), decreases the probability of halogen-halogen collisions, and thus the probability that the recoil atom will be caught in a reactive cage is correspondingly reduced. Similarly, in the gas phase the probability that the recoil atom will be held in a "cage" following a bond rupturing collision is much reduced.

Characteristic chemical forms of the (n,γ) reaction products are shown in Table 3. In the case of HBr, Suess identified the product as atomic bromine by observing its selective reactivity with acetylene. The reaction normally is photochemical and thus requires atomic Br. The predominance of reduced forms among the products has not been very satisfactorily explained. In the case of $KMnO_4$ in aqueous solution, Libby (*24*) has assumed the rupture of one or more manganese-oxygen bonds, and postulated formation of MnO_3^+, MnO_2^{+3} and even MnO^{+5}, or Mn^{+7}, if the oxygen atoms capture the bonding electron pairs because of greater electronegativity. These unstable species should react rapidly with the aqueous medium. Reactions which might occur are:

TABLE 3

Szilard-Chalmers Reactions

Target Compound	*Chief Disruption Products*
$NaClO_3$	Cl^0, Cl^-
BrO_3^-	Br^0, Br^-
IO_3^-	I^0, I^-
$KMnO_4$	MnO_2
$SeO_4^=$	Se
$SeO_3^=$	Se
$TeO_4^=$	Te
$AsO_4^=$	As^{+5}
AsH_3	As
HBr	Br
RX (Cl,Br,I)	X^0
ϕX	X^0

REDUCTION:

$$4MnO_3^+ + 2H_2O \rightarrow 3O_2 + 4H^+ + 4MnO_2 \text{ (summary of several steps)}$$

HYDROLYSIS:

$$MnO_3^+ + H_2O \rightarrow MnO_4^- + 2H^+$$

$$MnO_3^+ + OH^- \rightarrow MnO_4^- + H^+$$

In acidic or neutral solution nearly all the radioactive manganese is recovered as MnO_2, while in alkaline solution the chief product is MnO_4^-. Thus the reduction reaction appears to predominate in acid, and the hydrolysis by OH^- in alkaline solution.

Nuclear Fission

Measurements of the ionization produced by fission fragments, and of their range in matter by Jentschke (*25*), Flammersfeld (*26*) and others, have given about 175 Mev for the total kinetic energies of the two fragments. Mass numbers between 72 and 158 have been found, with the most frequent split (in U^{235}) at about 95 and 139. From equation 16, the kinetic energy values for these particles are found to be 104 and 71 Mev, respectively. This corresponds to an energy of 1.5×10^{-4} ergs for the light fragment. Its ve-

locity is $v = \sqrt{(2E/M)}$, or about 1.5 $\times 10^9$ cm per sec. This velocity can be compared with that of orbital electrons by use of the Bohr equation giving an approximation of the latter:

$$v = \frac{2\pi e^2}{nh} Z_{eff} \qquad (39)$$

For a fission fragment of atomic number 45, the effective nuclear charge, Z_{eff}, for a single electron in the N-shell ($n = 4$; 29th electron) is very approximately $45 - 28 = 17$ so that $v = 9 \times 10^8$ cm per sec, or somewhat less than that of the recoil nucleus. A similar calculation for one electron in the M-shell gives a value of $v = 2 \times 10^9$ cm per sec, which is somewhat greater than the recoil velocity. Thus the estimate suggests that a fission fragment loses its N, O, etc., electrons, and some of its M electrons, yielding an ion with charge $> 10e$, perhaps as high as $20e$. More precise treatments of the problem have been given by Knipp and Teller (*32*) and Bohr (*33*).

Perfilov (*27*) reported experimental values of about $20e$ from measurements of mv/e in observation of fission product recoil tracks on photographic plates. Lassen (*28*) deflected the recoils with a cyclotron magnet, and determined charge values of $20e$ for the light fragment and $22e$ for the heavy fragment. As yet the chemical behavior of these energetic, highly ionized atoms has not been described.

* * *

NOTE: The valuable assistance of Prof. C. D. Coryell and Prof. M. Deutsch of MIT is gratefully acknowledged.

BIBLIOGRAPHY

1. O. Hahn, F. Strassmann, *Naturwissenschaften*, 1938 ff.
2. Nuclei Formed in Fission, *J. Am. Chem. Soc.* **68**, 2411 (1946)
3. J. C. Jacobsen, *Phys. Rev.* **70**, 789 (1946)
4. D. R. Hamilton, *Phys. Rev.* **71**, 456 (1947)
5. R. F. Christy, E. R. Cohen, W. A. Fowler, C. C. Lauritsen, T. Lauritsen, *Phys. Rev.* **72**, 698 (1947)
6. C. W. Sherwin, *Bull. Am. Phys. Soc.* **22**, No. 6, 5 (1947)
7. W. F. Libby, *J. Am. Chem. Soc.* **69**, 2523 (1947)
8. H. Suess, *Z. physik. Chem.* **B45**, 312 (1940)
9. H. Geat, R. R. Edwards, T. H. Davies, Plutonium Project Record, IX B, Chap. 3
10. E. L. Feinberg, *J. Phys.* (USSR) **4**, 424 (1941)
11. C. Gerthsen, E. Grimm, *Z. Physik* **120**, 476 (1943)
12. C. Chamie, San-Tsiang Tsen, *J. Phys. Radium* (8), **2**, 46 (1941)
13. L. J. LeRoux, C. S. Lu, S. Sugden, *Nature* **143**, 518 (1939)
14. D. C. DeVault, W. F. Libby, *Phys. Rev.* **55**, 322 (1939)
15. J. C. Willard, *J. Am. Chem. Soc.* **62**, 256 (1940)
16. D. C. DeVault, W. F. Libby, *J. Am. Chem. Soc.* **63**, 3216 (1941)
17. E. P. Cooper, *Phys. Rev.* **61**, 1 (1942)
18. G. T. Seaborg, G. Friedländer, J. W. Kennedy, *J. Am. Chem. Soc.* **62**, 1309 (1940)
19. H. Bethe, "Elementary Nuclear Theory," (John Wiley and Sons, New York, 1947)
20. J. C. Willard, Am. Chem. Soc. Meeting, April, 1947, Atlantic City, N. J.
21. R. R. Edwards, unpublished
22. L. Szilard, T. A. Chalmers, *Nature* **134**, 462 (1934)
23. W. F. Libby, *Science* **93**, 283 (1941)
24. W. F. Libby, *J. Am. Chem. Soc.* **62**, 1930 (1940)
25. W. Jentschke, *Z. Physik* **120**, 165 (1943)
26. A. Flammersfeld, P. Jensen, W. Gentner, *Z. Physik* **120**, 450 (1943)
27. N. A. Perfilov, *Compt. Rend. Acad. Sci.* (USSR), **28**, 4268 (1940)
28. N. O. Lassen, *Kgl. Danske Videnskab. Selskab, Mat.-fys. Medd.* **23**, No. 2, (1945)
29. E. Rutherford, J. Chadwick, C. D. Ellis, "Radiations from Radioactive Substances," Section 31, (Cambridge University Press, New York, 1930)
30. H. D. McGee, *Phil. Mag.* **13**, 1 (1932)
31. W. Mund, P. Capron, H. Jodogne, *Bull. Soc. Chim. Belg.* **40**, 35 (1931)
32. J. Knipp, E. Teller, *Phys. Rev.* **59**, 659 (1941)
33. N. Bohr, *Phys. Rev.* **59**, 270 (1941)
34. E. J. Konopinski, *Phys. Rev.* **72**, 518 (1947)
35. E. G. Bohlman, J. E. Willard, *J. Am. Chem. Soc.* **64**, 1342 (1942)
36. E. Segrè, R. S. Halford, G. T. Seaborg, *Phys. Rev.* **55**, 321 (1939)
37. R. R. Edwards, F. B. Nesbett, A. K. Solomon, *J. Am. Chem. Soc.* **70**, 1670 (1948)
38. G. Wentzel, *Z. Physik* **43**, 524 (1927)

Nuclear Physics of the Deuteron and Other Two-Particle Phenomena—I*

The phenomenological approach to the problem of two-particle nuclear systems reviewed here is shown to provide a direct means for deducing the fundamental nuclear forces

By M. E. ROSE

Oak Ridge National Laboratory, Oak Ridge, Tennessee

THE PRIME IMPORTANCE of experimental and theoretical investigations of scattering of slow and fast neutrons and of protons by hydrogen nuclei has often been stressed in nuclear-physics literature. Together with the study of the properties of the deuteron which constitutes the bound or stationary state of the neutron-proton system, these problems may be said to form the keystone of nuclear physics. This becomes apparent when one considers that the description of all nuclear phenomena is almost entirely dependent on a knowledge of the forces acting between nuclear particles. Only with two-particle nuclear systems is the problem sufficiently simple to entertain any hope of obtaining such knowledge. Moreover, to the extent that nuclear forces act essentially between pairs of particles only, study of two-particle problems must take precedence over all others.†

One may attempt to deduce the nature of these forces in either of two ways:

1.) The deductive or field-theoretic approach wherein, on the basis of certain postulates concerning the interaction between mesons and nucleons, one attempts to account for the forces acting between the latter type of particles as a manifestation of the (virtual) emission and absorption of mesons by nucleons (*1*). Unfortunately the meson-field theory program has been beset by many difficulties and thus far has not been particularly successful.

2.) The inductive or phenomenological approach wherein one makes a model of the forces; that is, one assumes these forces to have a certain dependence on distance between nucleons and on other parameters and then compares the predictions of calculations based on these assumptions with the results of experiment. While such heuristic methods are somewhat less elegant than the methods of field theory, they offer greater hope of success in the near future. This article is entirely concerned with the attempt to deduce nuclear forces by this second method.

It will be recognized that in constructing models one follows the path used so successfully in the study of many other physical phenomena. The

* Part 2, the second half of this paper, will appear in the July NUCLEONICS. It includes, along with an appendix to the whole paper, a discussion of scattering of neutrons by ortho- and parahydrogen, *p-p* scattering, interaction with electromagnetic radiation, and noncentral forces.

† There is some theoretical reason for supposing that many-body forces, depending on the simultaneous coordinates of three or more particles, may exist. However, these forces are very probably of secondary importance and should be admitted only when the supposition of two-particle forces alone has demonstrably failed. In any case two-particle forces, which do exist, can be studied independently in two-particle phenomena.

situation may be compared with the deduction of the gravitational interaction from the empirical data of planetary motion. Unfortunately the nuclear problem seems somewhat less simple inasmuch as the nuclear forces appear to be more complicated in their dependence on distance and, moreover, are dependent on other quantities as well (see Section *I* below).

Aside from the problem of nuclear forces, the two-body problems are of particular significance for another reason connected with the techniques available for solving the problem at hand. This may be understood from a comparison with the atomic problem. In the interpretation of spectroscopic data and other problems pertaining to atoms, one starts with the important advantage that the interaction energy is essentially a known quantity—the Coulomb inverse square force between charged particles.*

The only problems which can be solved with essentially complete precision are those dealing with the motion of a single (valence) electron in the central field of the nucleus. This is the situation for the hydrogen atoms and hydrogen-like (alkali) atoms. For other atoms, with more than one valence electron, or with unclosed shells, the electrons move in the noncentral field due to the nucleus *and* the other electrons. However, because of the small electronic mass and the consequent rapid motion of these electrons, it is a good approximation to replace the interaction with other electrons by the average central field they produce. In this way, with the aid of elaborate numerical procedures, a highly accurate representation of the state of affairs in all atoms may be obtained.

The situation with nuclei is quite different. In place of the weakly interacting electrons in the long-range force field of the nucleus, we have strongly interacting nucleons subject to short-range forces (see *I* below). There is no predominant central particle as in the atomic case. On the average, nucleons are about 2×10^{-13} cm apart which is approximately the range of the nuclear forces. Their interaction energy is of the order of or greater than the kinetic energy $p^2/2M$, where p is the momentum and M the nucleon mass. The momentum is readily estimated from the uncertainty principle which, applied here, states that $pr_{av} \sim \hbar$ $(= h/2\pi)$ and r_{av} is the average distance apart. With $M = 1.6 \times 10^{-24}$ gr this gives an interaction energy of 5 Mev. In contrast, electrons in atoms, separated by distances of order 10^{-8} cm, interact with an energy of only a few ev. Thus, the approximation procedure described above cannot be applied to nuclei with any hope of success. Instead of considering one particle at a time, one must treat all of them simultaneously. This many-body problem is mathematically prohibitive, to say the least. However, the difficulty disappears in the case of very light nuclei, notably two-particle systems.

* Some complication enters because electrons, as well as atomic nuclei, possess an angular momentum due to spin and a magnetic moment, and these properties profoundly affect many atomic phenomena. However, these effects are now very well understood and quantitatively well accounted for.

I. Qualitative Consideration of Nuclear Forces

From a comparison of the binding energies of the deuteron (2.18 Mev) and the alpha-particle (28 Mev) one concludes that the interaction energy V between nucleons is of short range and has the form of a narrow deep well as pictured schematically in Fig. 1. Here $V < 0$, corresponding to attraction. The range r_0 of the interaction is defined so that V is essentially zero for

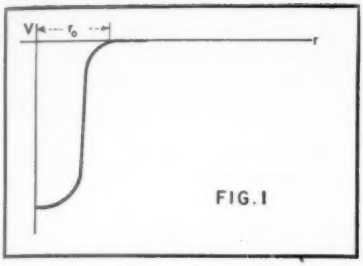

FIG. 1

the mutual distance between nucleons $r > r_0$.

The argument, according to Wigner, is as follows: If the range were large, then the ratio of binding energies would be approximately equal to the ratio of interacting pairs, *i.e.*, to 6. Actually the experimental ratio is 13, greater by a factor of about 2. With short-range forces we gain an advantage for the alpha particle in that additional attractions contract the nucleus sufficiently to bring all the pairs within the range of the nuclear forces, while in the deuteron the particles spend only a small fraction of the time within the range of mutual interaction. If the neutron and proton in the deuteron spent considerable time within the range of interaction, the kinetic energy $p^2/2M \sim \hbar^2/2Mr^2_{av}$ would become too large to permit the formation of a stable deuteron. The existence of a narrow deep well is all that one can predict with certainty about the spatial dependence of the forces. However, for many questions, the details of the shape of the well is not of decisive importance as long as it is narrow and deep.

The scattering of neutrons by protons and by ortho- and parahydrogen molecules, discussed in *IV* and *V* below, shows that the interaction energy between neutron and proton depends on the total spin angular momentum of the system of two particles. In addition one must admit the possibility of a dependence of the interaction on the orbital angular momentum of the particles around their common center of gravity. This must be true not only for the forces between neutrons and protons but also for the forces between any pair of nucleons.

This fact follows from the basic empirical result that the binding energy of nuclei is closely linear with the number of particles in the nucleus, that is, proportional to the mass number A. If the forces were of the ordinary type, dependent only on the distance between particles, it would follow that the nuclear binding energy would increase as the number of pairs of particles, that is, with A^2. From the linear dependence of binding energy one must conclude that in some way each nucleon interacts only with its near neighbors or with a limited number of other nucleons no matter how many particles there are in the nucleus as a whole.

This situation is a familiar one in the behavior of certain types of molecules which exhibit the same property of saturation of binding. For example, two hydrogen atoms form a stable H_2 molecule but the binding of a third hydrogen atom to form stable H_3 is not possible. This phenomenon has been completely accounted for in the molecular case by recognition of the identity of the two electrons in the H_2 molecule as a consequence of which the electrons have the possibility of exchanging their roles. This exchange is complete in that not only the positional coordinates but also the spin coordinates of both electrons are interchanged. The formal recognition of this property* leads to forces which are spin-dependent and account for the saturation of binding energy.

In an analogous fashion, similar spin-dependent (Heisenberg) forces, but

* This amounts to introducing the fact that identical particles with spin ½ (in units $\hbar$) must conform to the Pauli exclusion principle.

with different spatial dependence, have been introduced in attempting to account for nuclear phenomena. These forces would have to be attractive for the ground state of the deuteron in which, from the measured spins of the particles ($\frac{1}{2}\ \hbar$ for neutron and proton, $1\ \hbar$ for the deuteron), the neutron and proton spins are parallel. The property of these spin forces is such that in the case of antiparallel spin orientation they provide repulsion. Now in the alpha particle (spin 0), the neutron and proton spins cancel and are antiparallel in pairs.* Consequently this type of spin-dependent force, acting alone, would not yield the highly stable configuration of two neutrons and two protons that the alpha particle is known to be. One would expect the deuteron to be very tightly bound, whereas, in actuality, the binding energy per particle is less for the deuteron than for any other stable nucleus.

To avoid this difficulty non-spin-dependent forces have also been introduced in the nuclear force model. However, to satisfy the requirement of saturation these must not be ordinary forces. It has been postulated by Majorana that such forces involve an exchange of the positional coordinates, but not the spins, of the interacting nucleons. While the detailed mechanism of such "exchanges" is of no concern for the following, it is helpful, for the purpose of forming mental pictures, to regard this exchange as taking place by virtue of the meson emission and absorption as described by Primakoff (*1*). It can be shown that such forces must then depend on the orbital angular momentum of the particles and that they also lead to saturation and therefore to linearity of binding energy with mass number.

The forces described above, as well as a third type involving exchange of spins only, are referred to as *exchange forces.* In each case, for a given spin and orbital angular momentum, the force or energy of interaction depends only on the magnitude of the vector distance between particles. Such forces are therefore central forces and, since no direction in space is preferred, they lead to a spherically symmetric distribution of both neutrons and protons around the center of gravity of the nucleus. Thus, nuclei would have no electric dipole moment or higher multipole moments including electric quadrupole. The latter is defined as

$$Q = [r^2(3\ \cos^2\theta - 1)]_{av}$$

where θ is defined as the angle between a fixed axis and the line joining the nucleon to the center of gravity. For a spherically symmetric nucleus $(\cos^2\theta)_{av} = \frac{1}{3}$ and $Q = 0$. However, the deuteron has been observed to have a quadrupole moment (*2*) whose measured value is

$$Q = 2.73 \times 10^{-27}\ \text{cm}^2 \qquad (1)$$

One must therefore conclude that the particles are not distributed in a spherically symmetric manner; in fact, the deuteron must be cigar-shaped because $Q > 0$. Also the nuclear forces cannot be wholly central. However, since Q is small compared to the "geometrical cross section" of the deuteron ($0.60 \times 10^{-24}\ \text{cm}^2$) one can conclude that the noncentral forces are comparatively small.

In the case of the deuteron, as in other nuclei with nonvanishing spin, there is a preferred direction in space, namely, the direction of the spin momentum. Therefore, the existence of a quadrupole moment demands the introduction of noncentral forces depending on the orientation of the vector

* It is also necessary to state that what is measured is the total angular momentum which is the vector sum of spin and orbital angular momenta. However, the orbital angular momenta of the nucleons in the alpha-particle are zero since otherwise there would be repulsion due to centrifugal force and we would not obtain the most stable configuration corresponding to the ground state.

joining neutron and proton relative to the spin direction. There is actually some logical basis for the introduction of noncentral forces from the field theory where these forces take a form resembling the interaction between two classical magnets. Since these forces are small—and for most of the phenomena to be considered their effect is only of order of a few percent in the final results (see *VIII*)—they shall be ignored in the main part of the discussion. A re-examination of the two-particle problems in the light of the existence of noncentral forces will be undertaken in section *VIII*.

II. The Data of Two-Particle Phenomena

The data pertaining to two-particle systems from which one may attempt to deduce the nuclear forces is obtained from the following experiments:

(1) The measurement of the binding energy of the deuteron, $\epsilon_1 = 2.18$ Mev. This gives information about the interaction between neutron and proton in the state with parallel spins and zero orbital angular momentum. In the notation of spectroscopy, this is the $^3S_1$ state.* The letter S implies orbital angular momentum $L = 0$. States with $L = 1, 2, 3 \cdots$ are denoted with the letters P, D, F respectively. The superscript 3 implies that spin angular momentum is unity and a vector of magnitude unity can have three orientations in which its component in a given direction is 0 and ± 1. In general, for a spin vector with magnitude S' the number of orientations, or the multiplicity, is $2S' + 1$. The subscript in the above notation is the total angular momentum J, which is the vector sum† of L and S' and whose magnitude for the ground state of the deuteron has the measured value 1.

(2) The scattering of neutrons by protons. Particular attention must be given to the scattering process in which the neutron energy is 10 Mev or less. As will be discussed in greater detail below, the scattering of neutrons in this energy range is appreciable only if the centrifugal repulsion, and therefore the orbital angular momentum, has the value zero. In this case the collisions are head-on and we speak of the scattering of S neutrons, ($L = 0$). For P neutrons, with orbital angular momentum 1, the centrifugal barrier corresponds to a classical distance of closest approach which, in the energy range cited, is greater than the range of the forces; consequently such neutrons do not interact appreciably with the proton and suffer very little scattering. Since the neutron and proton spins in the scattering process can be either parallel or antiparallel, the low-energy scattering provides information about the $^3S_1$ and $^1S_0$ interactions. For higher-energy scattering, which has not been sufficiently well investigated as yet, one would expect to obtain information about the ^3P and ^1P interactions, etc.

(3) The scattering of protons by protons. For protons of energy less than about 10 Mev, only particles with $L = 0$ can be scattered appreciably. However, protons are identical particles obeying the exclusion principle. Two protons cannot have the same quantum numbers and, since S protons have essentially the same orbital angular momentum, they must have opposite spin directions. Hence only the ^1S interaction can be studied in this

* Actually, because of noncentral forces the ground state contains a small admixture of ^3D, corresponding to orbital angular momentum equal to 2 units.

† According to quantum mechanical rules, vectors are added in such a way that the magnitude of the resultant may assume a finite number of values, with consecutive values differing by unity. When adding L and S' the magnitude of the resultant varies from $L + S'$ to $|L - S'|$. Of course, here $L = 0$ and $J = S'$.

energy range. Again at higher energies the P interaction would presumably come into play and the exclusion principle permits only the ^3P.* Measurements of the scattering up to 15 Mev have not as yet shown conclusive evidence for P scattering.

(4) The quadrupole moment of the deuteron.

(5) The scattering of very slow neutrons by ortho- and parahydrogen. Here one again measures the ^3S and ^1S neutron-proton interaction. In the scattering by a single proton, triplet and singlet scattering are incoherent. Consequently, as will be seen, one cannot determine from such measurements whether or not the ^1S state is stable. The comparison of scattering in ortho- and parahydrogen depends on interference effects and is coherent. On this basis the question of stability of the ^1S state can be settled. The same evidence can be obtained from the observations of neutron diffraction by hydrogen-containing crystals (*3*).

The experiments involving interaction of nucleons and electromagnetic radiation, photodisintegration of the deuteron, and radiative capture of neutrons in hydrogen yield no new information about forces. Here, in the photodisintegration, the ^3P interaction is involved in final state after the deuteron has been dissociated, but the effect of nuclear forces is a refinement beyond the reach of present experimental accuracy.

It will be seen that, aside from the small effect of noncentral forces, only three experimental parameters referring to neutron and proton are available from experiment: the binding energy of the ^3S bound state, and the ^3S and ^1S scattering; the latter is only incompletely measured by scattering with single protons. Therefore, in the central force approximation, a model with no more than three parameters may be adopted. Of course, one can measure the neutron-proton scattering at several energies. Agreement between theory and observations would then indicate that the parameters, range, and depths of potential wells, say, were energy-independent. On the other hand, if the parameters defined in terms of a specific spatial dependence for $V(r)$ are energy-dependent, this is an indication that the form chosen for $V(r)$ is incorrect. In fact, observation of the scattering at all energies can be used, in principle, to determine the analytical form of $V(r)$ which involves essentially the specification of an infinite number of parameters.

With noncentral forces a model with four parameters can be used. Since this involves an additional type of interaction at least one extra parameter is necessary.

For the specifically nuclear interaction between two protons, one has only the scattering measurements. However, as is discussed below, the requirement that the interaction parameters, range, and depth of well be energy-independent permits a determination of these two quantities. The requirement that the forces should be energy-independent has no logical basis other than the fact that energy dependence should be a relativistic effect and would therefore be expected to be small for nuclei. This is apparent inasmuch as the decisive parameter measuring the importance of relativistic effects is $\left(\frac{velocity}{c}\right)^2 \approx 5 \times 10^{-3} \ll 1$.

It will be noted that no direct information concerning neutron-neutron forces is forthcoming from a study of two-particle phenomena. Such information is first obtained when one considers the problem of accounting for the binding energy of H^3.

* The rule is: If L is odd (even), then S' is even (odd).

III. The Ground State of the Deuteron

In accordance with the above, a model with three parameters is used. In the absence of precise scattering measurements over a wide energy range, it is necessary to make an assumption for the analytical form of the potential well. Four models have been used:

(a) "Square" well

$$V(r) = -V_1 \text{ (constant)}, \quad r < r_0 \qquad (2)$$
$$= 0 \qquad r > r_0$$

(b) Exponential well

$$V(r) = -V_1 e^{-2(r/r_0)} \qquad (3)$$

(c) Gaussian well

$$V(r) = -V_1 e^{-(r/r_0)^2} \qquad (4)$$

(d) Meson potential

$$V(r) = -V_1 \frac{e^{-(r/r_0)}}{r} \qquad (5)$$

In each case V_1 (> 0) is the depth of the well for the triplet (S) interaction, r_0 the range. For the singlet (S) interaction, the depth is V_0 with the shape of the well otherwise identical with that pertaining to the triplet state. Thus, the assumption is made that the range is spin-independent. It will be noted that the parameters r_0, V_1, V_0 have a specific meaning only in terms of the special forms assumed in (2) . . . (5), so that the values of these parameters obtained by using different models need not be the same. For the sake of analytical simplicity, the square well (2) is used in the following.

For the ^3S ground state, the known binding energy provides one relation between the depth V_1 and range r_0:

$$\sqrt{M(V_1 - \epsilon_1)} \cot\left(\frac{r_0\sqrt{M(V_1 - \epsilon_1)}}{\hbar}\right) = -\sqrt{M\epsilon_1} \qquad (6)$$

Details of derivation are given in the Appendix published with the second half of this paper next month. A more convenient form of (6) is obtained by expanding in powers of r_0. With V_1 in units Mev and r_0 in units 10^{-13} cm, we have with sufficient accuracy

$$V_1 r_0^2 = 102 + 9.6 r_0 + 2.6 r_0^2 + \ldots \qquad (7)$$

It has been customary to adopt the values $r_0 = 2.8 \times 10^{-13}$ cm. The evidence for this value is rather indirect. First, one finds that this is the range which accounts for the proton-proton scattering with an energy-independent square well ^1S interaction. Second, the difference between the observed binding energies of He^3 and H^2 is very closely equal to the calculated value of the Coulomb energy due to the repulsion of the two protons in He^3. Since the spins of like particles are oppositely aligned in H^2 and He^3, one may conjecture that in the ^1S state, at least, the nuclear forces are independent of the presence or absence of charge on the nucleon. Therefore, the ^1S range in the neutron-proton interaction would be 2.8×10^{-13} cm and, on the basis of the assumed spin-independence of the range, this value would apply to the triplet interaction. For $r_0 = 2.8$ in (7) the well depth is 19.0 Mev.

Unfortunately, for the argument, the range can be deduced fairly directly from scattering measurements and the simple theory of the deuteron ground state. Using the ortho-para-hydrogen scattering measurements (*4*) one finds $r_0 = (1.5 \pm 0.4) \times 10^{-13}$ cm and from the neutron diffraction measurements $r_0 = (1.6 \pm 0.3) \times 10^{-13}$ cm. An average value, $r_0 = 1.55 \times 10^{-13}$ corresponds to $V_1 = 50.4$ Mev. In order to resolve this uncertainty, one may attempt to use the scattering data for high-energy neutrons by protons. Unfortunately a decision cannot be made partly because of the relative insensitivity of the scattering data with range and partly because of the complications due to the presence of noncentral forces (*5*).

It is convenient to treat the scattering problem and to present the results in terms of a coordinate system which moves with the velocity of the center of gravity of the two particles involved in the collision. This coordinate system will be referred to as the C system whereas actual observations are made in the laboratory or L frame of reference in which the proton is initially at rest. In the C system the total momentum of the two particles before and after collision is zero. Because the particles here considered have equal mass, the conservation of energy and momentum requires that the velocities before and after collision of each particle have the same value $\frac{1}{2}v$, where v is the initial velocity of the neutron in the L system. The collision on the C system is schematically represented in Fig. 2(a), where the full and dashed arrows represent velocity or momentum vectors before and after the collision, respectively, and ϑ is the scattering angle in the C system.

Translation of results back to the L system is carried out very simply. If θ and ϕ are the scattering angle of the neutron and the recoil angle of the proton, $\boldsymbol{v}$, $\boldsymbol{v}'$ and $\boldsymbol{v}''$ the initial, final neutron velocities and the recoil proton velocity, respectively, we have from energy and momentum conservation

$$v^2 = v'^2 + v''^2 \text{ and } \boldsymbol{v} = \boldsymbol{v}' + \boldsymbol{v}'' \qquad (8)$$

so that these vectors form a right triangle and

$$\theta + \phi = \pi/2 \qquad (9)$$

See Fig. 2(b). Adding the velocity $\frac{1}{2}\boldsymbol{v}$ to the final neutron and proton velocities in the C system, we find

$$\theta = \tfrac{1}{2}\vartheta \qquad (10)$$

The energy in the C system is the energy of two particles with velocity $v/2$; *i.e.*

$$E = 2 \cdot \tfrac{1}{2}M(v/2)^2 = \tfrac{1}{4}Mv^2 = \tfrac{1}{2}E_0$$

where $E_0 = \frac{1}{2}Mv^2$ is the neutron energy in the L system.

The purpose of the scattering observations is to measure the scattering cross section. The differential scattering cross section $\sigma(\vartheta)$ is defined as the number of neutrons scattered per second per solid angle at angle ϑ when there is one incident neutron per second per cm^2. The total cross section σ is defined as the total scattering rate per unit incident flux. Thus

$$\sigma = \int \sigma(\theta) d\Omega \qquad (11)$$

where $d\Omega = \sin\vartheta d\vartheta d\varphi$ is the element of solid angle. The total cross section is the same in C and L systems.

The quantum mechanical description of the scattering is the following. In the absence of scattering, the incident beam of neutrons traveling in the z direction with undisturbed momentum p is represented by a plane wave:*

$$\Psi_{\text{inc}} = e^{ipz/\hbar} \qquad (12)$$

With the scattered wave, we add a spherical wave progressing outward from $r = 0$ where the scatterer is located so that the total wave, far from the scattering center, is

$$\Psi = e^{ipz/\hbar} + f(\vartheta)\frac{e^{ipr/\hbar}}{r} \qquad (13)$$

Here $f(\vartheta)$ is the amplitude of the scattered wave which may depend on scattering angle. Since the density of particles in the outgoing wave is $|f/r|^2$, the total number passing in unit time through an element of area dS on a sphere of radius r with velocity v is $v|f(\vartheta)|^2/r^2 \times dS$. Now $dS = r^2 d\Omega$, and the density in the incident beam, from (12), is unity; incident flux $= v$, so that the scattering per solid angle is

$$\sigma(\vartheta) = v\frac{|f(\vartheta)|^2}{r^2}\frac{r^2 d\Omega}{v d\Omega} = |f(\vartheta)|^2 \qquad (14)$$

The methods of obtaining the scattering amplitude f depend on a solution of the wave equation already given

* Throughout we omit a time factor $e^{-\frac{i}{\hbar}Et}$ where E is the energy.

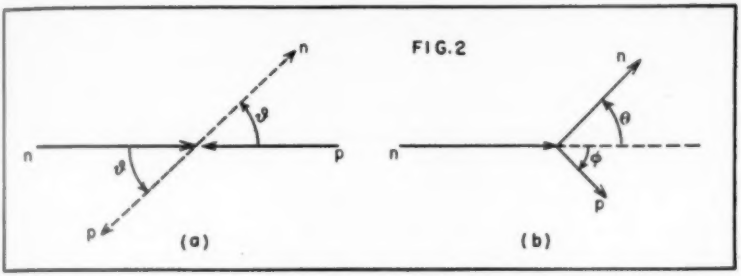

in the Appendix. We omit details† but present Fig. 3 as an aid to the understanding. Curve (1) represents a neutron wave in the absence of the potential well due to the proton. Its kinetic energy is everywhere the same and the (deBroglie) wavelength is constant. In the presence of the proton [curve(2)], the kinetic energy is greater because of the attractive force for $r < r_0$ and the wave starts out with a shorter wavelength corresponding to a more rapid oscillation. Beyond r_0, the kinetic energy is back to its undisturbed value and so is the wave length $\lambda = \hbar/p$. As a consequence of the potential hole, the wave has suffered a phase shift η which measures the effect of the scattering. It can be shown that, for the case illustrated, which is the scattering of S-waves or head-on collisions,

$$f(\vartheta) = \text{a constant in angle} \quad (15)$$

In fact, f is the lateral displacement in a horizontal direction between curves (1) and (2) outside the potential well.

The important conclusion to be drawn is that, in the C system, the *scattering of slow neutrons is isotropic.* According to (10), the observed scattering per unit solid angle in the L system is

$$\sigma_L(\vartheta) = \text{const. } \cos\theta \quad (16)$$

This result is well established by experiment for all neutron energies up to at least 10 Mev. At about this energy the neutron wavelength becomes equal to the range of the forces and the effect of the scattering of P waves should become observable.

In fact, if we consider a particle of mass M passing a scattering center with velocity v, the angular momentum is Mvd were d is the distance of closest approach. Quantum-mechanically, the orbital angular momentum takes on values $L\hbar$, where L is an integer. For P waves, $L = 1$ and the energy at which P scattering begins to be appreciable is that corresponding to $d = \hbar/Mv = r_0$ or $\lambda = r_0$. The observation of the consequent deviations from spherical symmetry in the angular distribution would be of the greatest importance since one can decide from the nature of such deviations (forward or backward scattering) whether the P interaction is repulsive or attractive. From quantitative information of this kind a decision as to the exchange nature of the forces can be made.‡

Until recently measurements by several investigators of the scattering at about 15 Mev gave conflicting re-

† The reader may consult H. A. Bethe, "Elementary Nuclear Theory" (John Wiley & Sons, Inc., New York, 1947).

‡ All force models must give the same attractive S wells so that one learns nothing of the orces from the scattering of S-neutrons.

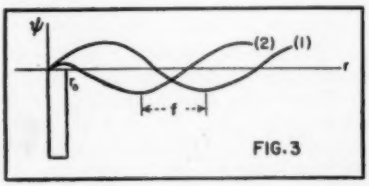

sults. However, the results of the Berkeley group using 90-Mev neutrons demonstrated fairly conclusively the exchange nature of the forces. At such high energies one must expect strong forward scattering if ordinary forces alone were operative. For small momentum losses, corresponding to small θ, the incident and scattered neutron waves have the same wavelength, and the consequent constructive interference favors small angle scattering. However, if exchange forces are present, the proton and neutron effectively interchange identity. The proton can also come out in the forward direction, the neutron in the backward direction. The observed results were that, in addition to the forward peak, there is also a backward peak. This provided the first direct evidence for the existence of exchange forces.

Returning to the scattering of slow neutrons, the total cross section for neutrons of energy E_0 with spin parallel to that of the proton is found to be

$$\sigma_1 = 4\pi f_1^2 = \frac{4\pi\hbar^2}{M}\frac{\beta_1}{\epsilon_1 + \frac{1}{2}E_0} \quad (17)$$

where the depth of the triplet well has been eliminated and the directly measured binding energy introduced by (6). The factor β_1 depends on r_0 and ϵ_1, and for small r_0 is given by

$$\beta_1 = 1 + r_0\sqrt{M\epsilon_1/\hbar} + \cdots$$

Since the measurements are usually made with hydrogen in molecular or combined form, it is necessary to restrict our consideration to energies for which the effect of molecular binding (omitted in the above) is negligible. The vibrational level spacing in molecules is of order 0.1 ev and above about 1 ev the proton may be considered free. At this energy and for a considerable range above it, σ is practically energy-independent. The cross section in this range, given by (17), is 4.30 barns, the measured value (6) is 21 ± 1 barn (1 barn = 10^{-24} cm^2).

This discrepancy, as Wigner was the first to recognize, is due to the omission of the singlet scattering. This is given by an expression corresponding to (17) with ϵ_1 replaced by $|\epsilon_0|$ where ϵ_0 is the energy in the singlet state.*

$$\sigma_0 = \frac{4\pi\hbar^2}{M}\frac{\beta_0}{|\epsilon_0| + \frac{1}{2}E_0} \quad (18)$$

Because the spin angular momentum for the triplet state is capable of three orientations and for the singlet state only one orientation is possible, and because all these are equally likely, in 3 out of 4 cases scattering will take place with parallel spins. Therefore,

$$\sigma = \tfrac{3}{4}\sigma_1 + \tfrac{1}{4}\sigma_0 \quad (19)$$

The necessity for singlet scattering different from triplet scattering is a direct indication of the spin-dependence of the nuclear forces.

Since the measured σ is so much larger than σ_1, it is clear that σ_0 must be large and, therefore, that $|\epsilon_0|$ must be small. Thus $\beta_0 \approx 1$. From the values quoted for the constants which enter σ, one finds $|\epsilon_0| = 0.069$ Mev. The sign of the singlet energy and, therefore, the question of the existence of a stable excited ^1S state cannot be decided on the basis of measurements described so far. This question is taken up in section V to be published next month.

BIBLIOGRAPHY

1. H. Primakoff, NUCLEONICS, **2**, No. 1, 2 (1948)
2. J. M. B. Kellogg, I. I. Rabi, N. F. Ramsey, J. R. Zacharias, *Phys. Rev.* **57**, 677 (1940); A. Nordsieck, *Phys. Rev.* **58**, 310 (1940)
3. C. G. Shull, E. O. Wollan, G. A. Morton, W. L. Davidson, *Phys. Rev.* **73**, 262 (1948)
4. R. B. Sutton, T. Hall, E. E. Anderson, H. S. Bridge, J. W. DeWire, L. S. Lavatelli, E. A. Long, T. Synder, R. W. Williams, *Phys. Rev.* **72**, 1147 (1947)
5. W. Sleator, Jr., *Phys. Rev.* **72**, 207 (1947)
6. H. B. Hanstein, *Phys. Rev.* **59**, 489 (1941)

* ϵ_1 was written in (17) since $\epsilon_1 > 0$. It should be emphasized that the meaning of ϵ_0 is mathematical rather than physical since what enters into the singlet cross section is r_0 and V_0 the singlet well depth; ϵ_0 is an abbreviation for a function of r_0 and V_0 given by (6) with ϵ_1 replaced by $|\epsilon_0|$ and, in view of the nonbound nature of the ^1S state (see Section V), with the sign of the right-hand side of (6) changed.

Beta-ray Measurements and Units

Authors have developed an instrument, using a photomultiplier tube and standard radioactive source, for making beta-ray measurements in terms of a newly proposed unit. Comments are made on the disadvantages of presently used units.

By M. BLAU and J. E. SMITH

Canadian Radium and Uranium Corp.
New York, New York

WITH THE INCREASED availability of radioactive isotopes for medical, biological and industrial research, the problem of suitable instrumentation, and consequently units of measurement, has presented itself. There is the need for a practical and rugged instrument for routine measurements covering a wide range of magnitudes, and for a convenient unit in which to express beta radiation.

The use of the units "millicurie" or "rutherford" (*1*) in measurements of the number of disintegrations per second neccessitates an exact knowledge of the disintegration schemes and the efficiency of the instrument for the particular type of radiation. In addition, other factors, *e.g.*, the absorption which the radiation suffers before entering the instrument, the amount of reflected radiation, and the exact geometrical arrangement, have to be known.

Actually the exact number of disintegrations can be determined only if comparative measurements are made using as a standard a known quantity of the same radioactive element and measuring both under exactly the same conditions;* otherwise, additional calculations, taking into account the variations, will be necessary.

A unit proposed especially for medical research is the "roentgen equivalent physical" or rep. According to the definition by Evans (*1*), a dose of 1 rep is obtained if the energy lost by ionization processes in one gram of tissue (1 sq cm of irradiated surface) is equal to the energy loss of one roentgen of gamma radiation absorbed in 1 gm of air. In the same paper, the meaning and significance of the roentgen unit for gamma and X-radiation is very extensively explained and the methods for measuring this unit are described.

Evans emphasizes that the roentgen does not involve any precise physical information about the quality and intensity of the radiation, but compares the ionization effect of radiation quantities. The ionization effect is measured in special ionization chambers, the so-called thimble chambers, which reproduce the conditions prevailing in the interior of an irradiated body.

No attempt will be made here to recommend replacement of the roentgen unit as far as X- and gamma radiation are concerned. However, in the case of beta radiation, it appears that a more convenient unit is desirable.

The most serious objection to the use of this unit is the impossibility of measuring it in a simple way. Even if

* A method for measuring the absolute radioactive strength was proposed by Wiedenbeck (*2*); however, this method necessitates complicated apparatus and highly skilled personnel.

measurements in small thimble chambers are made, it is difficult to arrive at a value for the total energy dissipated in the irradiated tissue without knowledge of the effective range of the beta particles.

The ionization effect produced in a volume element of air, *e.g.*, in one cc, is proportional to the energy loss caused by phenomena connected with the absorption processes. Furthermore, this value is proportional to the biological effect in a medium of similar absorption conditions.

In the case of penetrating gamma or X-radiation, the ionization effect in the small thimble chamber is proportional to that in large chambers containing 1 gm of air or offering a radiation path equivalent to about 800 cm in air and is similarly proportional to the energy dissipated in 1 gm of tissue. Therefore, the ionization current in the thimble chamber expressed in r units, for instance, is a measure of the biological effectiveness.

On the other hand, the beta radiation of most of the radioactive isotopes cannot penetrate 1 gm per sq cm of tissue or an equivalent amount of air, and correct results can only be obtained using ionization chambers large enough to cover the total range of the beta radiation under investigation. However, the dimensions required for this purpose would make the method inconvenient and impractical.

An additional criticism of the rep is explained by the following:

Assume that we are working with beta radiation of an average energy of 0.4 Mev. One millicurie, or 3.7×10^7 beta particles of this radiation, if completely absorbed, gives approximately 8.5×10^4 ergs per hour, or 4.25×10^4 ergs per hour if the tissue is irradiated from the outside and reflected radiation does not interfere. Therefore, the total energy available is about 500×83 ergs.

However, if we follow the definition

$$1 \text{ rep} = \frac{83 \text{ erg}}{\frac{1 \text{ gm}}{\text{cm}^2} \text{ tissue}}$$

we would correlate to this amount of available energy a biological effect of $\frac{4.25 \times 10^4}{83 \times 0.12} = 4280$ rep because the average range of the particles in question will be about 0.12 gm per sq cm of tissue.

Selecting now a radiation of 1.6 Mev, an average energy four times as great, and an equal number of particles, we would associate with this larger amount of total energy available a smaller dose of only 2600 rep because the average range of the beta particles in this case is about 0.76 gm per sq cm.

Thus, it seems that the rep unit is not entirely satisfactory. Whereas it indicates the ionization density in the affected tissue, it does not take into account the amount of tissue which actually is affected, nor does it give any information about the total energy administered.

The complexity of living matter and the interdependency of parts of the body to the whole make it logical to assume that the total energy supplied must also be of biological importance. Therefore a unit of dose indicating this amount, and at the same time the range of energy of the radiation would be more convenient and suggestive than a purely theoretical value like the rep which may even lead to erroneous conclusions.

A more convenient unit would be a quantity proportional to the total number of ions formed by the incident radiation. It is self-evident that there exist different methods which when accordingly applied would give the desired value in terms of the proposed unit.

The purpose of this paper is to describe a convenient and practical measurement method which can be used by persons not very familiar with radioactive measurements. This method is based on the use of a photomultiplier

tube and appropriate low persistence fluorescent screens, emitting light in the range of maximum sensitivity of the photocell. Because of the difficulty encountered with the dark current in this type of photocell, it is not advisable to extend the use of this method for intensities less than 1 to 5 microcuries, depending upon the energy of the particles.

For lower intensities, Geiger-Müller tubes, or the photomultiplier tube as a particle counting element (*3*), will have to be used and the energy of the particles leaving the sample will have to be determined by adequate absorption measurements. However, there is a definite lack of instruments for higher intensities and this consideration led to the development of the following method:

Theory

The beta particles striking the fluorescent screen are absorbed in the luminous compound and the energy dissipated along their path is transformed into energy of light. In the case of alpha particles (*4*) or cathode rays (*5*), the maximum light output is obtained when the thickness of the screen is equal to the range of the particles in the material or actually somewhat smaller because of the so-called "dead zone" which depends on the type of luminous compound. If the screen thickness is smaller, we do not utilize the total available energy and, in the opposite case, we lose light energy by optical absorption in the screen material.

The conditions are different if we deal with penetrating beta radiation whose path in the screen is approximately 1 mm and greater. Therefore, the light absorption is already appreciable for thicknesses much lower than the range of the particles.

If μ_1 is the absorption coefficient of the beta particles in the luminous compound, and μ_2* the optical absorption coefficient for the emitted light, the total light output L for a screen thickness t smaller than the range of the particles is given by

$$L \sim \int_0^t \mu_1 e^{-\mu_1 x} e^{-\mu_2 (t-x)}\, dx$$

$$= \frac{\mu_1}{\mu_2 - \mu_1} e^{-\mu_2 t}\left[e^{t(\mu_2 - \mu_1)} - 1\right]$$

$$= \frac{\mu_1}{\mu_2 - \mu_1}\left[e^{-\mu_1 t} - e^{-\mu_2 t}\right] \qquad (1)$$

In this equation, it is assumed that the beta radiation is absorbed according to a simple exponential law, which, for practical purposes, introduces only a negligible error.

The screen thickness t_{max} for which maximum light output is reached can be found by differentiation of equation 1 and is

$$\mu_1 e^{-\mu_1 t_{max}} = \mu_2 e^{-\mu_2 t_{max}} \qquad (2)$$

or

$$t_{max} = \frac{\ln \mu_2 - \ln \mu_1}{\mu_2 - \mu_1} \qquad (2a)$$

The absorption coefficient μ_2, which can be determined experimentally, remains constant for all measurements in which the same screen material is used. Therefore, equation 2 or 2*a* can be used to compute the value of μ_1, if, in the special problem, t_{max} has been established.

The light output L_{max} for t_{max} is proportional to

$$L_{max} \sim A \frac{\mu_1}{\mu_2 - \mu_1}\left(e^{-\mu_1 t_{max}} - e^{-\mu_2 t_{max}}\right) \qquad (3)$$

where A is the total amount of energy which is available from the incident radiation, corresponding to values of $\mu_2 = 0$ and absorption thickness of such an order of magnitude that $e^{-\mu_2 t}$ becomes zero.

Because all the constants μ_1, μ_2 and t_{max} can be measured or computed from the respective equations, the reading of the photocurrent at maximum light

---

* μ_2 also includes scattering, absorption, etc.

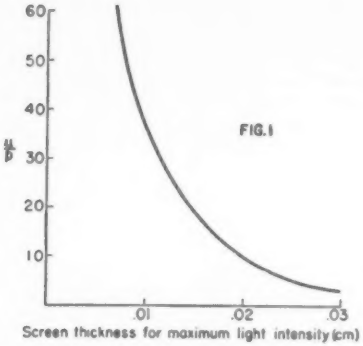

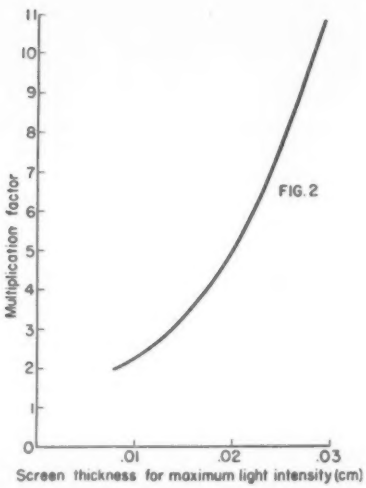

output is a measure of the total ionization energy available.

Using equation 2*a* and selecting a luminous compound with the effective density $\rho = 3.3$ and the light absorption coefficient $\mu_2 = 80$, we obtain the graph in Fig. 1, where μ_1/ρ, the mass absorption coefficient for the beta radiation, is plotted versus t_{max}.

From this curve, we can calculate the values $\mu_1 t_{max}$ and $\mu_2 t_{max}$ for different values of t_{max} and therefore, the factor $F = \frac{\mu_1}{\mu_2 - \mu_1}(e^{-\mu_1 t_{max}} - e^{-\mu_2 t_{max}})$ in equation 3. Figure 2 represents $M = 1/F$ as a function of t_{max}. M is the multiplication factor with which the reading of the photocurrent at maximum light output has to be multiplied to obtain the total energy corresponding to the radiation incident on the screen.

Figure 3 gives the functional relationship between the energy of the beta particles and the respective values of t_{max}. The curve was calculated using the energy-range data for beta rays (*6*) on the assumption that $e^{-\mu R} = 0.00068$. The latter relation can be determined from this same curve, using known values of μ and R for certain elements.

In Fig. 4 are plotted the respective values of particle range in mg/cm² versus t_{max}. These graphs may be useful for the calculation of the volume element which actually is affected by the ionization process.

Experiment and Calibration

A source of RaD-E-F deposited in a shallow disc of 0.5 × 1 cm² and covered with an aluminum foil of 0.5 mm thickness was brought to a distance of 4.5 mm from the screen surface which was directly in front of the window of the photomultiplier tube. The light output of the photocell was measured with screens of various thicknesses* and the curve of Fig. 5 represents the functional relationship between photocurrent and screen thickness. The maximum current is obtained at a screen thickness of 0.15 mm. From Fig. 1, it can be seen that this thickness corresponds to $\mu/\rho = 16.6$, which is in fair agreement with the experimental value of 16 (*7*) for the beta particles from RaE.†

* We wish to express our appreciation to Dr. S. Isenberg of General Luminescent Corporation, Chicago, who prepared the screens.

† The difference is due to experimental errors (*7*), especially in the determination of the light absorption coefficient.

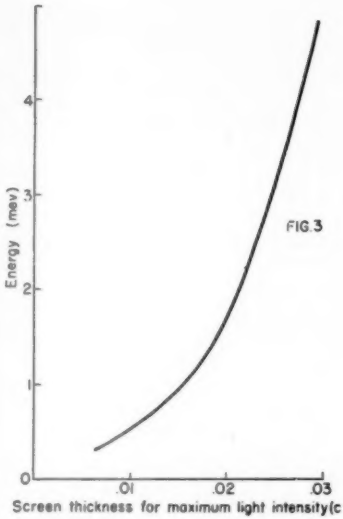

FIG. 3

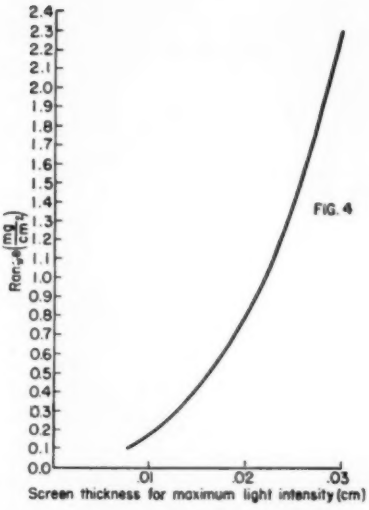

FIG. 4

From the curve in Fig. 2, we can establish the multiplication factor with which the photocurrent at optimum screen thickness has to be multiplied to give a magnitude proportional to the total energy available.

All measurements are corrected for the same sensitivity of the photocell by using a radioactive light standard (*8*) based on the alpha emission of a radium preparation. However, in order to obtain absolute values of the radiation energy present, in millicurie × ergs, the combination of photocell and fluorescent screen has to be calibrated.

For lack of a pure beta-ray source of known radioactive strength, we used a radon capillary of 0.1 mm glass thickness. The energy loss due to absorption and scattering in the glass wall is 45%. The light effect due to the gamma radiation can be neglected in comparison to the beta radiation.

Figure 6 gives the photoelectric current in arbitrary units versus the screen thickness *t*. The maximum value of ordinate multiplied by the corresponding value from Fig. 2 is a measure of the total beta radiation energy emitted.

The beta particles of RaB + RaC in equilibrium with 1 gm of radium produce, when completely absorbed, $3.25 \times 10^{14} \pm 6.4 \times 10^{14}$ ion pairs in standard air.

The measurements were made with a radon capillary of 1.64 millicurie at a distance of 4.5 mm from the screen.

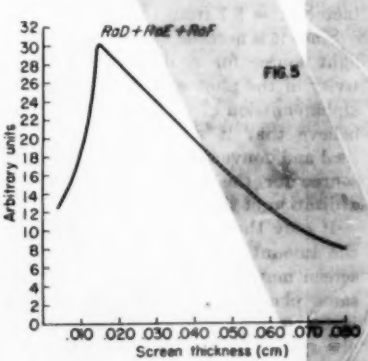

FIG. 5

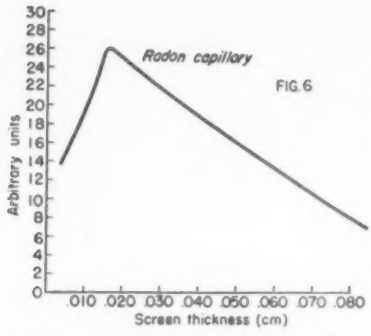

To overcome the difficulty of correctly computing the solid angle of the incident radiation, we calculate the total number of ion pairs for the total radiation emitted in the half sphere and assume that any other preparation of equal dimensions, and at the same distance, will strike the screen with the same fraction of the half-sphere radiation.

The beta radiation leaving the radon capillary would give rise to 4.33×10^{11} ion pairs, if the half-sphere radiation is measured and if an amount corresponding to the 45% absorption within the glass is subtracted. This value of 4.33×10^{11} ion pairs corresponds, in our specific experimental arrangement, to a photocurrent of 21.4 microamperes, obtained from Fig. 6, multiplied by the factor $M = 3.7$ from Fig. 2.

Since it is necessary to use a constant light source for controlling the sensitivity of the photocell (in our case the alpha emission of a radium source), we believe that it would be more practical and convenient to utilize the same source for the calibration and standardization of the instrument.

If only the light output depends on the amount of energy dissipated in the screen material, one should expect the same photocurrent for equal energies, irrespective of the somewhat different absorption mechanisms for alpha and beta particles.

The percentage of alpha particle energy emerging from the preparation was determined by the measurement of the ionization current due to the alpha particles and comparison of this value with the gamma activity of the foil.

This foil, provided with a diaphragm of 0.5×1.5 sq cm, was measured in the photocell arrangement at the same distance as the radon capillary with a screen of necessary thickness corresponding to the range of the alpha particles.

In order to take into account the differences in area between the exposed radium foil and the radon capillary, measurements with a stronger foil were made using a diaphragm of 0.5 mm and 0.1 cm width. From the relationship, current (.5)/current (.1) = $5f$, we find the factor f with which the value of the photocurrent has to be multiplied in order to obtain geometrical conditions identical with that of the radon capillary. In other words, we assume that the quantity of radium deposited on an area of 0.5×1.5 sq cm is concentrated on an area of 0.1×1.5 sq cm.

Taking the above corrections into account, we arrive at the number of ion pairs, $n = 6.8 \times 10^{10}$, produced per second by the alpha particles leaving the preparation.

The experimental value of photocurrent* corresponding to this quantity is 13.3 microampere, found after having subtracted the effect due to the beta particles of RaB + RaC.

Comparing now the two experimental values of the beta radiation from the 1.63 millicurie radon capillary and the alpha radiation from the radium preparation, we find the relation

$$C_{\beta,\,\text{radon}} : C_{\alpha,\,\text{Ra}} = 6.03,$$

where C = current.

The two calculated values of ion pairs are

* The correction factor due to the light absorption in the screen is negligible.

$IP_{\beta,\,\text{radon}} : IP_{\alpha,\,\text{Ra}} = 6.36$,

where IP = ion pairs.

The relationship between the photocurrent obtained with the RaD-E-F preparations mentioned above and the corresponding value with the radon capillary are given by

$$C_{\beta,\,\text{RaD}} : C_{\beta,\,\text{radon}} = 1.23$$

This relationship was obtained by taking into consideration the respective values of the multiplication factors, as was done previously. If the energy of the beta radiation from 1 millicurie (RaB + RaC) [according to heat measurements (*9*)] is 2.57 times the energy of the beta radiation from 1 millicurie RaE, the photocurrent would correspond to an apparent* radioactive strength of 2.82 millicuries.

If the mean energy of the beta radiation of RaE is 0.35 Mev, the photocurrent should correspond to an ionization value equivalent to 5.32×10^{11} ion pairs.

Now, if we compare the photocurrents obtained with the RaD source and the alpha standard, we get

$$C_{\beta,\,\text{RaD}} : C_{\alpha,\,\text{Ra}} = 7.42$$

and therefore find that the number of ion pairs is 5.05×10^{11}. The RaD-E-F source was furthermore compared with a set of decayed radon seeds filled at a known time with a known amount of radon. The amount of RaE in the seeds was calculated to be 0.412 millicurie. The loss due to absorption and scattering in the 0.08 millimeter glass wall of the seeds was measured to be 33%. The radon seeds were combined and measured in an ionization chamber and compared to the ionization current of the RaD-E-F preparation. The relation between the two currents was found to be

$$C_{\text{RaD}} : C_{\text{seeds}} = 10.8$$

Therefore, the ionization current produced by the RaD-E-F preparation corresponds to

$$C_{\text{RaD}} \sim 0.412 \times 0.67 \times 10.8$$
$$= 2.98 \text{ millicurie}$$

The agreement between the theoretical and experimental values is satisfactory and proves the applicability of the radioactive light standard for this type of measurement. The deviation of 6% is probably due to experimental errors, especially in the measurement of absorption coefficients. It is an interesting fact from an experimental and theoretical standpoint that the efficiency of the luminous compound is the same for alpha and beta particles if the absorption of the radiation is properly taken into account.

The great advantage of using a constant radioactive source is evident. Furthermore, this procedure provides measurements completely independent of the type of beta radiation under investigation and, therefore, represents an absolute method of beta measurements. It is intended to extend and test this method for various artificially radioactive elements.

Furthermore, it seems likely that the method could be improved by the use of organic phosphors like naphthalene (*3c*). These phosphors are more transparent to their fluorescent light than inorganic phosphors. Therefore, the thickness of the fluorescent layer, corresponding to the maximum light output, is greater, thus improving the sensitivity of the method. For calibration and standardization purposes, a constant beta or gamma source is more advisable than alpha-particle-emitting sources.

There still remains the problem of expressing the results in the most convenient unit.

From the measurements, we obtain directly the optimum screen thickness, which furnishes us with the energy or range, respectively, (Fig. 3 or Fig. 4) of the radiation. On the other hand, Fig. 2 gives us the multiplication factor

* The self-absorption of the beta radiation in the radioactive layer and the absorption in the aluminum foil are not taken into consideration.

FIG. 7. Photomultiplier tube and power supply enclosed in lightproof box.

with which the photocurrent at optimum screen thickness has to be multiplied. The result compared with the photocurrent due to the radioactive alpha standard is a direct measure of the total ionization energy (the product of number of millicuries times ergs).

If it is desirable to know the quantity of ions per unit energy or unit range, Fig. 3 or Fig. 4 has to be consulted.

This method enables us to obtain one of the proposed units, either Q or Q/E or Q/R, where Q is the total number of ions, E the energy and R the range of radiation.

Description of Apparatus

A 931-A photomultiplier tube, with its 900-volt battery power supply, was enclosed in a lightproof metal box (Fig. 7). The photocell was mounted in a horizontal position and directly beneath it was fastened a circular disc with ten fluorescent screens mounted on radii of the disc. The disc was movable so that it was possible to place each one of the screens, in succession, directly under the photocell window. The radioactive preparation under investigation was placed on a small table directly beneath the disc and in the same line with the tube window. The output current was detected and measured by a microammeter. For very small activities the current of the photocell was amplified by a conventional d-c amplifier.

BIBLIOGRAPHY

1. R. D. Evans, NUCLEONICS **1**, No. 2, 32 (1947)
2. M. L. Wiedenbeck, *Phys. Rev.* **72**, 974 (1947)
3. (a) R. S. Sherr, *Rev. Sci. Instr.* **10**, 767 (1947); (b) J. S. Allen, *Rev. Sci. Instr.* **10**, 739 (1947); (c) J. W. Coltman, Fitz-Hugh Marshall, NUCLEONICS **1**, No. 3, 58 (1947)
4. M. Blau, B. Dreyfus, *Rev. Sci. Instr.* **16**, 245 (1945)
5. H. W. Leverenz, *J. Optical Soc. Am.* **27**, 25 (1937)
6. M. D. Kamen, "Radioactive Tracers in Biology," p. 48 (Academic Press, Inc., New York, 1947)
7. G. Hevesy, F. A. Paneth, "A Manual of Radioactivity," p. 229 (Oxford University Press, London, 1938, 2nd Ed.)
8. M. Blau, I. Feuer, Radioactive Light Sources, *J. Optical Soc. Am.* **36**, No. 10, 576–870 (1946)
9. Ellis, Wooster, *Proc. Roy. Soc.* **A117**, 109 (1927); Mosley, Robinson, *Phil. Mag.* **28**, 327 (1914); Gurney, *Proc. Roy. Soc.* **A109**, 540 (1925); Meitner, Orthmann, *Z. Physik* **60**, 143 (1930)

NUCLEONIC EVENTS

GERMAN REPRESENTATIVE TO AID EDITORIAL BOARD

Last month NUCLEONICS announced commencement of the formal cooperation of six European scientists with its Editorial Board. To this distinguished list of scientists, NUCLEONICS is pleased to add the name of Dr. Hans Kopfermann, who will represent Germany. A brief sketch of Dr. Kopfermann's achievements is presented below:

Hans Kopfermann

(Germany)

Dr. Kopfermann, author of the book "Nuclear Moments," completed his studies at Göttingen University in 1924 and participated in the significant research done at the famed Institute for Physical Chemistry (Kaiser Wilhelm-Institute) in the late 1920's. This period, devoted chiefly to research on optics and nuclear moments, was highlighted by his discovery of negative dispersion.

A Rockefeller Foundation fellowship, awarded in 1932, gave him two fruitful years of nuclear physics research under Niels Bohr in Copenhagen. After four more years spent at the Kaiser Wilhelm-Institute in Berlin, Dr. Kopfermann left to accept a professorship at Kiel University in 1937. In 1942 he transferred to Göttingen. The Nazi government did not attach war significance to his research, enabling him to continue a relatively normal routine during these years.

As head of the nuclear research division of Göttingen University's physics department, Dr. Kopfermann, besides lecturing, directs a modest laboratory. Nuclear charge distribution and betatron research are the channels along which he and his five assistants are directing present efforts.

EDITOR'S NOTE: *The future scope of German nuclear physics research remains in doubt, pending further clarification of pertinent provisions under Allied Control Council Law 25 (Control of Scientific Research). This factor plus equipment shortages leads Dr. Kopfermann and his associates to expect better results from theoretical rather than experimental research in the immediate future. They are hopeful of progress in the betatron field, providing stringent limitations are not imposed. Likewise, they view German cosmic-ray research optimistically.*

REPORT ON PHYSICS RESEARCH IN SWITZERLAND

Research in physics in Switzerland is being carried on in the following places —the Eidgenössische Technische Hochschule, or the Federal Institute of Technology in Zürich, which is the only Swiss university, and also six other universities, each supported and governed by its own canton. They are the Universities of Zürich, Basel, Bern, Lausanne, Geneva, and Neuchatel. Research in physics is also going on in several independent institutes, probably the best known being Hochalpine Forschungstation Jungfraujoch. Most of the research in industrial research laboratories is on a small scale with the exception of that at the Brown Boveri Company (Baden).

Several of the research centers have set up nuclear physics divisions.*

In the Federal Institute of Technology (known as "ETH") nuclear research is centering around photonuclear effect with the Li 17-Mev

* Survey made by the Office of Naval Research (London office).

gamma ray; photodisintegration of the deuteron; K-capture problems utilizing a curved-crystal spectrometer; absolute intensity of gamma rays; (p,n) reactions, mainly in sulfur; and beta-ray spectrography.

At the University of Basel (under the direction of P. Huber) nuclear physics research is concerned with properties of Geiger-Müller counters; neutron reactions in ionization chambers at high temperature, particularly for obtaining Q-values; and the electron multiplier as a counter.

The University of Geneva's physics department, directed by J. Weigle, has set up a nuclear physics division which is studying absorption and diffraction of neutrons from the (d,d) reactions; nuclear induction by the Bloch method. (Other studies are being made on X-ray diffraction and bent crystal for gamma-ray diffraction, also microwaves at 1.25 cm for diffraction studies of crystal models.)

Jungfraujoch is conducting research in cosmic rays and the ozone layer of the atmosphere. No special nuclear physics program is under way at present.

At the Brown Boveri Company, research is not concerned specially with nuclear research. However, under R. Wideroë, there is a research program on betatron development. Also, there is a microwave program, including the study of magnetrons.

OAK RIDGE TO GIVE ISOTOPE TECHNIQUE COURSES

Announcement is made of a series of three one-month courses to be held at Oak Ridge this summer in the techniques of using radioisotopes. The courses will be conducted by the Oak Ridge Institute of Nuclear Studies.

The courses will be held from June 28 to July 23, August 2 to August 27, and August 30 to September 24. Application forms and additional information may be obtained from Dr. Ralph T. Overman, acting head of the Institute's Department of Special Training, P. O. Box 117, Oak Ridge, Tennessee.

The course will not attempt to cover any special field of application in chemistry or biology but will be based on simple chemical experiments selected and designed to give participants a maximum knowledge and ability in the techniques of handling and carrying on research with radioisotopes. Participants in the second of the three courses will be selected by the Atomic Energy Commission. Personnel of the other courses will be selected from qualified applicants, with preference given to persons connected with organizations which are now engaging in research utilizing radioisotopes, or planning such research. Thirty-two participants will be selected for each course.

A fee of $25.00 will be charged for the course. Participants will be expected to pay their own travel and living expenses. Dormitory or hotel accommodations will be provided in Oak Ridge at the usual rates.

BROOKHAVEN, BERKELEY TO BUILD LARGE ACCELERATORS

Plans for construction of two huge particle accelerators have been announced by the Atomic Energy Commission. A 30-foot, three-billion-electron-volt proton synchrotron will be built at the Brookhaven National Laboratory, Upton, New York, and a 110-foot, six-billion-electron-volt synchrocyclotron will be built at the Radiation Laboratory of the University of California, Berkeley.

Design of the $3,000,000 Brookhaven machine, construction of which will take three years, was done by a group at Brookhaven, headed by M. S. Livingston, chairman of the accelerator project at the Long Island laboratory.

The Berkeley machine will cost $9,000,000, and it will take approxi-

mately five years to be completed. Nearly finished with the design is a group which includes William Brobeck, Robert Serber, Robert Thornton, E. M. McMillan, Wilson Powell, and W. Panofsky. The cyclotron will have a ring-shaped magnet, requiring about 10,000 tons of steel. The radius of the magnet will be 55 ft; its length, from the outside limits, will be 140 ft. The magnet will operate from a 5,000 kw source.

KODAK SCIENTISTS RECORD TRACK OF ELECTRON

Eastman Kodak Company has announced that its scientists, using a new photographic emulsion, have successfully recorded tracks of electrons. This is believed to be the first definite identification of electron tracks, the company indicated. Tracks were reported from the University of Montreal in 1946. But the Kodak tracks, first obtained at the company's research laboratory at Harrow, England, and later in Rochester, are long enough to remove all doubt as to their identity.

The number of developed silver grains per track in the emulsion ranges from six to a maximum of twenty-eight. The length of the path in the emulsion is about 0.002 in.

GE ESTABLISHES GRADUATE SCHOOL AT HANFORD

A graduate school of nuclear engineering has been established by the General Electric Company for its employees at the Hanford Works, Richland, Washington. Five institutions —University of Washington, Washington State College, University of Oregon, Oregon State College and the University of Idaho—have agreed to co-operate by granting credit toward degrees for work done. F. Ellis Johnson, formerly engineering dean at the University of Wisconsin, has charge of the program for GE, which operates the plant for the Atomic Energy Commission.

BRITISH PROPOSE RADIOACTIVITY HEALTH BILL

A bill to protect the health of workers and the public from the harmful effects of exposure to radioactive substances, natural or artificial, has been introduced in the British House of Lords. Radium and radon and certain irradiating apparatus, principally X-ray tubes, are covered by its provisions.

Regulations by the appropriate minister will impose codes similar to those under the British Factories Act for the protection of employees in hospitals, laboratories and industrial establishments not already covered by legislation, where radioactive substances or irradiating apparatus are manufactured, treated, stored, or used. The disposal of radioactive waste will be controlled and regulations may be made to prevent injury during the transport of these substances.

Only medical and dental practitioners, or persons working under their directions, who hold a license from the Minister of Health, will be allowed to use certain apparatus and radioactive substances for treating patients. The supply of such substances to the public in the form of medicines or toilet preparations will be illegal except under the authority of a prescription from a licensed practitioner.

The bill also empowers the Minister of Supply to manufacture, process, and distribute radioactive substances and to make orders prohibiting or regulating their import and export.

AEC SETS MINIMUM PRICES FOR URANIUM

The Atomic Energy Commission has announced a three-point program for stimulating the discovery and production of domestic uranium. The major elements of the program are: government guaranteed ten-year minimum prices for domestic refined uranium, high-grade uranium ores and mechani-

cal concentrates; a bonus of $10,000 for the discovery and production of high-grade uranium ores from new domestic deposits; and government guaranteed three-year minimum prices for the low-grade carnotite- and roscoelite-type uranium-vanadium ores of the Colorado plateau area and government operation of two vanadium-uranium plants there.

Circulars describing the ore-buying program are available from the AEC offices at Washington, D. C.; Grand Junction, Colorado; and 70 Columbus Ave., New York, N. Y.

GERMAN RESEARCH GROUPS FORM SOCIETY

A society of German research institutes, known as the "Max Planck Gesellschaft zur Förderung der Wissenschaften," was formed recently. The new society has been approved by the Bipartite Board, after consultation of German representatives with the proper authorities.

Charter institutes of the new society include the following (name of director appears in parentheses):

BRITISH ZONE: Kaiser Wilhelm Institute (K. W. I.) for Instrument Design, Göttingen (Konrad Beyerle); K. W. I. for Physics, Göttingen (Werner Heisenberg).

AMERICAN ZONE: K. W. I. for Medical Research (Richard Kuhn), Institute for Chemistry (Richard Kuhn), and Institute for Physics (Walter Bother), all at Heidelberg.

NEWSON TO CONSULT ON REACTORS

Henry W. Newson, formerly a member of the design committee (in charge of control) for the high-flux pile at Oak Ridge, has been retained as a full-time consultant on nuclear reactor design by the H. K. Ferguson Company, industrial engineers and builders who are erecting the pile at the Brookhaven National Laboratory.

MIT ESTABLISHES GRADUATE SCHOOL AT OAK RIDGE

A school of engineering practice for graduate training in the engineering aspects of atomic energy is being established by MIT for its own engineering students in the production plants of the Atomic Energy Commission operated by the Carbide and Carbon Chemicals Corporation at Oak Ridge, Tenn., according to an announcement by Thomas K. Sherwood, dean of engineering of MIT.

Admission to the new school is restricted to graduate students in the several engineering departments of MIT who have been in residence at MIT at least one term. The program is open only to United States citizens and every student must be cleared by the AEC before he will be considered for admission.

Walter G. Whitman, head of the department of chemical engineering at MIT, will be in charge of the new school of engineering practice, and the educational program at the Oak Ridge station of MIT will be directed by William A. Reed, with one or more assistant directors.

SECOND BRITISH PILE TO START OPERATION

Britain's large-scale atomic energy pile will be in operation this summer, according to a recent announcement from the Ministry of Supply. This is the second British pile to be set up by the Atomic Energy Establishment at Harwell, Berkshire. It is said that the big pile will produce enough radioactive isotopes to supply the needs of all the medical and other scientific research workers investigating peaceful uses of atomic energy in Great Britain. It will also provide the first domestic application of atomic energy—by providing the heat for all the buildings at the Harwell research station.

The second pile will be a big brother

to the "GLEEP" (Graphite Low Energy Experimental Pile) which was set going last year. Production of isotopes —which will have a much greater activity than those now produced in the GLEEP—will be stepped up considerably.

The GLEEP itself produced in March a record total of over 120 samples of chemicals transformed into radioactive forms by exposure in the pile. A third of these were used at Harwell; the rest went to hospitals and research laboratories all over the country. So far, isotopes of about 30 elements have been produced. The one prepared in the largest quantity has been radiosodium, most of which has been used in hospitals for diagnostic purposes, particularly in vascular diseases. Other isotopes have gone to cancer research institutions, among others.

Products of the Harwell piles are to be packaged and distributed by the government-controlled Radiochemical Center at Amersham, Buckinghamshire. Considerable progress has been made at Harwell in designing safe packages for shipment of radioactive materials, so that if an accident befell in transit no radioactive substance would escape. —*McGraw-Hill World News*

GENERAL ELECTRIC FORMS NUCLEONICS DEPARTMENT

The formation of the Nucleonics Department, General Electric Company, with responsibility for the operation of the Hanford Works at Richland, Washington, and for contractual administration and negotiations in connection with the G-E Nucleonics Project has been announced by Charles E. Wilson, company president.

Roy C. Muir, who recently retired as company vice president and general manager of the Apparatus Department, has returned to active service as general manager of the new department, Mr. Wilson announced. Headquarters are at the Hanford Works, atomic energy plant which GE is operating for the Atomic Energy Commission.

The G-E Chemical Department formerly had responsibility for the activities now centralized in the new department. Mr. Wilson stated that the Knolls Atomic Power Laboratory here will continue to be operated by the company's Research Laboratory for the Atomic Energy Commission.

Future Issues Will Feature . . .

RADIOTOXICITY OF INHALED OR INGESTED RADIOACTIVE PRODUCTS

. . . by *Waldo E. Cohn*

PARTICLE DETECTION WITH MULTIPLIER TUBES

. . . by *James S. Allen*

INTERACTION OF ISOTOPIC RADIATION WITH MATTER—II

. . . by *Rex G. Fluharty*

NEUTRON DIFFRACTION AND ASSOCIATED STUDIES

. . . by *E. O. Wollan* and *C. G. Shull*

PRODUCTS and MATERIALS

LEAD SHIELD

Instrument Development Laboratories, 229 W. Erie St., Chicago 10, Ill. The model 3030 lead shield consists of a lead cylinder of 1¾ in. wall thickness, with a center space which accomodates the widely available glass Geiger counters, ¾ in. in diameter and 8½ in. long. Since this shield weighs 96 lbs, it has

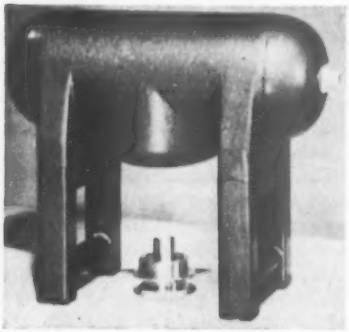

been designed with two handles to permit moving it around. The shield comes with a cable connector on one end and a built-in sample holder which provides reproducible geometries.

GEIGER TUBES

Tracerlab, Inc., 55 Oliver St., Boston, Mass. Beta-gamma end-window Geiger tubes are available in two types: the TGC-1 which has a mica window 3–4 mg/cm² and the more sensitive TGC-2, with a mica window less than 2 mg/cm², especially designed for high efficiency detection of low-energy emitters such as carbon-14 and sulfur-35. The tubes are of the self-quenching type and are said to have a life in excess of 10^8 counts. Both tubes are

mounted on standard, four-prong glazed ceramic tube bases.

PORTABLE DETECTOR

Technical Associates, 3730 San Fernando Rd., Glendale 4, Calif. The model F-3 has been designed for detecting and indicating relative intensities of beta, gamma, cosmic and X-radiation. Two sensitivity ranges are provided—low range, full-scale meter deflection indicates 0.5 mr/min;

high range, 0.017 mr/min. A counting-rate meter circuit affords means of making quantitative checks, and an amplifier operates earphones for aural monitoring. The Geiger tube is housed in a probe, which in turn is carried in a compartment in the lower section of the case. The probe window may be opened for checking beta radiation.

D-C POWER SUPPLY

Rowe Engineering Corp., 2422 N. Pulaski Rd., Chicago 39, Ill. The type IPS10000 10 kv Iso-volt d-c power supply provides a source of continuously variable d-c voltage from 1,000 to 10,000 volts at current drains up to 5 ma. Regulation of 0.1% is claimed. The apparatus is operable from a source

of power of 105–130 volts a-c, 60 cycles. Power drain is approximately 350 watts at full load. Overall dimensions of the unit are 22 in. wide by 41¾ in. high by 17½ in. deep. Weight is approximately 225 pounds.

D-C POWER SUPPLY

Furst Electronics, 800 W. North Ave., Chicago 22, Ill. The model 710-SR power supply has a range of 600–1,500 volts d-c at 0–1 ma, continuously adjustable. The output voltage is claimed to vary less than 0.01% of the

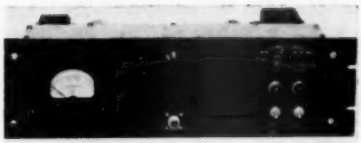

output voltage per volt change of line voltage and less than 1 volt with variations of output current between 0–1 ma (internal impedance is less than 1,000 ohms). An input of approximately 50 watts is required from a 115 volt a-c line.

END-WINDOW COUNTER

Instrument Development Laboratories, 229 W. Erie St., Chicago 10, Ill. The model D31 end-window Geiger tube is designed for use on an upright-style or socket-type sample holder. It has an all-glass envelope with a mica window at the end, and is a symmetrical cylinder either with or without a socket which can be provided if desired. Standard window thickness is 2–4 mg/cm². Thinner windows can be provided upon request. The tube is said to have a plateau from 1,100 to 1,300 volts, with a slope of 3% per

hundred volts. Life of the tube is guaranteed at 10^8 counts without a quench circuit, and the tube life can be prolonged with the use of the proper quench circuit.

URANIUM DETERMINATION

Fisher Scientific Co., 717 Forbes St., Pittsburgh 19, Pa. A new method* has been developed for determining the concentration of uranium in solution. Using the dropping mercury electrode system provided by the Fisher Elecdropode, the method can be employed to determine uranium when its concentration is within the range of 10^{-4} molar to 5×10^{-3} molar. The sample solution is first treated by the addition of a potassium chloride-hydrochloric acid solution, then placed in the Elecdropode cell. Nitrogen is passed through the solution for a minute, then the mercury electrode system is set at a dropping rate of one drop each three seconds. Potential of -0.5 volts is then applied to the electrodes and a galvanometer reading is made. This reading is then referred to the calibration curve and the concentration of uranium in the unknown sample is noted. The calibration curve is prepared by plotting galvanometer readings for different concentrations of uranyl chloride.

When iron is present along with uranium, it is merely necessary to treat the sample with hydroxylamine and warm to 50° C for 10 min before proceeding with the regular method. In the event that organic acids are present, the sample is first ashed. Phosphates which might also interfere are separated chemically before a determination is made.

DIFFUSION PUMPS

Recent experiments have been made using glycerine as the working medium in diffusion pumps. The tests were initiated by the **Services Electronics Research Laboratory at Baldock, England.** Efficiencies up to 80% of the theoretical value have been obtained, it is claimed. The increased pumping speed attainable with glycerine will be used in pumps being designed for the new Cavendish cyclotron.

TWO COMPANIES SYNTHESIZE RADIOACTIVE COMPOUNDS

Tracerlab. Inc., 55 Oliver St., Boston, Mass., has made arrangements with the AEC to manufacture and stock a number of compounds tagged with carbon-14. A partial list of C^{14}-tagged compounds which will be available within the next six months follows (in order of priority): barium carbide; acetylene; sodium cyanide; methyl alcohol and methyl iodide; carboxyl-labeled acetic acid, acetyl chloride, ethyl acetate; benzene; methylene-labeled ethyl alcohol, ethyl iodide; methyl-labeled acetic acid, acetyl chloride, ethyl acetate; and methyl-labeled ethyl alcohol, ethyl iodide.

Prices have not yet been determined but it is expected that they will be in the range of $200 to $500 per millicurie for most compounds. The minimum amount for sale will normally be one millicurie but, in some instances, smaller quantities will be available on request. All compounds will be packaged in sealed glass ampoules and,

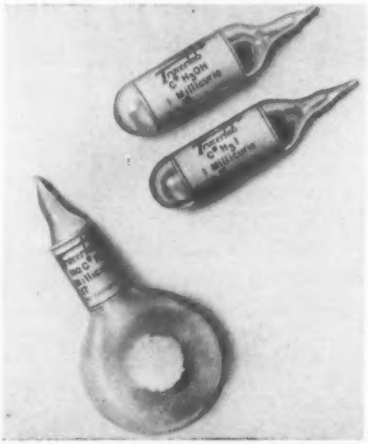

* This material is taken from *The Laboratory* **17**, 143 (1948), publication of the Fisher Scientific Co.

whenever possible, will have a minimum dilution of activity. However, the specific activity will not usually be greater than one millicurie per millimole since in some cases it has been found that the internal absorption from materials of very high specific activity may promote decomposition.

To obviate any uncertainty, standards for correlating the Tracerlab millicurie with that of Oak Ridge will be set up to permit the customer to obtain activity measured in accordance with the Oak Ridge millicurie. Standards of purity will be set up for each compound.

Barium carbide, tagged with C^{14}, is available for immediate delivery at $150 per mc with a specific activity of 2 mc per mmole. The cost of the C^{14} is included in this price. The compound contains small amounts of carbon as an impurity and upon treatment with dilute acid is said to give approximately a 60% yield of acetylene. The millicurie strength of the barium carbide is based upon a measurement of total activity present including some unreacted C^{14}.

Acetylene is available at a cost of $350 per mc. The specific activity is 2 mc per mmole and the volume of acetylene at standard conditions is approximately 11 cc per mc.

Sodium cyanide is available at $250 per mc. It has an activity of approximately 1 mc per mmole and is in the form of dry sodium cyanide containing about 2 mmoles of excess sodium hydroxide per mole of sodium cyanide.

Groups desiring synthesized compounds should contact Tracerlab first to determine availability and cost. Then the customer should apply for the compound desired by submitting Form 313, "Application for Radioisotope Procurement," to the Isotopes Division, U. S. Atomic Energy Commission, P. O. Box E, Oak Ridge, Tenn., for the required number of millicuries of C^{14} incorporated into the desired compound, stipulating the supplier. After approval by the AEC, Form 374 will be furnished the buyer by the AEC. This should then be sent to the supplier.

Texas Research Foundation, Renner, Texas, is also synthesizing radioactive compounds in cooperation with the AEC. Working on a non-profit basis, this company will, at the outset, synthesize compounds containing radioactive carbon, phosphorus and sulfur.

Synthesized compounds can be obtained in the same manner as from Tracerlab.

NUCLEONICS PRODUCTS AVAILABLE

Eldorado Mining and Refining, Ltd., P. O. Box 379, Ottawa, Ontario. This company lists the following products as being available:

Polonium—as bulk nitrate crystals or in the form of a plated electrode of specified activity; very suitable as source of alpha radiation.

Neutron sources—radium-beryllium and polonium-beryllium neutron sources are available, depending upon requirements. The polonium-beryllium source is a convenient generator of fast neutrons with a very low background of gamma radiation.

Gamma-ray standards—a series of standards consisting of radium salt sealed in a thin-walled platinum container. These are filled to a very close tolerance and are certified by the National Bureau of Standards.

Gamma Sources for Industrial Radiography—high density radium sources for use in nondestructive testing by gamma radiography. Have considerably reduced diameter compared to other sources.

Limited quantities of RaD, prepared as a beta and alpha source or mixed with beryllium to form a neutron source with negligible gamma background, are also available.

ABSTRACTS

CHEMICAL PUBLICATIONS

Beta-ray counters, R. S. Krishnan (Indian Inst. of Science, Bangalore), *Current Sci.* **17,** 37–43 (1948). The construction and characteristics of some beta-ray counters suitable for measuring the activity of low-energy beta particles are described. Circuits for a suitable amplifier and stabilized high-voltage unit for use with these counters are given.

"Analytical boundary" method for the determination of transference numbers, A. P. Brady (American Cyanimid Co., Stamford, Conn.), *J. Am. Chem. Soc.* **70,** 911–914 (1948). The theory and operation of a cell for measuring transference numbers which combine the Hittorf and moving boundary techniques are described. A radiotracer technique was used in which the leading and unknown solutions are of identical composition but contain a radioactive isotope of the ion or ions under investigation. Thus, Na^{22} was used to trace Na, and Br^{82} was used to follow Cl^- in NaCl. Ordinary counting methods were used.

The self-diffusion coefficients and transference numbers of the small ions in colloidal electrolytes, A. P. Brady, D. J. Salley (American Cyanimid Co., Stamford, Conn.), *J. Am. Chem. Soc.* **70,** 914–919 (1948). Radiotracer techniques employing Na^{22}, Na^{24}, and Br^{82} were used to determine the transference numbers and self-diffusion coefficients for two anionic and two cationic surface active agents. The tracer technique obviates errors which may arise if equilibria involving various micelle types are not fast compared to diffusion or electrical transport.

The application of the halogen-metal interconversion reaction to syntheses with isotopic carbon, A. Murray, III, W. W. Foreman, W. Langham (Los Alamos Scientific Lab., N. Mex.), *J. Am. Chem. Soc.* **70,** 1037–1039 (1948). The halogen-metal interconversion reaction was adapted to the microsynthesis of biologically important *p*-aminobenzoic acid and nicotinic acid labeled with C^{14} in the carboxyl groups, and having extremely high specific activities (about $2–3 \times 10^7$ disintegrations per min per mg).

Some exchange experiments involving hexacyanoferrate (II) and hexacyanoferrate (III) ions, R. C. Thompson (Univ. of California, Berkeley), *J. Am. Chem. Soc.* **70,** 1045–1046 (1948). A rapid electronic exchange between hexacyanoferrate (II) and hexacyanoferrate (III) ions in neutral solution, 1.0 M hydrochloric acid, and 0.05 M sodium hydroxide was observed. No exchange of iron atoms was observed between the following pairs of ions: iron (III) and hexacyanoferrate (III), iron (III) and hexacyanoferrate (II), iron (II) and hexacyanoferrate (II), and iron (II) and hexacyanoferrate (III).

Rate of exchange of cellulose with heavy water, V. J. Frilette, J. Hanle, H. Mark (Polytechnic Inst. of Brooklyn), *J. Am. Chem. Soc.* **70,** 1107–1113 (1948). Cellulose reacts very rapidly with heavy water, if sufficiently agitated, but the reaction is of limited extent. In none of the experiments were all of the hydroxyls exchanged, even at the end of a week. The falling-drop method was used to measure D_2O concentration. The extent of the exchange reaction gave a measure of the accessibility of the cellulose sample, and of the amount of amorphous material present.

The chemical properties of elements 94 and 93, G. T. Seaborg, A. C. Wahl (Univ. of California, Berkeley), *J. Am. Chem. Soc.* **70,** 1128–1134 (1948). Using the radioisotopes 94^{239} and 93^{239}, the chemical properties of elements 94 and 93 were studied. The chemical symbols Pu and Np are suggested for elements 94 and 93, respectively. In the reduced states, the precipitation reactions of these elements are similar to those of the 3+ rare earths and actinium, and of the 4+ cerium, thorium and uranium. Np and Pu exhibit a higher oxidation state with properties similar to those of 6+ uranium. For both elements the standard oxidation-reduction potential from the metal to the reduced ionic state is greater than +0.5 v. For the reduced to the oxidized ionic state, the standard potential for Np is about −1.35 v and for Pu, −1.0 to −1.4 v. The properties of Pu and Np indicate that a new rare-earth-type group of elements starts at the upper end of the periodic table with actinium or thorium.

The synthesis of uric acid containing isotopic nitrogen, L. F. Cavalieri, V. E. Blair, G. B. Brown (Sloan-Kettering Inst. for Cancer Research, New York), *J. Am. Chem. Soc.* **70,** 1240–1242 (1948). An improved synthesis of uric acid, suitable for the incorporation of N^{15} in positions 1 and 3, is described.

The mechanism of the oxidation of uric acid studied with isotopic nitrogen as a tracer, L. F. Cavalieri, G. B. Brown, (Sloan-Kettering Inst. for Cancer Research, New York), *J. Am. Chem. Soc.* **70,**1242–1243(1948). Using N^{15} as a tracer it has been shown that the oxidation of uric acid to allantoin with alkaline potassium permanganate proceeds through a symmetrical intermediate. Oxidation with either nitric acid or chlorine results in a direct cleavage of the imidazolone ring to produce alloxan.

On the dynamic state of antibodies, E. C. Kooyman, D. H. Campbell (California Inst. of Tech., Pasadena), *J. Am. Chem. Soc.* **70,** 1293–1294 (1948). Using C^{14} leucine as a tracer in rabbits, it was found that the order of magnitude of the radioactivity found in the passive antiserum was about one-fifth to one-sixth of the serum proteins. It is thought that an exchange takes place with the injected or passive transfer antibody.

Chemical reactions produced by ionization processes, J. O. Hirschfelder (Univ. of Wisconsin, Madison), *J. Phys. Colloid Chem.* **52,** 447–450 (1948). Chemical reactions produced by ionizing radiation may be studied by considering the following fundamental steps: primary processes consisting of primary and secondary ionizations, excitation without ionization, reactions between ions and neutral molecules and negative-ion formation; neutralization of the ions; and reactions of the free radicals and ions.

Electron microscopy of radiation polymerization products, J. H. L. Watson (Henry Ford Hospital, Detroit), *J. Phys. Colloid Chem.* **52,** 470–474 (1948). The acetylene polymers formed by alpha-ray bombardment, corona discharge, and catalysts were examined under the electron microscope and found to be sufficiently different in physical shape and size to be distinguished from one another.

. . . I. W. RUDERMAN

LIFE SCIENCE PUBLICATIONS

The therapeutic use of radioactive elements in malignancy, P. Hahn, C. Sheppard (Cancer Research Lab., Meharry Med. College, Nashville, Tenn.), *Ann. Inst. Med.* **28,** 598–606 (1948). An evaluation of radioactive isotopes in medicine and allied fields. Criteria for therapeutic usefulness such as selectivity, biological behavior, toxicity, etc., are discussed. Nearly all of the known radioisotopes are tabulated, giving half-life, type of radiation, chemical behavior, and comment concerning their use. Suggested techniques in the therapeutic use of the radioactive elements are included.

The accumulation of radioactive iodide by the thyroid gland in normal and thyrotoxic subjects and the effect of thiocyanate on its discharge, M. Stanley, E. Astwood (Joseph H. Pratt Diagnostic Hosp., Boston), *Endocrinology* **42,** 107–123 (1948). Thyroid hormone synthesis was almost completely inhibited after the administration of antithyroid medication but the human thyroid gland was still able to collect appreciable quantities of radioactive iodine believed to be in the form of iodide ion. The collected iodine was promptly though not completely discharged from the thryoid gland after administration of thiocyanate or large quantities of ordinary iodine.

The extent of uptake in thyrotoxic patients was much greater than normal and the rate of discharge was more rapid after administration of thiocyanate or normal iodide. The difference is sufficient so that active thyroid hyperplasia may be detected. The degree of previous hormone inhibition determines the extent of loss of collected radioiodide occasioned by a standard thiocyanate dose. Thus the quality of antithyroid therapy can be determined early in the course of treatment without interrupting medication. The duration of action of a single dose of antithyroid compound may be readily determined.

Site of action of acetylcholine, M. Rothenberg, D. Sprinson, D. Nachmansohn (Depts. of Neurol. and Biochem., College of Physicians and Surgeons, New York), *J. Physiol.* **11,** 111–116 (1948). Squid axons were exposed to solutions of N^{15}-labeled trimethylamine and to similarly labeled acetylcholine. At varying intervals after exposure, the axoplasm was extruded and the penetration of isotope determined. At the end

of 25 minutes the isotope concentration within the axoplasm was 40% of the external concentration and rose to 80% at the end of an hour for the axons exposed to the trimethylamine. By contrast, acetylcholine did not penetrate into the interior to any appreciable extent. These results are believed to explain why the pharmacological effect of acetylcholine is limited to the synapse in contrast to the physiological role of the ester in the surface membrane during conduction of nerve and muscle fibers.

The distribution pattern of sulfur-labeled methionine in the protein and the free amino acid fraction of tissues after intravenous administration, F. Friedberg, H. Tarver, D. Greenberg (Univ. of California Medical School, Berkeley), *J. Biol. Chem.* **173,** 355–361 (1948). Fasting rats were injected intravenously with methionine labeled with radiosulfur and its distribution in the proteins and free amino acid fraction of the tissues determined. The labeled sulfur was rapidly incorporated into the protein and a stabilisation of the tagged sulfur within the various organs followed. The largest incorporation occurred in the intestinal mucosa, followed by the pancreas, spleen, kidney, plasma, liver, testis, heart, brain and muscle. The red blood cell protein activity rose continuously while that of the other organs showed a continual downward trend. The rate of incorporation into the proteins of the stomach mucosa of dogs similarly injected was very low.

The effect of growth on the incorporation of glycine labeled with radioactive carbon into the protein of liver homogenates, F. Friedberg, M. Schulman, D. Greenberg (Univ. of California Medical School, Berkeley), *J. Biol. Chem.* **173,** 437–438 (1948). A graph of C^{14}-methylene-labeled glycine uptake by proteins of homogenates of rat liver as a function of body weight indicates that the growth of tissues is the result of increased activity of protein synthesis. The rate of protein synthesis is strikingly high in the fetus and decreases rapidly early in life and more slowly as maturity is approached.

Synthesis of chloracetic acid and glycine labeled with radioactive carbon in the carboxyl group, R. Ostwald (Radiation Laboratory and Dept. of Chemistry, Univ. of California, Berkeley), *J. Biol. Chem.* **173,** 207–209 (1948). Glycine labeled in the carboxyl group with C^{14} was prepared from sodium acetate via chloracetic acid in an over-all yield 42%.

Introduction of radioactive sulfur (S^{35}) into the penicillin molecule by biosynthesis, S. Howell, J. Thayer, L. Labaw (Veneral Disease Research Lab., Staten Island, N. Y.), *Science* **107,** 299–300 (1948). It was shown that in the uptake of radioactive sulfur in the biosynthesis of penicillin there is no differentiation between radioactive sulfur and ordinary sulfur.

Glycine as a precursor of purines in yeast, R. Abrams, E. Hammarsten, D. Shemin (Chem. Dept., Karolinska Institutet, Stockholm), *J. Biol. Chem.* **173,** 429–430 (1948). The experiments reported indicate that the synthesis of nucleic acid purines in yeast using glycine occurs in the same manner as does the uric acid synthesis using glycine in humans and pigeons.

Determination of the fate of phosphorus in the laying hen by means of radiophosphorus (P^{32}), J. O'Neil, J. Jowsey, C. Lee, M. Reade, J. Spinks (Univ. of Saskatchewan, Saskatoon), *Science* **107,** 295–296 (1948). About 5% of a dose of radioactive phosphorus fed to hens as calcium phosphate at a single feeding appeared in the eggs subsequently laid. In hens fed equal doses of radioactive calcium phosphate on succeeding days, the radiophosphorus content of the eggs laid rose until a constant level of 5% of the daily dose was reached in each day's egg output. The eggs continued to show activity long after the doses were discontinued indicating that the radiophosphorus was being obtained from the muscles and bones.

α-Aminoadipic acid in arginine formation, J. Dubnoff, H. Borsook (California Inst. of Tech., Pasadena), *J. Biol. Chem.* **173,** 425 (1948). α-Aminoadipic acid is shown to aminate citrulline and the relative reaction rates indicate that lysine is converted to α-aminoadipic acid.

Studies in protein metabolism with compounds labeled with radioactive carbon. II. The metabolism of glycine in the rat, D. Greenberg, T. Winnick (Univ. of California Med. School, Berkeley), *J. Biol. Chem.* **173,** 199–204 (1948). Fasting rats were given glycine containing radioactive carbon in the carboxyl group. In most of the organs examined, radioactivity reached a peak in 6 to 18 hours and thereafter the activity

approached a common lower level. Intestines, bone marrow, liver, kidney, plasma, spleen and lung were the more active organs. Muscle, red blood cells, and brain were the least active. Activity in the red blood cells was still rising at the end of 5 days.

About 60% of the C^{14} activity in the hydrolysate of the proteins was accounted for as glycine. Much smaller amounts were found in aspartic acid, arginine and glutamic acid. None was found in proline, serine and tyrosine. Half of the administered C^{14} was eliminated as expired carbon dioxide at the end of 18 hours while 4% was eliminated in the urine. Urea, hippuric acid, and free-glycine accounted for the bulk of the urinary radioactive carbon.

α-Aminoadipic acid: a product of lysine metabolism, H. Borsook, C. Deasy, A. Haagen-Smit, G. Keighley, R. Lowy (California Inst. of Tech., Pasadena), *J. Biol. Chem.* **173,** 423–424 (1948). Lysine labeled in the ε-position was prepared and incubated with guinea-pig liver homogenate, amino acid mixture corresponding to casein except for lysine, and α-ketoglutarate in isotonic solution. Chromatographs indicated the formation of α-aminoadipic acid by the de-amination of lysine. Evidence is presented indicating that the process is enzymatic and that the radioactivity did not come from contamination by the labeled lysine originally added.

The permeability of the human placenta to sodium in normal and abnormal pregnancies and the supply of sodium to the human fetus as determined with radioactive sodium, L. Flexner, D. Cowie, L. Hellman, W. Wilde, G. Vosburgh (Depts. of Embryology and Terrestrial Magnetism, Carnegie Inst. of Washington, Baltimore, Md.), *Am. J. Obstet. Gynecol.* **55,** 469–480 (1948). Measurements were made using radioactive sodium of the changes in rate of placental transfer per unit weight of placenta in normal pregnancies from the ninth week of gestation until term. There is an increase of permeability of about 70 times in this period. The permeability of the human placenta to sodium is similar to that of other members of the hemochorial group.

Chronic hypertension and cardiac disease in a small series of cases did not affect the rate of transfer. Of the two cases of pre-eclampsia observed, one showed a marked reduction of permeability. The fetus receives as much sodium at the twelfth week and 1100 times as much at the fortieth week as is incorporated into the growing tissues.

Techniques for *in vivo* tracer studies with radioactive carbon, H. Skipper, C. Bryan, L. White, Jr., O. Hutchinson (Southern Research Inst., Birmingham, Ala.), *J. Biol. Chem.* **173,** 371–381 (1948). Apparatus is described which is designed to absorb mouse respiratory CO_2 which may possibly contain radioactive carbon C^{14}. A procedure is given for the oxidation of tissues prior to radiocarbon determination. A method for determining the analysis of radiocarbon in the gaseous state is described.

The preparation of sodium acetate labeled with radioactive carbon in the methyl group, B. Tolbert (Univ. of California, Berkeley), *J. Biol. Chem.* **173,** 205–206 (1948). Carbonating labeled methyl magnesium iodide in a vacuum system yielded sodium acetate with C^{14} in the methyl group. The yield was about 75% on a small scale.

Biological precursors of uric acid. I. The role of lactate, acetate and formate in the synthesis of the ureide groups of uric acid, J. Sonne, J. Buchanan, A. Delluva (School of Med., Univ. of Pennsylvania, Philadelphia), *J. Biol. Chem.* **173,** 69–79 (1948). $C^{13}O_3$, $HC^{13}OOH$, $CH_3C^{13}OOH$, $NH_2CH_2C^{13}OOH$, $CH_3CHOHC^{13}OOH$, $C^{13}H_3C^{13}HOHCOOH$ were synthesized and fed to fasting pigeons. The uric acid excreted was degraded so that both ureide carbon atoms could be analyzed for isotope content. The labeled atoms of the compounds other than acetic and formic acids were not used in ureide synthesis. Acetate is believed to be the source of the ureide carbon and it is believed that formate is an intermediate or may be converted into an intermediate of this reaction. α,β-labeled lactate is also believed to be an intermediate.

CO_2 and the carboxyl groups of lactate and pyruvate are not precursors of formate in the pigeon. The carboxyl group of lactate is not a direct precursor of urea in the rat, indicating that the carbon of urea and ureide carbon of uric acid have separate metabolic origins.

Biological precursors of uric acid. II. The role of lactate, glycine and carbon dioxide as precursors of the carbon chain and nitrogen atom 7 of uric acid, J. Buchanan, J. Sonne, A. Delluva (School of Med., Univ. of Pennsylvania, Philadelphia), *J. Biol. Chem.* **173,** 81–97

(1948). CO_2 was shown to be the source of carbon 6 of uric acid, and the carboxyl carbon of glycine to be the source of carbon 4 of uric acid. It was indirectly demonstrated that the amino nitrogen of glycine is probably the source of nitrogen 7. The α-carbon of glycine is believed to be the source of carbon 5. The assimilation of CO_2 into carbon 6 is believed to occur by a reaction not previously described. It is believed that lactate is converted to glycine by reactions involving the conversion of serine to glycine. Glycine and acetate are not directly interconvertible in the metabolism of the pigeon. It is suggested that a 3-carbon intermediate formed by a reaction involving CO_2 and the α-carbon of glycine may be a step in the metabolism of glycine.

Studies in protein metabolism with compounds labeled with radioactive carbon. I. Metabolism of D,L-tyrosine in the normal and tumor-bearing rat, T. Winnick, F. Friedberg, D. Greenberg (Univ. of California Med. School, Berkeley), *J. Biol. Chem.* **173,** 189–197 (1948). C^{14} administered in the form of tyrosine to tumor-bearing rats is rapidly incorporated into the proteins of the various organs. The highest isotope concentrations were found in intestinal mucosa, kidneys and plasma, followed by liver and spleen. Lower concentrations were found in testis, brain and muscle. The tumor proteins had high activity and contained much of the total protein-bound C^{14}. Almost all of the radioactivity of the proteins was due to tyrosine. Small C^{14} concentrations were found in the dicarboxylic acids. Analysis of urinary tyrosine, urea, creatinine, hippuric acid and ketone bodies indicated the presence of C^{14}.

. . . BERNARD KANNER

PHYSICAL PUBLICATIONS

Yield of neutrons from photo-neutron sources, B. Russell, D. Sachs, A Wattenberg, R. Fields (Argonne National Lab., Chicago, Ill.), *Phys. Rev.* **73,** 545–549 (1948). The absolute number of neutrons per second per curie of incident gamma rays was investigated. The gamma radiation was from sources produced by irradiation in a pile, and the number of neutrons was determined by comparison with a Ra-(α,n)-Be source of known neutron yield, using a "long counter." The absolute values are uncertain by as much as 25%, because the number of gamma rays per second emitted by the sources was calculated from the neutron activation cross sections and the pile flux, but the relative values are quite reliable.

Disintegration of positive and negative mesons in different absorbers, N. Nereson (Univ. of New Mexico, Albuquerque), *Phys. Rev.* **73,** 565–569 (1948). Using a magnetic field to separate the positive and negative mesotrons, along with absorbers of low and high atomic number, electrons from the decay of the mesotrons in the absorber were studied. Coincidence and anticoincidence circuits allowed determination of delayed counting rates. The results agree with previous investigations. Positive mesotrons decayed in all absorbers tried (boron, carbon, aluminum, and iron); negative mesotrons decayed with lifetimes greater than 0.6 microseconds only in boron and carbon. This indicates that negative mesotrons tend to be captured by absorbers of high atomic number before decaying.

New experiments concerning the surplus gamma-radiation from rocks, V. F. Hess, J. D. Roll (Fordham Univ., New York), *Phys. Rev.* **73,** 592–595 (1948). The excess of gamma-ray activity from certain igneous rocks over that to be expected from the content of radioactive elements might be attributable to cosmic-ray effects. The ionization from crushed rock samples was investigated in an iron house. In the case of granite, the excess ionization was the same in an underground station as above ground, so that the excess could not have been due to the effect of cosmic radiation.

Gamma-radiation from granite, W. D. Urry (Carnegie Inst., Washington, D. C.), *Phys. Rev.* **73,** 596–601 (1948). By adding amounts of uranium, thorium and potassium equal to the amounts calculated to be present, the ionization is found to be doubled in the case of gamma-ray activity of Quincy granite. This indicates that the ionization is fully accounted for, contrary to previous results. The discrepancy may have arisen in the computation of the expected ionization because of an incorrect value for the gamma radiation from potassium.

The beta-spectra of Cu^{64} as a test of the Fermi theory, C. S. Cook, L. M. Langer (Indiana Univ., Bloomington), *Phys. Rev.* **73,** 601–607 (1948). The

positron and negatron spectra of Cu^{64} have been measured with a double-focusing spectrometer of high resolution and intensity, so constructed as to almost eliminate scattering. Very thin source, backing, and counter window allow accurate measurements of the relative distribution down to about 10 kev. Departures from the Fermi plot are definitely observed, below 0.27 Mev for positrons and 0.19 Mev for negatrons. There are more of both at low energies than given by the theory, and the positron-electron ratio is higher than predicted at low energies, agreeing with the results of Backus. A simple linear combination of the possible beta interactions does not account for the experimental results.

Total cross section of Fe, Ni, and Bi for fast neutrons, H. H. Barschall, C. K. Bockelman, L. W. Seagondollar (Univ. of Wisconsin, Madison), *Phys. Rev.* **73,** 659–665 (1948). The neutron cross sections were measured from 10 to 500-kev neutron energies with 20-kev resolving power, and from 200 to 1400-kev with 150 kev resolution. High resolution measurements show resonances in Fe and Ni but not in Be, spacing being about 50 kev for Fe and 100 kev for Ni. Experiments with thick targets at lower resolving power were performed to compare results with the Weisskopf theory. Discrepancies exhibited in the comparison may be caused by an uncertainty in the knowledge of the constants on which the calculations are based.

Resonances in the disintegration of fluorine and lithium by protons, T. W. Bonner, J. E. Evans (Rice Inst., Houston, Texas), *Phys. Rev.* **73,** 666–674 (1948). Gamma radiation from bombarded elements showed resonances in the case of fluorine at intervals of the order of 100 kev with experimental widths of the order of 10 kev. The absolute cross section was calculated to be of the order of 10^{-26} cm^2 at resonance, and the partial widths due to proton re-emission varied from 10 v to 5.7 kev. In the case of lithium, the asymmetry of the resonance curve precluded explanation by the single-level dispersion formula.

On the recoil of the nucleus in beta decay of Kr^{85}, J. C. Jacobsen, O. Kofoed-Hansen (Inst. for Theoretical Physics, Univ. of Copenhagen, Denmark), *Phys. Rev.* **73,** 675–679 (1948). The recoil nuclei from the disintegration of Kr^{85} produced in fission of uranium are allowed to collect on aluminum foils whose activity is then measured. By putting a retarding potential on a grid of wire gauze, something can be learned about the energy distribution of the recoils. The maximum energy is determined with good accuracy, but poor resolution overestimates the number of small energy. The average recoil energy is 29 ev; the maximum recoil energy is 51.5 ± 2 ev, which agrees closely with the value calculated from the maximum energy 2.4 Mev of the beta particles as determined by absorption.

Relaxation effects in nuclear magnetic resonance absorption, N. Bloembergen, E. M. Purcell, R. V. Pound (Harvard Univ., Cambridge, Mass.), *Phys. Rev.* **73,** 679–712 (1948). In the magnetic resonance absorption process, the new equilibrium state requires the transfer of energy to the degrees of freedom (internal) other than the spins. This involves the spin-lattice interaction described by the spin-lattice relaxation time T_1, measuring the time required for the establishment of thermal equilibrium. The width of the absorption line is determined partly by the interaction among the magnetic nuclei, measured by a characteristic time T_2'. The line width and relaxation times were measured under widely varying conditions (the latter vary from 10^{-4} to 100 sec), and are explained theoretically by considering the effect of the thermal motion of the magnetic nuclei on the interaction of their spins.

Slow neutron velocity spectrometer studies of H, D, F, Mg, S, Si, and quartz, L. J. Rainwater, W. W. Havens, Jr., J. R. Dunning, C. S. Wu (Columbia Univ., New York), *Phys. Rev.* **73,** 733–741 (1948). Using a paraffin sample gives 20.6 ± 1 barns for the free proton cross section for neutrons; at low energies, the value approaches four times as much. The free cross section of D is 3.3 ± 0.2 barns, obtained from D_2O. Magnesium shows no resonances but exhibits microcrystalline effects (rise in cross sections at low neutron energy). Sulfur has a very low cross section, indicating destructive interference between potential and resonance scattering amplitudes. Silicon exhibits no discernible resonances. Quartz shows a residual, incoherent scattering cross section of 1.25 barns (constant below 0.025 ev). It rises with energy to 9.2 barns at about 1 ev and then remains constant, indicating that this is the additive cross section for the free atoms scattering independently.

Energy distribution of protons from a target bombarded by 190-Mev deuterons, W. W. Chupp, E. Gardner, T. B. Taylor (Radiation Lab., Univ. of California, Berkeley), *Phys. Rev.* **73,** 742–749 (1948). When deuterons of the indicated energy strike a target, the neutrons may be stripped from the deuteron in a nuclear collision, the proton continuing on its way, just as the proton may hit the nucleus and the neutron, missing, may continue with about half the deuteron energy. The deuterons are produced by the 184-in. cyclotron, and the cyclotron magnetic field is used to separate protons of different energies. Carbon detectors using the $C^{12}(p,pn)C^{11}$ reaction, which has a constant cross section from 60 to 140 Mev, and photographic plates were used for proton detection. The energy distribution of the protons agrees with that calculated on the basis of Serber's transparent nucleus theory.

Proton widths of light nuclei, R. F. Christy, R. Latter (California Inst. of Tech., Pasadena), *Revs. Mod. Phys.* **20,** 185–190 (1948). In nuclear resonance experiments involving charged particles, it is useful to separate the known energy-dependent factors from the observed widths. This involves the square root of the (proton) bombarding energy and the barrier penetration factor, which can be calculated from Coulomb wave functions in terms of the energy and the proton angular momentum. Results are given for Li^7, Be^9, B^{11}, C^{12}, N^{14}, O^{16}, and F^{19}, proton widths being normalized to 1 at 1 Mev without barrier.

The energy and momentum relations in the beta-decay, and the search for the neutrino, H. R. Crane (Univ. of Michigan, Ann Arbor), *Revs. Mod. Phys.* **20,** 278–295 (1948). A critical evaluation is given of the characteristics of the beta-decay which lead to the neutrino hypothesis, including experiments which have gone to determine the energy and momentum relations which apply. The momentum experiments include those on recoil experiments using the *K*-capture process, measurement of nuclear momentum of electron emitters (Leipunski, Jacobsen and Kofoed-Hansen), and measurement of another quantity besides recoil momentum (Crane and Halpern, Sherwin, and Li^8 disintegration). Neutrino absorption is discussed and suggestions are made for further experiments to discover more about what we call "a neutrino."

The use of coincidence counting methods in determining nuclear disintegration schemes, A. C. G. Mitchell (Indiana Univ., Bloomington) *Revs. Mod. Phys.* **20,** 296–304 (1948). By avoiding instruments of high resolving power in measuring the beta and gamma-ray energies, low activity sources may be used. Two counters are placed near the radioactive source, and coincidences are measured between the gamma and beta rays of various energies and among the several gamma rays. In this manner the following can be determined: (*a*) whether there is more than one gamma per disintegration, (*b*) whether the lowest-energy beta ray leads to the ground state of the product, and (*c*) whether there are any low-energy groups of electrons associated with additional gamma-ray transitions. Coincidence counting arrangements are described, and sample experimental results given for simple and complex spectra.

Studies of self-absorption in gamma-ray sources, R. D. Evans, R. O. Evans (Massachusetts Inst. of Tech., Cambridge), *Revs. Mod. Phys.* **20,** 305–326 (1948). The theory of self-absorption in a source due to Compton effect, photoelectric effect, and pair production is given, with results, as a function of gamma-ray energy, density, and atomic number of the absorbing material. Self-absorption formulae are derived through use of the attenuating coefficient for various geometrical arrangements, including linear and cylindrical sources. Experimental arrangements for the measurement of self-absorption are described, including corrections for poor geometry. Application is made to radium assay by gamma-ray measurements.

The production of nuclear disruptions by the cosmic radiation, S. A. Korff (New York University), *Revs. Mod. Phys.* **20,** 327–333 (1948). The experimental techniques and results concerning the nuclear disruptions emitting heavily ionizing particles are summarized. Data may be obtained using cloud chambers, photographic emulsions, and ionization chambers. The initiating particles are usually uncharged (mainly neutrons). The energy of the burst rises slowly with the atomic number of the target nucleus. Together with the number of particles per "star," and neutron and proton production rates, these facts lead to certain conclusions about the cross sections for the production processes, and explain the

production of fast neutrons, electron-photon cascades, and secondary protons from the primary 6-Bev (and over) proton radiation.

Cosmic rays at 30,000 feet, R. V. Adams, C. D. Anderson, P. E. Lloyd, R. R. Rau, R. C. Saxena (California Inst. of Technology, Pasadena), *Revs. Mod. Phys.* **20,** 334–349 (1948). A cloud chamber was operated at various altitudes up to 30,000 feet, in a magnetic field of 7,500 gauss. Electron showers and single particles were compared as to frequency of occurrence. Energy measurements indicated that at 30,000 feet many of the particles in the range of momenta up to 10^7 gauss-cm are protons, whereas at sea level they are nearly all mesotrons. Large numbers of photographs of showers, disintegrations, and single particles are shown.

Cosmic-ray effects from solar flares and magnetic storms, H. V. Neher, W. C. Roesch (California Inst. of Tech., Pasadena), *Revs. Mod. Phys.* **20,** 350–352 (1948). The cosmic-ray data taken during a solar flare and following magnetic storm are given. The increase in intensity coinciding with the visual start of the flare may indicate a source for cosmic radiation, though small flares give no effect. The hypothesis of the current-sheet resulting in a change in the earth's dipole is discussed.

A new cosmic-ray telescope for high altitudes, A. T. Biehl, *et al.* (California Inst. of Tech., Pasadena), *Revs. Mod. Phys.* **20,** 353–359 (1948). A telescope is described which has an angular resolution of 15° but a high enough counting rate to make the relative probable error (at peak) in four minutes of counting 1.5%. The accidental coincidence rate is very low, a triple coincidence circuit being used.

Recent studies of the cosmic-ray latitude effect at high altitudes, A. T. Biehl, *et al.* (California Inst. of Tech., Pasadena), *Revs. Mod. Phys.* **20,** 360–366 (1948). Using the improved Geiger counter telescope, a number of balloon flights were made, all sets of equipment being compared with a common standard to reduce the results. The number of counts as a function of the weight of air above is given for a number of latitudes.

The absorption of high-energy electrons in cosmic radiation, W. L. Scheen (University of Amsterdam, Netherlands), *Physica* **13,** 669–688, (1947). By considering the notion of the "maximum particle" (that particle among the secondaries in a cascade which has the highest energy), a generalized cascade theory is constructed which gives the "range" in a material through which a particle or its most energetic secondary will penetrate.

A coincidence method of measuring a flux of fast neutrons, B. B. Kinsey, S. G. Cohen, J. Dainty, *Proc. Cambridge Phil. Soc.* **44,** 96–113 (1948). The protons projected by fast neutrons from a polythene layer in the forward direction are recorded using a triple coincidence counter, the circuit containing a discriminator to eliminate secondary electrons from gammas. Assuming isotropic neutron-proton scattering, the neutron flux may be calculated from the proton counting rate and the *n-p* cross section. The accuracy is estimated at from 5% to 15%, depending on how well the energy of the neutron and the *n-p* cross section at that neutron energy are known.

The stopping power of polythene and fast neutron flux measurements, D. H. Wilkinson, *Proc. Cambridge Phil. Soc.* **44,** 114–123 (1948). To use the "homogeneous ionization chamber" method for determining fast neutron flux, the gas and walls must have the same stopping power. Alpha-particle stopping powers were investigated for polythene and ethylene. These are found to differ by less than 1%, due to differences in polarizibility of gaseous and condensed states, changing of the electronic energy levels and, consequently, the average excitation potential, and alteration of the electron affinity.

The yield of Ba^{139} in the fission of natural uranium by fast and slow neutrons, E. Broda (Univ. of Edinburgh, Scotland), L. Kowarski (Collège de France, Paris), D. West (Chalk River Lab., Ontario, Canada) *Proc. Cambridge Phil. Soc.* **44,** 124–132 (1948). The yields per fission of Ba^{139}, as found by the beta-activity after chemical separation, are found to bear a ratio of 0.84 ± 0.03 for the cases of fast neutrons (from a Ra-Be) source and slow neutrons (those captured by Cd).

An electrical method for the determination of short-period activities and its use in the evaluation of the half-life of B^{12}, J. V. Jelley, E. B. Paul, *Proc. Cambridge Phil. Soc.* **44,** 133–139 (1948). The deuterons from a high-voltage ac-

DPi
HIGH VACUUM RESEARCH AND ENGINEERING

High Vacuum

make it, measure it, control it

with DPI equipment

Ten years of research, development, design and manufacturing have made DPI leading suppliers of high-vacuum equipment for work involving betatrons, cyclotrons, syncrotrons, syncro-cyclotrons, straight line accelerators, Geiger Mueller tubes.

DPI is currently producing more than 35 types and sizes of vacuum pumps and an extensive line of stills, chambers, gauges, controls, valves, recorders, and accessories.

For highly sensitive, sturdy, trouble-free apparatus to attain, measure and control high vacuum, look to DPI—pioneer in the field.

Vacuum Equipment Division

DISTILLATION PRODUCTS, INC.

781 Ridge Road West, Rochester 13, N.Y.
570 Lexington Ave., New York 22, N.Y.
135 So. LaSalle Street, Chicago 3, Ill.

celerating tube produced neutrons by bombarding a target. These neutrons produced short-period activity in another target. Deflector plates moved the beam rapidly onto and off the target, and the beta rays from activities induced by the neutrons were counted by a counter whose output was recorded by several delay channels. By varying the delay time, the number of beta-rays as a function of time after the cessation of neutron bombardment was obtained. The period of B^{12} activity was thus found to be $(27 \pm 2) \times 10^{-3}$ sec.

Sur la possibilité d'existence d'un type particulier de radio-activité phénomène de créatione, R. Daudel, M. Jean, M. Lecoin (Curie Lab., Paris), *J. phys. radium.* **8,** 238–243 (1947). A beta disintegration is discussed in which the electron emitted from the nucleus does not escape the Coulomb field but takes its place in an outer orbit. Eventually it emits a photon and falls into the atomic ground state. Considerations for the occurrence of such a process are discussed.

Discussion de nouvelle expériences sur les grandes gerbes de l'air (gerbes d'Auger), J. Daudin, A. Loverdo (École Normale Supérieure), *J. phys. radium* **8,** 233–237 (1948). A summary and discussion are given of results on the Auger showers of cosmic radiation, using coincidence counters. Various altitudes of measurement are included and quadruple-triple and triple-double coincidence ratios give information on the density of the showers. The variation of frequency of showers with density is the same for a number of different experiments.

De la validité de la loi en $1/V$ pour le vanadium et pour d'autres detecteurs de neutrons thermiques et de quelques propriétés du vanadium radioactif V^{52}, J. Martelly, *Ann. phys.* **2,** 555–648 (1947). The period of V^{52} is found to be 3.74 ± 0.01 min, and the energy of the gamma ray accompanying the disintegration is found by absorption measurements to be 1.46 ± 0.05 Mev, with 36 emitted per hundred betas. The neutron capture cross-sections of B, Ag, V, Dy^{164}, and Au are measured as a function of energy to verify the $1/V$ law in the thermal region. The energy of the neutrons is varied by use of boron capture, cadmium resonance, and changing the temperature of the paraffin which slows the neutrons down to thermal energy.

. . . HAROLD BROWN

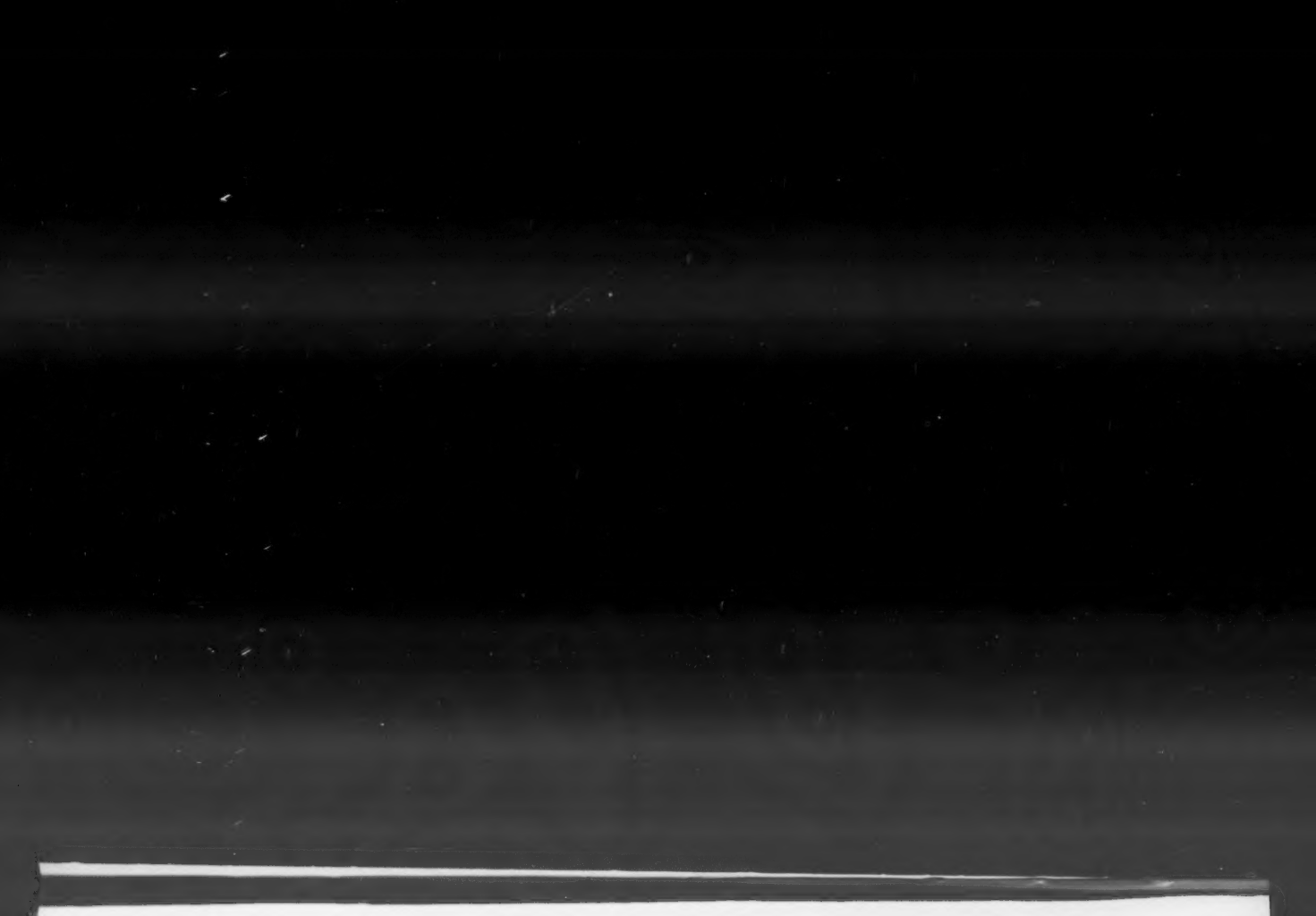

Keleket Dosimeter
Model K-100

The KELEKET DOSIMETER and CHARGING UNIT

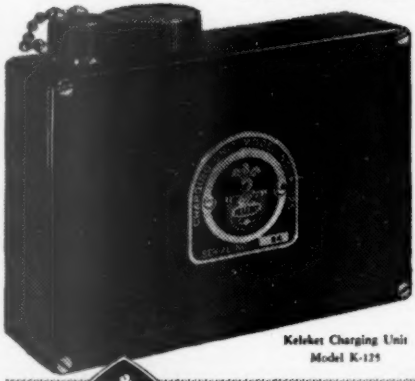

Keleket Charging Unit
Model K-125

The *"Landsverk" Dosimeter*, now manufactured by the Instrument Division of the Kelley-Koett Mfg. Company, is no larger than the average ball-pen . . . it can be clipped into the pocket.

Radiologists, X-ray technicians, research-workers and others working with X-ray equipment or radio-active materials can observe, at any time of the day, the total quantity of radiation he has absorbed.

The Dosimeter is an integrating-meter for the measurement of x- or gamma ray dosage . . . and is read by pointing the Dosimeter at a source of light and noting the distance the fibre image has moved on the scale. The scale reads directly in milliroentgens . . . and has a range from 0 to 200. (Twice the accepted normal dosage.)

The *Keleket Charging Unit* is a compact, portable voltage and light source enclosed in a waterproof, cast-aluminum case ($1\frac{15}{16}$" x $4\frac{15}{16}$" x $5\frac{5}{16}$") The charging unit will charge one or more Keleket Dosimeters.

YOUR INQUIRIES ARE INVITED

INSTRUMENT DIVISION
THE KELLEY-KOETT MFG. CO.
COVINGTON, KENTUCKY

Write! for "KELLEY-KOETT" Bulletin Q-2
which describes Dosimeter and Charging Unit.

Most complete line

of precise instruments for nuclear measurements

Instrumentation is the ladder by which science is climbing to new heights in the new field of nucleonics. Findings cannot be more accurate than the instruments used. No one knows this better than *i d l's* designers and craftsmen with their Manhattan District background and constant contact with today's vanguard of research, both academic and industrial.

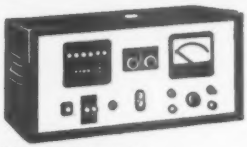

model 163 automatic scaler
Outstanding for precise research. Automatic scaler shutoff, scale selection plus "Count-o-matic" scale multiplier, and built-in register. A complete unit, without an equal for proved performance.

model 161 scaling unit
Highly flexible basic unit. Simple operation, extreme reliability. Built-in high-voltage supply. Facilities for clock and external register. Can also be furnished with built-in register.

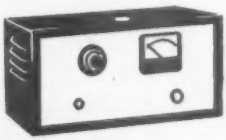

model 1090 high-voltage supply
Extremely accurate control from zero to 5000-volts (plus or minus). Continuously variable. Output varies less than .01% for a line voltage variation of 90 to 130-volts AC.

model 2610 portable beta-gamma count rate meter
Easily portable (weighs only 9½ pounds). Ideal for health or geological surveys, location of radioactive materials, x-ray monitoring, other uses.

model 3340 pocket chamber
Newest safeguard for monitoring exposure to gamma and x-ray radiation. Capacity of .2 roentgen. Clips to shirt pocket. Sturdy, shock-proof, moisture-proof, accurate. Each instrument numbered.

i d l's complete line comprises all the devices and accessories needed for radioactivity instrumentation in all its current applications. Please call upon us for catalog information or assistance in working out your technical problems.

idl

Instrument Development Laboratories

223-233 West Erie Street • Chicago 10, Illinois